

# **Investigation of the gut-brain axis in Parkinson's disease**

By

Tyler Cannon

Department of Microbiology and Immunology

McGill University, Montreal, Quebec, Canada

April 2021

A thesis submitted to McGill University in partial fulfilment of the requirements of the degree of  
Doctor of Philosophy

© Tyler Cannon, 2021

## **TABLE OF CONTENTS**

<b>ABSTRACT</b>	<b>1</b>
<b>RÉSUMÉ</b>	<b>3</b>
<b>ACKNOWLEDGEMENTS</b>	<b>5</b>
<b>CONTRIBUTION TO ORIGINAL KNOWLEDGE</b>	<b>7</b>
<b>CONTRIBUTION OF AUTHORS</b>	<b>8</b>
<b>LIST OF ABBREVIATIONS</b>	<b>10</b>
<b>PREFACE TO CHAPTER 1</b>	<b>13</b>
<b>CHAPTER 1: Introduction and literature review</b>	<b>14</b>
1. Parkinson's disease	14
1.1 – Pathophysiology and clinical features	14
1.1.1 – Dopaminergic neurodegeneration	15
1.1.2 – $\alpha$ -Synuclein and Lewy Pathology	17
1.1.3 – Mitochondrial dysfunction	19
1.1.4 – Immunological evidence	22
1.1.5 – Motor symptoms	25
1.1.6 – Non-motor symptoms	27
1.2 – Risk Factors	28
1.2.1 – <i>PINK1</i>	29
1.2.2 – <i>PRKN</i>	29
1.2.3 – <i>SNCA</i>	30
1.2.4 – Environmental factors	31
1.2.5 – Infection	32
1.3 – Clinical interventions	33
1.4 – Murine models of Parkinson's disease	35
1.4.1 – MPTP model	35
1.4.2 – Rotenone model	36
1.4.3 – 6-Hydroxydopamine model	37
1.4.4 – LPS injection model	37
1.4.5 – Human $\alpha$ -Synuclein overexpression model	38
1.4.6 – <i>Parkin</i> <sup>-/-</sup> mice	38
1.4.7 – <i>Pink1</i> <sup>-/-</sup> mice	39
2. Intestinal homeostasis and infection	39
2.1 – Intestinal overview	40
2.1.1 – Intestinal epithelial cells	41

2.1.2 – Intestinal immunology	44
2.1.3 – The gut microbiota	48
2.1.4 – The enteric nervous system	51
2.2 – Intestinal infection	53
2.2.1 – Enteropathogenic and enterohemorrhagic <i>Escherichia coli</i>	54
2.2.2 – <i>Citrobacter rodentium</i>	56
2.3 – Host response to intestinal infection	59
2.3.1 – Innate immunity	59
2.3.2 – Adaptive immunity	61
3. The gut-brain axis in Parkinson's disease	62
3.1 – Gastrointestinal dysfunction and Parkinson's disease	63
3.2 – $\alpha$ -Synuclein spread along the gut-brain axis	65
3.3 – The microbiota in Parkinson's disease	67
<b>PREFACE TO CHAPTER 2</b>	<b>70</b>
<b>CHAPTER 2: Intestinal infection triggers Parkinson's disease-like symptoms in <i>Pink1</i><sup>-/-</sup> mice</b>	<b>71</b>
Abstract	71
Main Text	72
Methods	88
Extended Data	100
Supplementary Information and Videos	112
Acknowledgements	115
Data Availability Statement	115
<b>PREFACE TO CHAPTER 3</b>	<b>116</b>
<b>CHAPTER 3: Characterization of the intestinal microbiota during <i>Citrobacter rodentium</i> infection in a mouse model of infection-triggered Parkinson's disease</b>	<b>117</b>
Abstract	117
Introduction	117
Gut Bacterial Diversity	120
Taxonomic Analysis of the Gut Bacterial Microbiota	123
Short-Chain Fatty Acid Analysis	128
Concluding Remarks	132
Acknowledgements and Funding	133
Disclosure Statement	133

<b>CHAPTER 4: Discussion</b>	<b>134</b>
4 – Overview	134
4.1 – A two-hit model for familial Parkinson’s disease	136
4.2 – Mitochondrial antigen presentation	139
4.3 – The anti-mitochondrial immune response	142
4.4 – The gut microbiota and short-chain fatty acids	146
4.5 – Revisiting <i>Pink1</i> <sup>-/-</sup> mice as a model for Parkinson’s disease	148
4.6 – Conclusion	150
<b>REFERENCES</b>	<b>152</b>
<b>APPENDIX</b>	<b>179</b>

## ABSTRACT

Parkinson's disease (PD) is a neurodegenerative disorder that results in the specific destruction of dopaminergic neurons in the brain. Inherited familial forms of PD have been strongly associated to several genetic recessive mutations in genes such as *PINK1*; however, previous studies utilizing *Pink1*<sup>-/-</sup> mice have failed to recapitulate a PD-like phenotype. Recently, a novel function for the PINK1 protein was discovered wherein PINK1 inhibits mitochondrial antigen presentation (MitAP) on MHC I in macrophages exposed to lipopolysaccharide (LPS), suggesting that PD may be immunological in nature and influenced by external factors such as infections. Furthermore, a growing body of evidence has recently implicated the gut in PD via the gut-brain axis: inflammatory bowel disease correlates with increased PD incidence rates in humans, and several studies have now highlighted how a PD-derived microbiota can exacerbate symptoms in a PD mouse model. This thesis investigates the mechanisms of the gut-brain axis in PD; thus, we hypothesize that the gut can regulate disease onset in *Pink1*<sup>-/-</sup> mice.

Given that LPS can induce MitAP in PINK1-deficient cells, we infected wild-type (WT) and *Pink1*<sup>-/-</sup> littermate mice with the intestinal pathogen *Citrobacter rodentium*, a Gram-negative murine model for *Escherichia coli* infections. We observed a significant induction of MitAP in splenic dendritic cells and the subsequent formation of anti-mitochondrial CD8<sup>+</sup> T cells uniquely in *Pink1*<sup>-/-</sup> mice upon infection. Notably, *C. rodentium* infection was sufficient to induce infiltration of these anti-mitochondrial CD8<sup>+</sup> T cells into the central nervous system. Performing four serial infections resulted in a PD-like motor phenotype in *Pink1*<sup>-/-</sup> mice, characterized by the decreased ability to descend a pole. Treatment with L-DOPA, a dopamine precursor, rescued this phenotype, suggesting a deficiency within the dopaminergic system of these mice.

Due to the mounting evidence implicating the gut microbiota to PD, we also investigated whether *C. rodentium* infection is altering the intestinal microbiota over the course of infection in our model. Performing 16S ribosomal RNA gene sequencing on fecal samples during infection revealed no significant disturbances to the diversity of the microbiota during infection and that the microbial communities remained comparable between genotypes. A trend was observed for an increase in the genus *Akkermansia* in WT mice post infection, a microbe associated with anti-inflammatory signatures. Short-chain fatty acid analysis revealed a significant increase in butyric acid only in *Pink1*<sup>-/-</sup> mice, compared to an increase in isobutyric acid in WT mice.

The findings in this thesis suggest that the intestinal environment is a key regulator of disease development in *Pink1*<sup>-/-</sup> mice, highlighting the importance of the gut-brain axis in PD.

## RÉSUMÉ

La maladie de Parkinson (MP) est une maladie neurodégénérative qui engendre la destruction spécifique des neurones dopaminergiques dans le cerveau. Les formes familiales héritées de la MP ont été fortement associées avec plusieurs mutations génétiques récessives dans des gènes comme *PINK1*; mais, des études précédentes qui utilisent des souris *Pink1*<sup>-/-</sup> n'ont pas réussi à récapituler un phénotype similaire de MP. Récemment, une nouvelle fonction pour la protéine PINK1 a été découverte où il se trouve que PINK1 inhibe la présentation de l'antigène mitochondrial (MitAP) sur le complexe majeur d'histocompatibilité I dans les macrophages exposés au lipopolysaccharide (LPS). Cela suggère qu'il est possible que la MP est de nature immunologique et est influencée par des facteurs externes comme les infections. Aussi, il y a maintenant beaucoup d'évidences qui impliquent l'intestin dans la MP via l'axe intestin-cerveau: les maladies inflammatoires de l'intestin sont corrélées avec une augmentation des taux d'incidences de la MP chez les humains, et plusieurs études maintenant suggèrent comment un microbiote dérivé d'un patient MP peut exacerber les symptômes dans un modèle de souris pour la MP. Cette thèse étudie les mécanismes de l'axe intestin-cerveau dans la MP; c'est pourquoi nous proposons l'hypothèse que l'intestin peut réguler la manifestation des symptômes similaires de la MP chez les souris *Pink1*<sup>-/-</sup>.

Avec l'information que la LPS peut induire MitAP dans les cellules déficientes en PINK1, nous avons infecté des souris de type sauvage (WT) et *Pink1*<sup>-/-</sup> de la même portée avec le pathogène intestinal *Citrobacter rodentium*, un modèle Gram-négatif pour les infections *Escherichia coli* chez les souris. Nous avons observé une induction significative de MitAP dans les cellules dendritiques spléniques et la formation subséquente des cellules T CD8<sup>+</sup> anti-mitochondriales

uniquement chez les souris *Pink1*<sup>-/-</sup> infectées. Notamment, l'infection avec *C. rodentium* était suffisante pour induire une infiltration de ces cellules T CD8<sup>+</sup> anti-mitochondriales dans le système nerveux central. Nous avons observé que quatre infections en série ont abouti à un phénotype moteur seulement en les souris *Pink1*<sup>-/-</sup>, caractérisé par une capacité réduite à descendre un pôle. Traitement avec la L-DOPA, un précurseur de la dopamine, a pu renverser ce phénotype et suggère un déficit dans le système dopaminergique de ces souris.

Parce qu'il y a maintenant beaucoup d'évidences qui impliquent le microbiote intestinal dans la MP, nous avons également étudié si l'infection avec *C. rodentium* modifiait le microbiote intestinal au cours de l'infection dans notre modèle. Le séquençage du gène ribosomique 16S sur des échantillons fécaux pendant l'infection n'a révélé aucune perturbation significative associée à la diversité du microbiote pendant l'infection et que les communautés microbiennes sont restées comparables entre les génotypes. Une tendance a été observée pour une augmentation du genre *Akkermansia* chez les souris WT après l'infection, un microbe associé à des signatures anti-inflammatoires. Une analyse des acides gras à chaîne courte a révélé une augmentation significative de l'acide butyrique uniquement en les souris *Pink1*<sup>-/-</sup> et une augmentation de l'acide isobutyrique en les souris WT.

Les résultats de cette thèse suggèrent que l'environnement intestinal est un régulateur très important dans le développement de la maladie chez les souris *Pink1*<sup>-/-</sup>, soulignant l'importance de l'axe intestin-cerveau dans la MP.



## ACKNOWLEDGEMENTS

As I prepare to submit this thesis, I have come to realize that my time in graduate school has been defined by the remarkable people I have met along the way. My colleagues, mentors, and coworkers have been immense sources of inspiration that have challenged me to grow as a person. I am now honored to call these people some of my closest friends. I thus recognize the futility in writing these acknowledgements – to properly give credit to the impact everyone has had on me is nothing short of impossible.

First and foremost, I would like to thank my Ph.D. supervisor, Dr. Samantha Gruenheid, whom I have had the privilege of training with for all these years. She generously took a chance on me when I was just starting out as an undergraduate and continued to supply me with opportunities to succeed throughout my graduate school career. Thank you for your constant support, patience, and mentorship. Above all else, thank you for constantly exemplifying what it means to truly be a scientist.

I would also like to thank my research advisory committee – Dr. Martin Richer, Dr. Michel Desjardins, and Dr. Heidi McBride – and all the other collaborators involved in this work. Thank you for your guidance and help on approaching this project from an interdisciplinary perspective.

I would also like to acknowledge all of my coworkers, past and present, whom I've worked with over the years. I always looked forward to coming into the lab to discuss life, go for drinks, try new foods, or to bond over failed experiments. I must thank Dr. Eugene Kang, who was not only my first mentor who taught me how to use a pipette, but also my first friend in the lab. Also, Dr. Natalie Giannakopoulou, who was always willing to drop everything to go get some coffee and listen in times of need. I also want to thank Lei Zhu and Christina Gavino for constantly

lending me a helping hand. To Dr. Ahmed Fahmy, Dr. Jorge Cueva-Vargas, and Camberly Hernandez – thank you for always being open to collaboration and having fun along the way. Finally, to the current graduate students of the Gruenheid lab – Brendan Cordeiro, Lindsay Burns, and Jessica Pei – thank you all for being amazing friends, sources of inspiration, and fantastic trivia partners. I never imagined we would be going through a pandemic together, but I could not imagine doing it with anyone else.

To my better half, Gabrielle Lavoie-Gregoire – thank you for always being my partner in crime and believing in me, no matter how many times I say I want to go back to school. I am also immensely grateful for all of my friends outside of academia, including Harsh Laul, who have all been an endless source of support and fun away from campus – thank you all.

Finally, I would like to thank my family: my sister Tabatha, my brother Scott, and especially my mother Helen Kavalieratos and my father Rick Cannon. You have not only believed in me at every step but pushed me to become everything I am. None of this would have been possible without you.

## CONTRIBUTION TO ORIGINAL KNOWLEDGE

1. Live Gram-negative, but not Gram-positive, bacterial infections are capable of inducing mitochondrial antigen presentation via the sorting nexin-9 dependent pathway in cells deficient in either PINK1 or Parkin.
2. *Pink1*<sup>-/-</sup> mice infected with the Gram-negative intestinal pathogen *Citrobacter rodentium* induces mitochondrial antigen presentation in splenic dendritic cells and subsequent expansion of anti-mitochondrial CD8<sup>+</sup> T cells.
3. This thesis provides the first evidence that *Pink1*<sup>-/-</sup> mice can experience PD-like phenotypes when exposed to an environmental trigger; repeated infection with *C. rodentium* induced the loss of tyrosine hydroxylase-positive axonal varicosities in the striatum and motor impairment that was reversed with L-DOPA treatment
4. The first 16s rRNA gene analysis comparing the intestinal microbiota between wild-type and *Pink1*<sup>-/-</sup> mice over the course of *C. rodentium* infection revealed no large-scale diversity or taxonomic shifts. Exceptionally, *Akkermansia muciniphila*, a microbe associated with anti-inflammatory responses, was observed to be higher in wild-type mice post infection.
5. This is the first work to compare the levels of short-chain fatty acids over the course of *C. rodentium* infection and to compare wild-type mice to *Pink1*<sup>-/-</sup> mice. Analysis showed that infection raised butyric acid levels in *Pink1*<sup>-/-</sup> mice and isobutyric acid levels in wild-type mice.

## CONTRIBUTION OF AUTHORS

The work presented in this thesis was published, or is in preparation for publication, as follows:

### Chapter 1:

Introduction and literature review

The literature review was written by TC and edited by SG.

### Chapter 2:

**D. Matheoud\***, **T. Cannon\***, A. Voisin, A.M. Penttinen, L. Ramet, A.M. Fahmy, C. Ducrot, A. Laplante, M.J. Bourque, L. Zhu, R. Cayrol, A. Le Campion, H.M. McBride\*\*, S. Gruenheid\*\*, L.E. Trudeau\*\*, and M. Desjardins\*\*, *Intestinal infection triggers Parkinson's disease-like symptoms in *Pink1*(-/-) mice*. Nature, 2019. **571**(7766): p. 565-569.

\* Co-first authors

\*\* Co-corresponding authors

DM and TC helped conceive and perform most experiments. AV, AMP and LR helped perform brain/neuron analyses and behavioural tests. CD, AL, MJB and LZ helped with the animals and some experiments. ALC performed flow cytometry analyses. HMM, SG, LET and MD conceived the experiments, analyzed the results and supervised the project. DM, TC, HMM, SG, LET and MD wrote the manuscript.

### Chapter 3:

**T. Cannon**, A. Sinha, L.E. Trudeau, C.F. Maurice, and S. Gruenheid, *Characterization of the intestinal microbiota during *Citrobacter rodentium* infection in a mouse model of infection-triggered Parkinson's disease*. Gut Microbes, 2020. **12**(1): p. 1-11.

TC and SG conceived and performed the experiments. TC and AS performed the data analysis.

TC and SG wrote the manuscript and generated the figures with contributions from AS, L-ET, and CFM. L-ET provided the mice for the experiments. SG supervised the project.

### Chapter 4:

Discussion and conclusion

The discussion and conclusion were written by TC and edited by SG.

## LIST OF ABBREVIATIONS

PD	Parkinson's disease
aSyn	$\alpha$ -Synuclein
TH	Tyrosine hydroxylase
DAT	Dopamine reuptake transporter
VTA	Ventral tegmental area
SNc	Substantia nigra pars compacta
MPTP	1-methyl-4-phenyl-1,2,3,6-tetrahydropyridine
LPS	Lipopolysaccharide
PINK1	PTEN-induced putative kinase 1
LRRK2	Leucin-rich repeat kinase 2
Snx9	Sorting nexin 9
MitAP	Mitochondrial antigen presentation
CNS	Central nervous system
BBB	Blood brain barrier
CSF	Cerebral spinal fluid
COMT	Catechol- <i>O</i> -methyl transferase
MAOB	Monoamine oxidase B
GI	Gastrointestinal
ENS	Enteric nervous system
M-cell	Microfold cell
Muc2	Mucin 2
SCFA	Short-chain fatty acid
GALT	Gut-associated lymphoid tissue
DC	Dendritic cell
Treg	Regulatory T cell
Ig	Immunoglobulin
ILC	Innate lymphoid cell
A/E	Attaching and effacing
EPEC	Enteropathogenic <i>Escherichia coli</i>

EHEC	Enterohemorrhagic <i>Escherichia coli</i>
T3SS	Type-3 secretion system
LEE	Locus of enterocyte effacement
Tir	Translocated intimin receptor
N-WASP	Neural Wiskott-Aldrich syndrome protein
ARP2/3	Actin-related protein 2/3
GB3	globotriaosylceramide
EspFu	<i>Escherichia coli</i> secreted protein F from prophage U
EspF	<i>Escherichia coli</i> secreted protein F
EspG	<i>Escherichia coli</i> secreted protein G
NleA	Non-LEE encoded effector A
Map	Mitochondria-associated protein
Rspo2	R-spondin 2
PRR	Pattern recognition receptor
TLR	Toll-like receptor
MyD88	Myeloid differentiation primary response 88
NF- $\kappa$ B	Nuclear factor $\kappa$ B
RAG2	Recombinant activating gene 2
IBD	Inflammatory bowel disease
SIBO	Small intestinal bacterial overgrowth
MHC	Major histocompatibility complex
HSV-gB	Herpes simplex virus glycoprotein B
OGDH	Oxoglutarate dehydrogenase
HK	Heat killed
GzB	Granzyme B
IL	Interleukin
DN	Dopaminergic neurons
FBS	Fetal bovine serum
PFA	Paraformaldehyde
PBS	Phosphate-buffered saline

CD	Cluster of differentiation
FACS	Fluorescently activated cell sorting
HC	Hematopoietic cells
IFN	Interferon
TGF	Transforming growth factor
TNF	Tumor necrosis factor
H&E	Hematoxylin and eosin
Ctl	Control
WT	Wildtype
ASV	Amplicon sequence variant
PCoA	Principal coordinate analysis
ANCOM	Analysis of the composition of the microbiota
MDV	Mitochondrial-derived vesicles
IRF3	Interferon regulatory factor 3
TBK1	TANK-binding kinase 1
STING	Stimulator of interferon genes
cGAS	Cyclic GMP/AMP synthase
UPR	Unfolded protein response
PDC	Pyruvate dehydrogenase complex



## **PREFACE TO CHAPTER 1**

The intestinal tract and the brain are intertwined in their physiology, the two systems regulating each other to maintain homeostasis in what has been coined the gut-brain axis. Over the years it has become clear that a dysregulation in either system could influence the other, suggesting that neurological diseases may be initiated in the gut. Parkinson's disease, although characterized as a neurological movement disorder, is commonly associated with gastrointestinal dysfunction. This thesis aims to explore the molecular mechanisms underlying the gut-brain axis in Parkinson's disease. This first chapter provides a literature review of the field to date and is divided into three sections. The first section focuses on Parkinson's disease and summarizes the current proposed etiological mechanisms, clinical information, and the current mouse models used to study the disease. The second section discusses the gastrointestinal system, describing the cellular and molecular pathways necessary for maintaining homeostasis and the impact of attaching/effacing intestinal pathogens. Finally, the last section discusses the current models and recently published data linking intestinal dysfunction to Parkinson's disease.

## **CHAPTER 1: Introduction and literature review**

### **1. Parkinson's disease**

Parkinson's disease (PD) is a complex and progressive neurodegenerative disorder first described over 200 years ago [1]. It is currently the second most common neurodegenerative disease worldwide affecting 0.3% of the general population and as high as 4% in people over the age of 65 [2, 3]. Over 90% of PD cases are idiopathic in nature with no known cause and motor impairments appearing later in life [4]. The remaining 10% of cases are familial forms of PD that are caused by inheriting monogenic mutations in one of several PD-related genes. Familial PD is also sometimes referred to as early-onset PD as clinical symptoms generally manifest before the age of 50 [5]. PD is characterized by motor deficits that arise due to the specific destruction of dopamine-producing (dopaminergic) neurons [1]. The exact cause of neurodegeneration remains unknown. PD is also accompanied by an array of non-motor symptoms that can precede motor impairment by over a decade in patients, implicating other physiological systems in disease progression. The clinical complexity of PD is only worsened by the fact that the disease-defining motor symptoms only arise once 70-80% of all dopaminergic neurons have been destroyed [6], leaving preventative measures difficult to implement. Currently there is no cure for PD with most therapeutic interventions focusing mainly on symptom management.

#### **1.1 – Pathophysiology and clinical features**

Which events are needed to initiate neurodegeneration remains a contentious area of research. Several hypotheses have been proposed, including genetic mutations that alter cellular physiology [4, 7, 8], the seeding of spreadable misfolded proteins in molecules such as  $\alpha$ -synuclein (aSyn) [9], and the development of immune pathology [10]. It is unlikely that there is a single unifying mechanism that can be applied to all PD patients, with the possible the exception of monogenic familial forms of the disease. Nonetheless, the outcome of such events is always the same – the significant destruction of dopaminergic neurons. The progression of PD pathology is gradual, and it takes years for the neurological damage to accumulate and manifest as a clinical motor deficit. Furthermore, it is now known that the autonomic nervous system is also affected in PD patients, leading to the development of non-motor systems in peripheral tissues [11].

### **1.1.1 – Dopaminergic neurodegeneration**

Dopaminergic neurons are primarily responsible for the secretion of the neurotransmitter dopamine [12, 13]. Dopamine itself is unable to cross the blood brain barrier and is synthesized locally by neurons via modification of the amino acid tyrosine [14, 15]. Tyrosine hydroxylase (TH) is initially used to convert tyrosine into L-DOPA, which then undergoes decarboxylation into dopamine [14-16]. As such, staining for the enzyme TH is commonly used for the identification of dopaminergic neurons in brain tissue sections [13, 17, 18]. TH levels themselves have been shown to sometimes decrease with time in both elderly monkeys and humans and believed to be cause of age-related decline in dopaminergic function [19, 20]. Once secreted, dopamine can act on target cells via a G-protein coupled receptor that functions by modulating ion transporters and adenylyl cyclase, which are necessary for both the propagation of the action potential and cell

survival/protein synthesis [21-26]. Dopamine receptors are largely classified into two subgroups: D1, which activates adenylyl cyclase, and D2, which inhibits [25, 27]. Both receptors are involved in PD and targeted by clinical interventions, but researchers have noted that knocking out D2 receptors in murine models resulted in decreased movement akin to PD-like pathology [28], although this has been difficult to replicate [29]. Secreted dopamine within the synaptic space can be scavenged by dopaminergic neurons via a dopamine reuptake transporter (DAT), a monoamine transporter that functions via coupling to sodium ion import [30, 31]. Due to the possibility that TH may be downregulated with age, DAT staining is routinely used to counterstain dopaminergic neurons [13].

Anatomically, dopaminergic neurons in mammalian brains can be primarily found in the retrorubral field, the ventral tegmental area (VTA), and the substantia nigra pars compacta (SNc) [32, 33]. PD results in the specific destruction of dopaminergic neurons within the SNc [34, 35]. The exact mechanism leading to their unique susceptibility remains unknown. The axons of these dopaminergic neurons originate at the cell soma within the SNc but extend outwards and becomes highly arborized to form synapses within the striatum [13]. One study noted that virtually any random point chosen within the striatum will be within 0.5  $\mu\text{m}$  of at least one dopaminergic neuron axon terminal [36]. This connection to the striatum is called the nigrostriatal pathway and is largely responsible for fine motor control and movement coordination [3, 37]. The number of axon terminals from a single SNc neuron are orders of magnitude larger than other dopaminergic neurons, which is speculated to be a reason for their unique susceptibility [35]. The energy demand required to maintain a successful action potential along a dopaminergic neuron axon was determined to follow a power law, growing exponentially with both the number of branches and

total surface area [35], providing a potential mechanism as to how these neurons may be vulnerable from an energetic standpoint

Although the mechanism by which SNc dopaminergic neurons die in PD is unknown, a prominent feature of aging neurodegenerative diseases is the observation that axons degenerate first, moving in a retrograde fashion from the axon terminal towards the cell soma [38]. This phenomenon, coined “dying-back”, is also observed in PD [39-41]. Recent evidence in both murine models and human studies suggests that axonal degeneration can arise before symptom onset [42]. There have been several proposed mechanisms for the axonal degradation of SNc dopaminergic neurons that will be explored in the following sections [38], including protein misfolding [43], over-reliance on mitochondrial output [33], and inflammation [44].

### **1.1.2 – $\alpha$ -Synuclein and Lewy Pathology**

The aSyn protein is 140 amino acids long and, although ubiquitous, is more abundantly found in neural tissue [45]. The native structure of aSyn *in vivo* is disputed, although it is now believed to exist under homeostatic conditions in an unstructured monomeric form [46]. It is most commonly found surrounding pre-synaptic vesicles but can also be found in most subcellular compartments [47]. No definitive function for aSyn has been identified yet [48], although knocking out the gene in mice led to decreased striatal dopamine levels and altered dopamine release, suggesting it might play a role in synaptic vesicle release [49].

Pathologically, aSyn can assemble into one of two highly ordered aggregates depending on their location: Lewy neurites in cellular processes, and globular structures called Lewy bodies in the main cell soma [48]. Recent evidence has found that the aSyn oligomers that are found

earlier in disease are actually more toxic to TH<sup>+</sup> neurons than the end-stage fibrils both *in vivo* in rats and *in vitro* in mammalian neuronal cultures [50, 51]. The end-stage fibrillar forms of aSyn have been noted to have prion like ability on monomeric aSyn, and, notably, can transmit cell to cell [51]. *In vivo* analysis in mice revealed that healthy neuronal stem cells transplanted into the hippocampus of aSyn overexpressing mice lead to the propagation of aSyn fibrils into transplanted cells [52]. Further, in an *in vitro* human dopaminergic cell model, human aSyn fibrils were shown to cause the formation of novel aSyn oligomers, which induced cellular damage and apoptosis, causing the release of aSyn fibrils which were subsequently taken up and induced novel fibril formation in surrounding cells [53]. Pre-formed aSyn fibrils were also observed to spread in a retrograde fashion from striatal neurons to SNc dopaminergic neurons in wild-type C57BL/6/C3H mice, which is believed to be supportive of the “dying back” hypothesis [54].

A growing body of literature has now also highlighted how aSyn preformed fibrils injected into the gut of mice can induce PD-like pathology. Indeed, aSyn preformed fibrils were able to propagate via the vagus nerve and result in SNc dopaminergic neuron death in aged C57BL/6 mice [55, 56]. Supporting this notion, Braak and associates have staged the propagation of Lewy pathology in post-mortem human brains from sporadic PD patients, showing that aggregated aSyn originates from the olfactory bulb and dorsal motor nucleus of the vagus nerve, spreads to the limbic system and SNc, and eventually overtakes the neocortical areas of the brain [9, 57]. The observation that Lewy pathology seems to spread from the nasal olfactory bulb and from the gut via the vagus nerve, both of which are barriers exposed to the environment, has led to the hypothesis that external factors may seed initial aSyn misfolding [58, 59]. A recent study has noted that the curli protein from *Escherichia coli* can exacerbate the formation of Lewy pathology within the brain of aSyn overexpressing mice [60].

From a genetic standpoint, overexpression via multiplication of the aSyn gene *SNCA*, loss of genetic regulation, or mutations that promote aSyn misfolding are sufficient to cause monogenic familial PD [48, 61]. Post-translational modifications are also believed to instigate aSyn misfolding, as phosphorylated forms of aSyn are also commonly found in Lewy bodies in both human patients and mouse models. The most common post-translational modification observed in Lewy bodies (>90%) is phosphorylation at serine residue 129 [62]. Oxidation of tyrosine residues has also been shown to promote the accumulation of toxic oligomeric forms of aSyn [63], which is believed to be one mechanism by which the high mitochondrial demand required by dopaminergic SNc neurons might initiate pathology.

Despite Lewy pathology being long regarded as a hallmark of PD, as it appears in both idiopathic and familial forms of the disease, it is possible for PD pathology to develop and progress in its absence. A meta-analysis of monogenic familial PD cases caused by the genes *PINK1*, *PRKN*, or *LRRK2* has revealed that SNc dopaminergic neuronal death occurs without the development of Lewy pathology in more cases than not [64]. Further, it has also been observed that, in some cases, clinical symptoms of PD can worsen without the existing Lewy pathology worsening [65]. This evidence has put into question the necessity and causality of Lewy pathology in PD and remains a debated area of research.

### **1.1.3 – Mitochondrial dysfunction**

Mitochondria are incredibly bioactive organelles that can undergo oxidative respiration to generate cellular energy. As a result, cells with high energy demand, such as SNc dopaminergic neurons, are particularly susceptible to mitochondrial dysfunction [33]. A link between

dysfunctional mitochondrial respiration and PD was first established when exposure to 1-methyl-4-phenyl-1,2,3,6-tetrahydropyridine (MPTP), a compound that can disrupt the electron transport chain via inhibition of complex I, led to dopaminergic neurodegeneration in humans [66]. MPTP becomes MPP<sup>+</sup> when oxidized, which is able to be taken up by the DAT receptor on SNc dopaminergic neurons [67], explaining its selective toxicity. Since then, a number of studies have shown that other complex I inhibitors, such as the pesticide rotenone, can also lead to similar SNc neurodegeneration and the development of clinical PD symptoms in humans and murine models [68-70]. Inside the cell this class of chemicals cause a number of additional mitochondria-related issues such as the increased release of reactive oxygen species [71], which in turn can oxidize cytoplasmic molecules like  $\alpha$ Syn and seed misfolding [63].

Genetic analyses have linked loss-of-function autosomal recessive mutations in the genes *PINK1* and *PRKN* to familial monogenic forms of PD [72-75]. The *PINK1* gene generates the protein PTEN-induced putative kinase 1 (PINK1), a kinase that is imported into mitochondria via translocon proteins where it is degraded by proteases under homeostatic conditions [76]. However, when a mitochondrion becomes dysfunctional and loses its membrane potential, PINK1 is no longer fully imported and becomes stable on the outer mitochondrial membrane where it is able to phosphorylate its cytoplasmic substrates [76]. The *PRKN* gene generates the protein Parkin, an E3 ubiquitin ligase that is phosphorylated and activated by stabilized PINK1. Parkin is able to ubiquitinate both adaptor and mitochondrial proteins, which eventually leads to the recruitment of membranes from the endoplasmic reticulum that encapsulates the dysfunctional mitochondria and targets them for lysosomal degradation [73, 77]. This process, known as mitophagy, is a routine function of cellular turnover orchestrated by PINK1 and Parkin, and loss of function mutations in either of them leads to an accumulation of dysfunctional mitochondria within the cell [78]. As



previously mentioned, the significant energy demand of SNc dopaminergic neurons is believed to make them particularly susceptible to dysfunctional mitochondrial buildup.

However, mitochondrial dysfunction as a trigger for neurodegeneration, similar to other PD hypotheses, also remains disputed. In particular, the extreme nature of chemicals like MPP<sup>+</sup> and their propensity to be taken up uniquely by dopaminergic neurons makes it arbitrary that they would cause PD-like pathology. Further, there is a distinct lack of literature demonstrating direct causality between defective mitophagy and neurodegeneration. In *Drosophila* models, loss of either the pink1 or parkin protein resulted in muscular apoptosis and mitochondrial morphological defects, but no significant dopaminergic neurodegeneration [79]. Similarly, *Pink1*<sup>-/-</sup> mice experience a buildup of dysfunctional mitochondria with lowered energy output, but fail to show signs of SNc dopaminergic neurodegeneration [80]. This was also confirmed in a separate study which showed that *Pink1*<sup>-/-</sup> mice did not display any classic PD-like neurodegeneration in the SNc or standard clinical phenotypes but did experience some loss of olfactory sensation and hind paw discoordination [81]. This body of work suggested that *Pink1*<sup>-/-</sup> mice are not a robust model for PD. *Prkn*<sup>-/-</sup> mice were also determined to not be a sufficient model for PD, as they experienced no loss of secreted dopamine in striatal tissue and no significant motor impairment [82].

Researchers have noted that mitophagy can occur in the absence of PINK1 in SNc dopaminergic neurons in mice via a PINK1-independent pathway [83], suggesting that PINK1-mediated mitophagy may not be vital for cellular homeostasis. In this regard, the usefulness of PINK1 and Parkin deficient mice as models of PD have been put into question; however, it remains to be determined if this also translates to humans. New research has demonstrated a novel role for PINK1 and Parkin in the repression of mitochondrial antigen presentation (MitAP) on MHC I in response to bacterial lipopolysaccharide (LPS) [84]. Here it was discovered *in vitro* that RAW

264.7 cells with inherently low levels of Parkin or primary splenic dendritic cells from *Pink1*<sup>-/-</sup> mice were susceptible to MitAP following LPS stimulation. This pathway resulted in the release of unique mitochondrial derived vesicles in a sorting-nexin 9 (Snx9) dependent manner that carried mitochondrial cargo for degradation and presentation on MHC I. This research has suggested a novel immunological function for PINK1 and Parkin with regards to repressing anti-mitochondrial autoimmunity, and also suggests *Pink1* and *PRKN* related PD may be influenced by environmental factors such as Gram-negative infection.

#### **1.1.4 – Immunological evidence**

The central nervous system (CNS) is largely considered to be an immune-privileged site [85]. The blood brain barrier (BBB) – formed by endothelial cells, pericytes, and astrocytes – largely prevents peripheral immune cell infiltration into the CNS [85, 86]. Within the brain, no major lymphatic system is present to facilitate immune invasion [85-87]. Recently a major lymphatic vessel was discovered near the skull surface in the brain dura; however, its function in neuroimmunology remains largely unknown [88]. Cerebral spinal fluid (CSF) circulates throughout the brain ventricles and spinal cord and is the collection of filtered blood from capillaries within these areas [89]. CSF does filter through to the cervical lymph nodes at the base of the skull, however it's been noted that CSF contains no major antigen presenting cells and only a subset of memory CD4<sup>+</sup> T cells [90]. The protective meningeal layers of the brain do contain most immune cell populations, but how they are trafficked there remains unknown and they do not enter the main brain parenchyma [91]. Within the CNS, the most abundant immune cell present are microglia, a specialized type of tissue resident macrophage [92]. Under homeostatic conditions

microglia prune synapses and engulf debris but are also capable of responding to infectious agents and presenting antigens on MHC II [92]. Notably, the SNc and striatum are where microglia are most abundant [93].

Neuroinflammation is a key signature of PD pathology, with increased levels of the cytokines IL-1 $\beta$ , TNF $\alpha$ , TGF- $\beta$ , IFN $\gamma$ , and IL-6 having been found in post-mortem PD patients' brains, CSF, and nigrostriatal regions [94, 95]. These inflammatory signatures are also observed systemically in serum analyses, notably with IL-6 and TGF- $\beta$  [96]. Inflammation is known to weaken the BBB and allow larger molecules and peripheral immune cells to infiltrate the CNS. Indeed, intravenous injection of LPS to induce systemic inflammation is widely used as a model to induce BBB permeability in mice, as it results in endothelial destruction and disruption of astrocytes [97, 98]. Cerebral endothelial cells also express higher levels of IL-6 and TNF $\alpha$  receptors that induce endothelial activation and adhesion molecule expression [99, 100], making the CNS particularly vulnerable under systemic inflammatory conditions.

Increased recruitment and activation of microglia (microgliosis) into the nigrostriatal region of the brain is an early hallmark of PD pathogenesis [101, 102]. It is now widely accepted that microgliosis is the source of the observed pro-inflammatory cytokines and suggests that microglia may function as an early instigator of disease progression. Murine studies have shown that injection of LPS into the nigrostriatal area that acted on TLR4 uniquely found on microglia was sufficient to induce local microgliosis, secretion of pro-inflammatory cytokines, and eventual dopaminergic neurodegeneration [103, 104]. In both mouse and human primary microglia cultures, aSyn was shown to activate microglia via TLR1/2 and shift them towards a pro-inflammatory phenotype [105, 106], providing evidence that aSyn-mediated neurodegeneration may also be exacerbated by immunological factors. Microglia, being professional antigen presenting cells, may

also act as a key component for the activation of the adaptive immune response in PD [92]. Indeed, the gene responsible for the MHC II molecule HLA-DRA that is uniquely expressed in microglia was recently identified as a risk factor for PD [107].

The adaptive immune response is also believed to be a key player in PD pathogenesis. Both CD4<sup>+</sup> and CD8<sup>+</sup> T cells, but not B cells or NK cells, have been identified in the SNc of post-mortem PD patient brains [108]. Anatomically, these cells were located close to dopaminergic neurons and blood vessels, indicating they likely trafficked there across the BBB [108]. The exact T cell responses that dominate in PD remains elusive. In humans, an increase in activated Treg cells is associated with PD cognitive decline [109], although this has been hard to validate [110] and the opposite is found in mouse models [111]. In mice, treatment with MPTP induces a dominant Th17 response, and the cytokine IL-17 alone is sufficient to exacerbate neurodegeneration [112]. Th17 T cells have also been shown to be able to kill human neuronal cultures *in vitro* [113]. The exact antigens that can illicit these T cell responses is unknown and remains a debated area of research. A recent study of peripheral blood from PD patients found the presence of autoreactive CD4<sup>+</sup> and CD8<sup>+</sup> T cells that could respond to either soluble monomeric or fibrillar forms of  $\alpha$ Syn, suggesting autoimmune mechanisms in PD [114].

The observation of CD8<sup>+</sup> T cells in the SNc of PD patients is particularly striking as it provides a potential immunological mechanism by which dopaminergic neurons can be destroyed. In post-mortem brains from PD patients, dopaminergic neurons in the substantia nigra were observed to express higher levels of MHC I molecules than any other examined neuron group [115]. This work, in corroboration with previous studies, also found cytotoxic CD8<sup>+</sup> T cells surrounding the dopaminergic neurons. Further *in vitro* analysis of dopaminergic neurons cultured from C57BL/6 mice showed upregulated surface expression of MHC I following treatment with

IFN $\gamma$  or pre-conditioned media from microglia treated with LPS, linking microgliosis and susceptibility to CD8<sup>+</sup> T cell destruction [115].

Together this information has led to the notion that PD pathogenesis may have immunological origins. A major difficulty in establishing causality between the immune system and PD initiation, however, is timing: once a patient has been diagnosed with PD they are already in the late stages of dopaminergic neurodegeneration. It is thus difficult to determine whether the inflammation observed is causal to SNc dopaminergic neuronal death, or a consequence. The observation of microgliosis early in disease development suggests a causal role, but this remains to be formally proven. A major limitation to the models thus far is the necessity of a triggering event for the initial source of inflammation, such as LPS directly injected into the SNc, or MPTP treatment instigating neuronal death directly. What this event may be – if one is even needed – in human PD cases is unknown.

### **1.1.5 – Motor symptoms**

Clinical onset of motor symptoms occurs in PD patients once 70-80% of SNc dopaminergic neurons are lost [6]. The destruction of the nigrostriatal pathway results in loss of fine motor movement and coordination, leading to the motor symptoms of the disease [3]. There are four characteristic motor symptoms of PD: tremors, rigidity, bradykinesia, and postural instability [116]. Recently, two more symptoms, freezing gait and parkinsonian gait, are also being recognized as hallmark PD symptoms [116]. Despite the limited number of conventional motor symptoms, diagnosis of PD remains complicated since the course of symptom onset, severity of symptoms, and the order in which they appear can vary widely between patients.

Bradykinesia is generally the symptom that manifests first and is considered to be essential – a diagnosis of PD is immediately put into question if a patient presents without bradykinesia [117]. Bradykinesia presents as a delayed initiation of voluntary actions with the eventual reduction in overall velocity and frequency of actions [117, 118]. From a pathophysiological perspective, the mechanism behind bradykinesia is unknown; however, studies have noted strong correlations between loss of SNc dopaminergic neuron density and bradykinesia severity, regardless of PD diagnosis [119]. In general, a pre-requisite for a PD diagnosis is the development of bradykinesia and at least one other PD motor symptom [117].

The remaining motor symptoms – tremors, rigidity, and postural instability – are all associated with increased susceptibility to PD prior to diagnosis [120]. Tremors are the most recognizable symptom of PD but are not present in all patients. Tremors have been reported to be present in up to 70% of PD patients at time of diagnosis, and up to 75% of PD patients experience tremors at one point in their disease [121]. PD tremors are characterized as resting tremors as they are continuous even while avoiding voluntary movement, differentiating them from active tremors that are seen in other neurological conditions [116]. Usually, tremors are unilateral and affect only distal areas such as the hands, although cases of postural tremors also exist in rare cases [122]. Recent evidence has highlighted that tremor symptoms correlate with a loss of a specific population of dopaminergic neurons within the retrorubral field [123]. Rigidity presents as increased muscular stiffness in both proximal and distal body parts. It is generally accompanied by the “cogwheel” appearance in which forced movement of the limb is stuttered [124]. Severe rigidity, notably within the trunk, can lead to the hunched posture associated with parkinsonian gait and postural instability [125]. Postural instability appears later in disease development and its severity is influenced by a number of motor and non-motor symptoms. Postural instability is

caused by a loss of reflexes when challenged with sudden changes in movement and, as a result, is the major cause of falls [126]. Freezing gait is characterized by the sudden and transient inability to move and is considered to be one of the most debilitating motor symptoms of PD [127]. Freezing gait appears in approximately 40-50% of patients and is also affected by the severity of rigidity, bradykinesia, and postural instability [128].

### **1.1.6 – Non-motor symptoms**

The non-motor symptoms of PD are often overlooked by the general public but have immense implications on the lives of PD patients. Indeed, non-motor symptoms are often reported to be significant causes of distress compared to motor symptoms that can be managed with medication. Contrary to motor symptoms that only appear after most dopaminergic neurodegeneration has occurred, non-motor symptoms can appear as early as a decade prior to diagnosis [116, 129]. Non-motor symptoms include psychiatric symptoms, sensory symptoms, and autonomic dysfunction [130].

Psychiatric symptoms of PD can include depression, loss of organizational abilities, and hallucinations, all of which can occur either before or after diagnosis [130]. Hallucinations at early stages are transient and non-threatening [131]. As disease progression continues, PD patients can develop more severe dementia and cognitive impairment [131]. Hallucination can occur in up to 40% of patients but are mostly seen in late-stage patients [131]. Depression is also a common side effect of PD, having been reported in one third of patients [132]. Sensory symptoms present as a loss of smell and generalized muscle achiness [133]. Loss of smell is a particularly striking symptom as it appears in over 80% of patients and is commonly noted to occur prior to diagnosis

[134]. The pathological staging done by Braak and associates had shown that aSyn pathology begins in the olfactory bulb and dorsal motor nucleus vagus nerve [57], suggesting a potential mechanism for the early loss of smell; however, this still remains to be formally proven.

Autonomic dysfunction has long been regarded as an early indicator of PD pathology and includes dysregulation of the sympathetic, parasympathetic, and enteric nervous systems [135]. The mechanism underlying autonomic dysfunction remains unknown to date. Orthostatic hypotension – a drop in blood pressure upon standing – is commonly observed in PD patients and contributes to postural instability [136]. Notably, up to 90% of PD patients experience gastrointestinal issues including decreased gastric motility and constipation [137]. The gastrointestinal symptom of constipation can occur over a decade prior to diagnosis [137]. The enteric nervous system's connection with the vagus nerve has been postulated to play a role in the early stages of aSyn pathology observed by Braak and associates [57]. The early and prominent nature of gastrointestinal symptoms has led researchers to believe that the gut may play a role in initiating PD pathogenesis.

## **1.2 – Risk Factors**

Upon discovery that environmental factors such as MPTP exposure could induce pathology [138], epidemiological evidence had originally supported the notion that PD was a classical non-genetic disorder [139]. However, with the development of modern molecular genetic tools, a number of genetic loci have since been identified that influence PD outcome. PD is now recognized as a complex disorder with influences from both environmental and genetic factors. Monogenic early-onset forms of PD are still considered to be entirely influenced by the inheritance of a single



mutated gene with near 100% penetrance [4, 139]. In contrast, in idiopathic PD, single nucleotide polymorphisms in an array of genetic loci are only weakly associated with disease outcome, and idiopathic PD is considered to be primarily influenced by environmental factors [6].

### **1.2.1 – *PINK1***

Loss of function *PINK1* mutations are associated with autosomal recessive, early-onset, monogenic forms of PD [140]. A number of studies had suggested that acquiring heterozygous *PINK1* mutations are also associated with increased risk of PD [141-143]; however, a recent meta-analysis found this to not be the case [143]. The PINK1 protein consists of a mitochondrial targeting sequence, a large kinase domain, and a C-terminal regulatory domain [144]. Most mutations found were either missense or nonsense (over 60 identified to date), but a few rare cases of entire exon deletions have also been noted [4]. Observed PD-causing mutations can be found in all exons, but approximately two thirds of the mutations are located in the kinase domain [4, 145-148]. Over 40% of patients with *PINK1*-related PD have mutations that cause truncation of the protein, the most frequent mutation being Q456X in exon seven [4, 143].

### **1.2.2 – *PRKN***

The *PRKN* gene was the first to be associated with autosomal recessive PD [4]. *PRKN* mutations have been shown to cause PD pathology very early in life, usually affecting patients before the age of 40, but can also affect those as young as under 20 in what is called juvenile PD [149, 150]. Patients with *PRKN* associated PD showed loss of SNc dopaminergic neurons in the

absence of Lewy pathology [151, 152], although exceptions have been found [153]. The *PRKN* gene is the second largest known gene in the human genome and spans 12 exons encoding for a ubiquitin-like domain, three really-interesting-new-gene domains, and an in-between-ring domain [154]. The latter four domains are responsible for interaction with ubiquitination machinery necessary for carrying out the ubiquitin ligase activity of Parkin [154]. Over 200 published mutations have been identified within the *PRKN* gene including single nucleotide polymorphisms, single nucleotide deletions, and entire exon deletions [155]. Over 50% of the mutations observed occur in exons 1-4 and affect the ubiquitin-like domain that is necessary for activation of the protein [155]. Contrary to *PINK1*, *PRKN* heterozygous mutations have been associated with increased PD risk [142, 156, 157].

### 1.2.3 – *SNCA*

The *SNCA* gene, encoding for the protein aSyn, is associated with both familial and sporadic forms of PD and the key component of Lewy pathology. Mutations in *SNCA* result in autosomal dominant PD. To date only 3 missense mutations have been associated to PD [158], the most prominent mutation being A53T that results in an 85% penetrance of the disease [7, 159]. Although aSyn exists under homeostatic conditions in an unstructured monomeric form [46], it can coil into a helical structure upon interaction with a lipid membrane [160]; notably, the point mutations associated with PD disrupt this function and promote a  $\beta$ -sheet structure, favouring aSyn aggregation and fibril formation. Fibrils can then promote the misfolding of non-mutated aSyn, giving rise to the dominant nature of aSyn mutations [161]. Duplication of the *SNCA* gene is also associated with increased risk of PD with a 33% penetrance [162], and a correlation has been

drawn between an increased number of *SNCA* gene copies and more rapid pathological progression [163].

#### **1.2.4 – Environmental factors**

Research into the effect of environmental factors on PD outcome has, to date, been largely correlative, and drawing causative conclusions remains a challenge. A 2016 meta-analysis of potential PD-causing environmental factors noted significant heterogeneity in the data, potential bias, and cases of reverse causation [164]. However, certain environmental factors were noted to strongly correlate with PD, including exposure to pesticides, hydrocarbons, rural living, and energy intake [164]. Two pesticides were strongly correlated with PD onset: rotenone, a mitochondrial complex I inhibitor, and paraquat, a superoxide producer that can cause oxidative damage to mitochondria [164-167]. Both pesticides were shown to increase the odds of developing PD by over two-fold [164, 167]. Rural living and farming are both also risk factors for PD [167]; however, these are considered to be a consequence of increased pesticide exposure in crops. Hydrocarbon exposure was shown to increase the odds of developing PD by over 30%, the most significant being exposure to carbon tetrachloride [168]. Increased food intake was weakly associated with increased PD risk; notably, subsequent analysis of each individual major macronutrient showed so significant increase in PD risk [169]. Medically, head injuries that result in loss of consciousness is associated with increased PD risk [170]; damage to the CNS is postulated to increase neuroinflammation and instigate PD pathology, although this remains to be proven [171]. Both constipation and depression are also strongly associated with PD, although these are now more recognized as prodromal signs of PD rather than risk factors [164, 172].

Smoking and exercise are both observed to be protective of PD [173, 174]. Nicotine is considered to be neuroprotective [175], although the extent to which smoking is protective of PD was likely exaggerated due to small-scale study bias [164]. Exercise is believed to be protective by increasing blood uric acid levels, which is also shown correlate inversely with PD [174].

### **1.2.5 – Infection**

There remains much debate about whether a link between infection and PD exists. The notion first came to be when there was a surge of encephalitic parkinsonism (cerebral inflammation presenting with Parkinson's disease-like symptoms) cases following the 1918 H1N1 Spanish influenza pandemic [176, 177]. Indeed, patients at this time were observed to experience cognitive decline, upper limb rigidity, and tremors [178]. Epidemiological evidence had shown that people born during the pandemic had up to a three-fold increased risk for PD [179]. The H1N1 virus is known to be neurotropic in humans, suggesting the virus may have either directly, or indirectly via induction of inflammatory responses, damaged SNc dopaminergic neurons [180]. Follow-up work in macaques showed that the H1N1 Spanish flu did not infect CNS tissue, but did induce cytokine profiles necessary for microgliosis [181]. There have also been theories that an infection could induce immunological sequelae within a system [178], meaning that inflammation could persist even if the infectious agent is no longer present, akin to lasting CNS inflammation that is observed in MPTP models once MPTP is removed [182]. These theories remain controversial and confounding factors are difficult to delineate – in the case of H1N1 Spanish flu, there was also a rise in the use of rotenone in farming at the time [178].

More recently, a number of studies have begun highlighting correlations between various infections and increased PD risk [183]. One of the most prominent findings is that gastric infection with *Helicobacter pylori* is associated with increased risk of PD [184]. One study noted that seropositivity to *H. pylori* was five times more likely in PD patients compared to control patients [185]. Notably, another study found that eradication of *H. pylori* in patients did not ameliorate their odds, suggesting that *H. pylori* does not need to be present for disease onset [184]. While some studies have noted that *H. pylori* eradication improved motor symptoms and clinical outcomes [186], more recent and thorough analyses determined this to not be true [187]. Viral infection with hepatitis C has also been associated with increased PD risk [183]. Less is known about the connection between hepatitis C and PD, but it is postulated that the increased interferon responses associated with infection may induce microgliosis in the CNS [188]. Fungal *Malassezia* infections and bacterial-causing pneumonia are associated with PD; however, these infections may be a result of comorbidities associated with PD [183]. Autonomic dysfunction of sebum production in PD may increase *Malassezia* infection, and a decreased ability to swallow effectively may increase risk of pneumonia [183].

### **1.3 – Clinical interventions**

The lack of a definitive and unifying pathophysiological mechanism for PD has led to an inability to develop preventative measures for the disease. Destruction of SNc dopaminergic neurons, however, remains consistent across PD patients. As a result, most current medications aim to limit PD symptoms via modulation of an aspect of the dopamine pathway [189]. Administration of L-DOPA, a precursor to dopamine that is still able to cross the BBB, is usually

one of the first treatments given to PD patients and acts by simply increasing the amount of dopamine available in the CNS [189, 190]. The conversion of L-DOPA to dopamine is irreversible and dopamine itself is unable to cross the BBB; therefore, L-DOPA is administered in conjunction with Carbidopa, an inhibitor of the L-DOPA decarboxylating enzyme that acts peripherally and increases the amount of L-DOPA that can cross the BBB [191]. One study has shown that those on L-DOPA retain persistent mobility improvements seven years after beginning treatment and over 92% of study participants continued to use L-DOPA by the end compared to patients who received other treatments like dopamine receptor agonists (50%) [192].

L-DOPA does become less effective as degeneration of the nigrostriatal region progresses. Increasing L-DOPA dosage is an option but is commonly accompanied by dyskinesia, which is the involuntary erratic movement of the body [193]. In these cases, lowered doses of L-DOPA can be combined with other treatments [189]. Dopamine receptor agonists are commonly used to supplement L-DOPA and function by directly activating D1 and D2 receptors, bypassing the need for dopamine [194]. While useful as a supplementation, dopamine receptor agonists used in high doses can cause impulse control disorders such as excessive spending and gambling in up to 40% of patients, leading to doctors prescribing it sparingly [195]. Under homeostatic conditions dopamine is degraded by catechol-*O*-methyl transferases (COMT) and monoamine oxidase B (MAOB) [196]. These two enzymes are also pharmacological targets used in PD treatments to prolong the effects of available dopamine [196]. COMT and MAOB inhibitors are routinely administered in conjunction with L-DOPA in order to minimize the dose of L-DOPA needed and prolong its effects [189, 196].

As PD symptoms worsen, surgical options for deep brain stimulation are available. Deep brain stimulation involves the implantation of wires in the subthalamic nucleus that are able to

send electrical impulses to mediate the downstream neural networks that are impacted by nigrostriatal degeneration [197]. When used in combination with L-DOPA, deep brain stimulation was shown to significantly increase motor performance [198]. The combination of effectiveness with L-DOPA makes deep brain stimulation a potential treatment avenue if the patient has already responded positively to L-DOPA [189].

## **1.4 – Murine models of Parkinson’s disease**

The complex nature of PD has made it difficult to successfully recapitulate all aspects of the disease in one unified model. Work in mice has largely involved two major strategies to study PD: the use of neurotoxic chemicals, and genetic models. Neurotoxic chemicals are useful for studying the end-stage of PD as they tend to destroy a significant portion of SNc dopaminergic neurons in mice but fail to completely recapitulate the earlier stages of the disease. For example, while useful to research motor impairments or mechanisms of dopaminergic neuronal cell death, these models fail to address the effects of prodromal symptoms, non-motor symptoms, Lewy pathology, or genetics on PD progression. Creation of several genetically-modified mouse lines has allowed further research into the influence of genetic aspects on PD; however, these have shown to be limited by their inability to recapitulate all late-stage manifestations of PD including motor symptoms, Lewy pathology, and significant SNc dopaminergic neurodegeneration.

### **1.4.1 – MPTP model**

The MPTP murine model has become one of the most widely used in the field to investigate PD pathology. Administration of MPTP is done intraperitoneally as a bolus in multiple doses over time where it is able to enter the bloodstream and cross the BBB [199]. Once in the CNS, MPTP is oxidized by monoamine oxidase B and taken up by DAT where it disrupts mitochondrial function [199]. This model results in significant destruction of the nigrostriatal pathway with marked loss of SNc dopaminergic neurons [200]. Notably, MPTP treated mice do not experience significant motor impairment or Lewy pathology [200, 201]; however, recent studies have observed prodromal symptoms in these mice including loss of olfaction and constipation [201, 202]. Despite its shortcomings, the MPTP model has shown significant usefulness in elucidating mechanisms of SNc dopaminergic neurodegeneration. Indeed, this model prompted research into the effect of mitochondrial dysfunction on dopaminergic neurons [200], and also recapitulates certain aspects of neuroinflammation such as microgliosis and Th17 immune responses [203].

#### **1.4.2 – Rotenone model**

Rotenone is a pesticide with lipophilic properties capable of crossing the BBB, entering cells, and disrupting mitochondrial complex I [204]. Although used in both mice and rats, rotenone is more commonly used in a rat model [204]. Rotenone can be administered orally, intravenously, intraperitoneally, intradermally, and intracranially, each method having particular benefits and drawbacks. Rotenone is toxic to a wide variety of organs including the heart and liver, making intracranial injections more favourable to localize damage to the CNS [204]. The rotenone model does result in destruction of SNc dopaminergic neurons and decreased TH staining, although it is not as selectively toxic as MPTP [204]. Mice administered rotenone do experience motor deficits



such as decreased movement in an open field and decreased endurance on a rotating rod [205]. Lewy pathology can also be observed in most routes of administration [204]. Oral administration of rotenone results in slowed gastric motility and conventional PD-like symptoms, which were shown to worsen with stress-induced gut dysfunction [206].

### **1.4.3 – 6-Hydroxydopamine model**

Administration of 6-hydroxydopamine must be done locally due to its inability to cross the BBB, where it can then be taken up by DAT and become oxidized in the cytoplasm of dopaminergic neurons and release damaging peroxides [207]. The 6-hydroxydopamine model very potently and specifically destroys SNc dopaminergic neurons and can be used to model the dying-back mechanism of neurodegeneration when administered into the striatum [199]. Mice given 6-hydroxydopamine experience motor impairment including slowed turn time and bradykinesia, and over-administration of L-DOPA to these mice are routinely used to model L-DOPA-induced dyskinesia [208]. No Lewy pathology is observed in this model.

### **1.4.4 – LPS injection model**

Given that neurons do not express the LPS receptor TLR4, injection of LPS is performed to study the effects of microglia-induced inflammation [199]. Systemic administration as well as local injection were both shown to induce microgliosis, increased TNF $\alpha$  secretion, and SNc dopaminergic neurodegeneration in C57BL/6 mice [209]. The effect of this model on motor phenotypes and Lewy pathology is less investigated. Two-hit models have shown that systemic

LPS can induce pathological aSyn misfolding from harmless oligomers injected into the CNS, suggesting that LPS-induced inflammation may seed misfolding [210]. This two-hit model also found signs of motor deficits including slowed movement and exploration.

#### **1.4.5 – Human $\alpha$ -Synuclein overexpression model**

In order to mimic Lewy pathology that is observed in humans caused by aSyn aggregation, mice overexpressing human aSyn were developed to mimic multiplication of the gene [211]. Mice expressing human aSyn under the Thy1 promotor (Thy1.aSyn) are noted to express aSyn in all brain regions akin to the late time point of Braak's Lewy pathology staging [211]. These mice do form aSyn aggregates including Lewy bodies containing aSyn phosphorylated at serine 129 in the substantia nigra and striatum, akin to human PD, but not the olfactory bulb [211]. Despite this, loss of olfaction is observed in these mice [212]. Thy1.aSyn mice also exhibit a progressive loss of striatal dopamine levels, losing 40% of striatal dopamine by 14 months of age [213]. Notably, complete SNc dopaminergic neuronal degeneration does not occur, but axonal arborization does decrease [211]. Motor deficits do develop in Thy1.aSyn mice including decreased locomotion and hunched postures [213]. This model has also been shown to induce microglial activation and induction of pro-inflammatory cytokines including TNF $\alpha$  early in their development [214].

#### **1.4.6 – *Parkin*<sup>-/-</sup> mice**

Although inheritance of a loss of function mutation in *PRKN* results in PD with near 100% penetrance in humans [4], *Parkin*<sup>-/-</sup> mice have largely failed in recapitulating the disease. Indeed,

*Parkin*<sup>-/-</sup> mice do not experience Lewy pathology or destruction of SNc dopaminergic neurons [82, 215, 216]. Most motor phenotypes are also not observed in *Parkin*<sup>-/-</sup> mice with the exception of one study that noted increased paw slipping while walking across a rod [215]. Nonetheless, it has been shown that *Parkin*<sup>-/-</sup> mice are more susceptible to MPTP insult, suggesting that Parkin may play a neuroprotective role in PD given MPTP's specificity for SNc dopaminergic neurons [217]. It has also been noted that *Parkin*<sup>-/-</sup> mice have altered levels of striatal dopamine, suggesting Parkin may play a role in either synapse function or dopamine release [215].

#### **1.4.7 – *Pink1*<sup>-/-</sup> mice**

Similar to *Parkin*<sup>-/-</sup> mice, *Pink1*<sup>-/-</sup> mice also largely fail to exhibit most PD pathological hallmarks. Although *Pink1*<sup>-/-</sup> mice do present with an accumulation of dysfunctional mitochondria, loss of mitochondrial membrane potential, and increased reactive oxygen species, they do not exhibit any loss of SNc dopaminergic neurons [80]. Mild motor impairment has been observed in these mice at 18 months of age but fail to recapitulate the severity and progressiveness of PD in humans [80, 81]. Some prodromal symptoms of PD have also been documented in *Pink1*<sup>-/-</sup> mice including loss of olfaction and altered gait which included decreased ability to stand on their hind paws [81]. *Pink1*<sup>-/-</sup> mice fail to model Lewy pathology and any other brain-related PD pathology [216]. The inability to effectively recapitulate PD pathology in mice has called into question the proposed mechanisms and our preconceived notions of familial forms of autosomal recessive PD.

## **2. Intestinal homeostasis and infection**

The mammalian gastrointestinal (GI) tract begins at the mouth and extends through the stomach, small intestine, colon, and rectum. Primarily, the GI tract functions to digest and absorb macronutrients, water, vitamins, and minerals [218]. Absorption of nutrients by intestinal epithelial cells largely occurs in the lower GI tract consisting of the small intestine and colon [218]. However, as a barrier to the external environment, the GI tract must also serve a protective function to foreign and potentially dangerous agents. Ingested pathogenic microbes that are capable of disrupting intestinal function pose a threat to our health; indeed, infectious diarrheal diseases remain a significant cause of morbidity and mortality in lower- and middle-income countries [219, 220]. In this regard multiple systems must work in concert to ensure proper homeostatic control and function of the GI tract. The immune system, working in coordination with the physical and chemical barrier that is created by intestinal epithelial cells, has the task of halting pathogenic infections from penetrating the mucosal intestinal layer and initiating disease [221].

## **2.1 – Intestinal overview**

Ingested food travels through the stomach into the small intestine. A more thorough digestion of food into base macromolecule monomers and their subsequent uptake primarily occurs in the small intestine, while the colon mostly absorbs water, vitamins, and minerals [221]. The small intestine possesses villi structures – protrusions of the intestinal mucosa – that greatly increases its surface area and allow more efficient nutrient uptake via enterocytes [221]. Invaginations of the mucosa create crypts where stem cells divide, differentiate, and transit up to the villi to replace dying cells that slough off [222]. The small intestine is divided into three segments: the duodenum that accepts partially digested food from the stomach through the pyloric

valve, the jejunum, and the ileum that empties through the ileocecal valve into the cecum and colon [221]. The colon does not possess villi structures but does have deep crypt architecture [221]. Transit of food through the gut occurs primarily by peristalsis induced by innervation of smooth muscle within the intestinal walls [223]. The gut is highly innervated by the enteric nervous system (ENS), a dense network of neurons in the gut wall that is part of the autonomic nervous system [223]. Further, the gut hosts a highly complex immune environment in order to control potentially dangerous agents ingested; however, the small intestine and colon are also colonized with trillions of commensal microbes that develop alongside us since first exposure at birth [224]. This collection of microbes, coined the gut microbiota, play essential functions necessary for homeostasis including aiding in digestion, secretion of metabolites [225], maintenance of epithelial cell barrier integrity [226], and proper development of the immune system [227]. The microbiota also plays a key role preventing the colonization of numerous potential pathogenic microorganisms [228]. Together these systems function to ensure proper homeostatic function of the gut.

### **2.1.1 – Intestinal epithelial cells**

The intestinal mucosa is comprised of a layer of smooth muscle tissue (muscularis mucosae), the lamina propria, and a single layer of intestinal epithelial cells that is exposed to the intestinal lumen [218]. Intestinal epithelial stem cells reside at the base of the crypts where they are able to divide and migrate up onto the villi, differentiating along the way into a multitude of cell types [222]. Enterocytes, which are the most abundant cell type, are absorptive cells whose primary function is uptake of digested nutrients from the intestinal lumen [229]. Enterocytes possess a brush border with microvilli protrusions that further aid in breaking down and

transporting nutrients into the cell. Although primarily absorptive, enterocytes also play a critical role in intestinal immunity; indeed, enterocytes possess TLR molecules on their basolateral side that can respond to invading pathogens [230]. Further, enterocytes are able to produce the antimicrobial peptide RegIII $\gamma$ , a molecule that has been reported to be a key mediator of host-microbial segregation throughout the gut [231]. Production of RegIII $\gamma$  was shown to be regulated by the TLR MyD88 pathway and also be induced by the IL-22 receptor also present on enterocytes [231, 232]. RegIII $\gamma$  targets bacterial peptidoglycan and induces pore formation that results in cell death [233]. Mice lacking RegIII $\gamma$  were shown to have increased invasion of the microbiota at the luminal surface and increased pro-inflammatory Th1 immune responses [231]. Microfold cells (M cells) are another differentiated epithelial cell type commonly found clustered over immunological structures in the lamina propria such as Peyer's patches and lymphoid follicles [234]. Less is known about M cells, but it has been found that they allow the passive and non-specific transcytosis of luminal contents into basolateral immune compartments for sampling by innate immune cells [229]. They have also been observed to engage in active transport in response to certain pathogens; for example, activation of M cell's surface receptor glycoprotein 2 by the *S. enterica* pilus protein FimH has been shown to induce active microbial uptake and transcytosis of the pathogen [235].

Intestinal homeostasis is also supported by a number of secretory cell types. Paneth cells provide an exception to most other differentiated intestinal epithelial cells; rather than migrating up villi, they remain within crypts [236]. Paneth cells are unique to the small intestine and secrete a number of antimicrobial molecules including lysozymes and defensins [236]. These molecules are known to protect the crypts from overt bacterial invasion [236]. Defensin deficiency was shown to cause susceptibility to *Salmonella enterica* infection, while overexpression of human  $\alpha$ -defensin

under a Paneth cell-specific promoter increased resistance [237]. These antimicrobials were also shown to diffuse into the intestinal lumen to keep the gut microbiota from infiltrating through the mucosal layer [238]. Goblet cells are another type of secretory cell that primarily produce and secrete mucins. The most abundant and common of these mucins is mucin 2 (Muc2) which forms the majority of the intestinal mucous layer [239]. Muc2 is able to form a highly dense structure of polymers that further limits bacterial invasion [239]. The small intestine is coated with a single layer of mucous, while the colon has two distinct layers: a dense inner layer that is impermeable to bacteria, and a looser outer layer that is heavily colonized by the microbiota [239]. Mice lacking Muc2 were shown to suffer from spontaneous colitis and be predisposed to colorectal cancer [240, 241]. The mucous layer, together with the enzymes and antimicrobial peptides generated from Paneth cells and enterocytes, form a highly effective chemical and physical barrier to most microbes. Enteroendocrine cells are hormone-secreting cells loosely scattered throughout the GI tract that respond to meal stimuli and bacterial metabolites [242]. G-protein coupled receptors on their cell surfaces are able to respond to stimuli such as microbiota-derived short-chain fatty acids (SCFAs) or sugar [243]. In response, enteroendocrine cells are able to secrete hormones that can regionally modulate gut such as serotonin that can affect the ENS or glucagon-like peptides that regulate insulin [244, 245].

Efficient modulation of intestinal permeability through the single layer of epithelial cells is vital to limit overt inflammation and disease. In addition to transcellular pathways, paracellular permeability (in between cells) must also be regulated. Intestinal epithelial cell tight junctions at the apical surface are formed by claudin and occludin proteins [246, 247]. Tight junctions limit permeability to microbes and large macromolecules, only allowing water and solutes to pass through [246]. Adherens junctions, formed by adherens and cadherins, also form on apical surfaces

but do not function in limiting paracellular permeability [248]. Instead, adherens junctions were shown to be highly dynamic and respond to stimuli to either tighten or loosen the connection between cells to allow for epithelial remodelling [248]. Both adherens and tight junctions are formed by transmembrane proteins that interact with the actin cytoskeleton on the cytoplasmic side of intestinal epithelial cells [249]. Tight junctions can be regulated by cytokines; pro-inflammatory cytokines including  $\text{IFN}\gamma$ ,  $\text{TNF}\alpha$ , IL-17, and IL-6 were all shown to increase paracellular permeability [246, 250].

### **2.1.2 – Intestinal immunology**

The gut has the largest compartment of immune cells in the body and has the monumental task of maintaining control of both commensal and invading microbes. Intestinal epithelial cells provide the first layer of defence in the form of physical and chemical barriers but can also provide help initiating immune responses via TLR-induced cytokines if microbes penetrate these layers [251]. The immune system in the intestine is complex and consists of both regional lymphoid structures called gut-associated lymphoid tissue (GALT) and conventional lymph drainage into secondary lymphoid organs [252]. The small intestine possesses GALT structures called Peyer's patches; non-capsulated lymphoid follicles tightly associated at the basolateral surface of epithelial cells [253]. Dendritic cells have been observed to be enriched near the epithelial cell region where M cells can transfer luminal antigens and pathogens for processing and presentation to adaptive immune cells [252]. Peyer's patches have been observed to contain both B cell follicles, germinal centers, and T cell zones [253]. The colon also contains GALT structures known as cecal and



colonic patches, both of which contain B and T cells, but only cecal patches were shown to be a major source of germinal centers and B cell antibody production [254].

Under homeostatic conditions dendritic cells are able to extend processes through the epithelial layer and sample luminal antigens for presentation on MHC II [255]. Invading microbes that breach the epithelial layer activate dendritic cells via TLRs resulting in digestion of the pathogen, increased presentation of MHC II, increased pro-inflammatory cytokine secretion, and upregulation of chemokine receptors [256]. Dendritic cells within the lamina propria that activate upon antigen exposure express the chemokine receptor CCR7 that targets them for afferent lymphatic vessels [256]. Most lymphatic vessels from the gut drain into surrounding mesenteric lymph nodes, although it has recently come to light that the colon also possess their own unique colon-associated lymph nodes [257]. Intestinal conventional dendritic cells are largely dominated by CD103<sup>+</sup> dendritic cells (CD103<sup>+</sup> DCs). Upon interaction with the appropriate T cell in the lymph node, T cell proliferation and differentiation can occur. CD103<sup>+</sup> DCs are able to metabolize vitamin A into retinoic acid, which promotes the differentiation of regulatory T cells (Treg) and expression of gut-homing integrins [258, 259]. The absence of pro-inflammatory cytokines in homeostatic conditions also favours Treg differentiation and tolerance to luminal microbes, while inflammatory cytokines secreted by dendritic cells via TLR signalling induce T cell subtypes that promote gut inflammation and clearance of the invading microbe [260, 261].

Macrophages comprise a large portion of innate immune cells within the lamina propria [262]. Intestinal macrophages, in contrast to macrophages in other systems, are relatively inert to TLR stimulation, secrete high levels of anti-inflammatory IL-10, and highly express MHC II [263, 264]. These macrophages express CX3CR1, which was shown to be necessary to extend processes through the epithelial layer into the lumen for antigen sampling akin to dendritic cells [265].

Resident CX3CR1<sup>+</sup> macrophages are believed to be vital in the local restimulation of Treg cells and maintenance of intestinal homeostasis, as impairment of these cells resulted in colitis, decreased Treg numbers, and increased inflammation in response to bacterial molecules [266, 267]. Macrophages that elicit pro-inflammatory responses to enteric pathogens were shown to be recruited from circulation via the chemokine CCL2 and be distinct from CX3CR1<sup>+</sup> macrophages [268].

Neutrophils are polymorphonuclear cells that are rapidly recruited to the gut following infection, representing 80% of leukocytes present in acute inflammation [269]. They function by phagocytosing invading pathogens, releasing cytotoxic granular contents, and forming neutrophil extracellular traps [270]. Epithelial cells, in response to TLR signalling from invading microbes, are able to secrete cytokines that in turn result in both the secretion of neutrophil-attracting chemokines and promote Th17 differentiation [271]. Th17 cells, via IL-17 secretion, can elicit potent neutrophil responses by both activating endothelial cells to secrete neutrophil-attracting CXCL1 and CXCL5. [272, 273]. Neutrophils have also been observed to secrete the chemokines CXCL10 and CCL2 which further recruit Th17 cells and circulating monocytes, creating a feed-forward loop that enhances the inflammatory response [273].

Lymphocyte populations within the gut are dispersed in the GALT, lamina propria, and between epithelial cells. Under homeostatic conditions Th1, Th17, Treg, and plasmacyte cell populations are found in abundance; Th2 was originally believed to also be present under homeostasis but was discovered to be absent in mouse colonies lacking parasitic infections [274]. As discussed, Treg cells function to limit overt inflammation and promote tolerance to commensals and food products within the intestinal lumen. Treg cells are found to be in greatest abundance towards the distal colon where the microbiota is most abundant [252]. Th17 cells are responsible

for responding to infections under inflammatory conditions; however, recently they have been shown to be a heterogeneous population [261]. Indeed, Th17 cells have been shown to sometimes co-express Treg transcription factors and perform inhibitory functions in *ex vivo* cells isolated from inflammatory bowel disease patients [275]. Follow up experiments also showed that pro-inflammatory cytokines can downregulate the Treg-properties of these cells and allow them to express more bona-fide Th17 cytokines [275]. This data suggests that Th17 cells within the colon may be plastic and convert between inhibitory and inflammatory phenotypes depending on antigen exposure.

B cells within the GALT provide the most immediate and largest source of antibodies for the intestinal environment [252]. B cells activation and transformation into antibody secreting plasma cells can occur with the aid of dendritic cells that carry antigens and produce retinoic acid [276]. Retinoic acid was shown to promote class switching to type A immunoglobulins (IgA) while simultaneously promoting IL-10 secretion and gut-homing receptor expression [277]. Plasma cell-derived IL-10 helps with Treg generation but was shown to be not necessary in knockout mouse models [278]. Secreted IgA is able to undergo transcytosis across epithelial cells with aid of specific immunoglobulin receptors, allowing IgA to bind and neutralize microbes in close proximity to the epithelium [279]. Neutralization via IgA add to the chemical and physical barriers present within the intestinal lumen and provides another mechanism of defense to pathogenic microorganisms.

Innate lymphoid cells (ILCs) display functional similarities to T cell subsets, but do not possess rearranged T cell receptors. The intestinal environment is enriched with ILC1s and ILC3s that secrete Th1- and Th17-type cytokine profiles respectively [280]. ILC2s, like Th2 cells, are not found in abundance in the gut [281]. With no distinct antigen receptors, ILCs are primarily

activated via cytokine receptors that, in turn, induce cytokine secretion that can rapidly ramp up local immune responses for efficient pathogen clearance [280]. For example, ILC3-secreted IL-17 and IL-22 was shown to be an instrumental early source of cytokines to initiate protective responses to enteric pathogens [282]. In this regard, ILCs are considered to a source of rapid early-response T cell cytokines without the need for antigen presentation or T cell differentiation.

### **2.1.3 – The gut microbiota**

Colonization of microbes in the gut is considered to begin at birth. Both genetic and environmental factors control the developing composition of the microbiota; however, most stable gut microbiotas begin to form between the ages of three and five and are dominated by the phyla *Bacteroidetes* and *Firmicutes* with minor contributions from *Proteobacteria*, *Verrucomicrobia*, and *Actinobacteria* [283]. The gut microbiota increases in both diversity and concentration along the GI tract, the colon alone housing more than  $10^{13}$  individual microbes [224, 284]. These microbes largely exist in an anaerobic environment and cannot survive in the presence of oxygen [285]. Factors such as changes in diet, antibiotics, and disease have been shown to drastically and rapidly shift the microbiota [286]. Establishing whether alterations in the microbiota are the cause or a consequence of disease has been difficult to elucidate in humans as most studies remain correlative. Experimental studies in mice, however, with the advent of germ-free mice and microbiota transplants, have begun to help elucidate some of the mechanisms by which the microbiota can affect intestinal homeostasis.

One of the primary functions of the microbiota is to aid in digestion and modulate energy intake by the host [287]. Mouse studies have shown that fecal microbiota transplants from obese

mice can confer the obesity phenotype [288], suggesting the gut microbiota is directly affecting the efficiency of energy absorption. This is further supported by mouse studies where germ-free mice are leaner than normal mice until colonized with a microbiota from a conventionally raised mouse [288]. Complex carbohydrate fermentation is largely accomplished by the gut microbiota and results in the production of SCFAs that can then be absorbed by enterocytes for energy. SCFA-derived energy is estimated to account for 10% of all energy intake by humans [289]. Further, when SCFAs are oxidized by the host for energy carbon dioxide is also released which aids in maintaining the anaerobic environment of the gut [290]. SCFAs can modulate hormone levels via activation of G-protein coupled receptors GPR43 and GPR41 on enteroendocrine cells [291], also affecting digestion and absorption. Induction of these receptors leads to secretion of the hormones leptin, which activates fat deposits [292], PYY, which slows gut motility to allow for more efficient caloric extraction [293], and glucagon-like peptides, which regulates insulin release and sugar uptake [294].

While the host immune system is responsible for keeping the microbiota in check, the host immune system can reciprocally be affected by the gut microbiota. Germ-free mice were shown to have decreased macrophage and neutrophil responses [295, 296], and decreased TLR and NOD expression [297, 298]. Loss of function mutations in NOD receptors have been shown to be involved in inflammatory bowel disease, suggesting that the gut microbiota may protect against inflammatory diseases by regulating these receptors [299]. Microbiota-derived SCFAs have been shown to modulate immune responses towards an anti-inflammatory phenotype. Indeed, the SCFA butyrate was shown to act as a histone deacetylase inhibitor, promoting the expression of FoxP3 and Treg differentiation [300]. Specific microbes can also directly affect immune responses: polysaccharide A from *Bacteroides fragilis* was shown to be engulfed by CD103<sup>+</sup> DCs and

promote Treg differentiation and subsequently protect from colitis [301], while colonization with segmented filamentous bacteria were shown to promote Th17 colonic immune responses [302].

Regulation of tight junctions is accomplished via both cytokine secretion and microbiota derived SCFAs to limit the spread of enteric pathogens [303]. Effective Treg differentiation and IL-10 secretion has been shown to enhance tight junctions while limiting pro-inflammatory cytokines that weaken them [304]. The SCFA butyrate was also shown to reduce trans-epithelial permeability both *in vitro* and *in vivo* [305]. Regulation of tight junctions was also shown to occur in distal organ sites such as the brain via similar mechanisms; indeed, germ-free mice were shown to have increased BBB permeability and microglia activation, and recapitulation of a normal microbiota was shown to enhance BBB integrity showing a causal relationship [306]. Butyrate was also shown to directly enhance BBB tight junction protein expression [307]. Prolonged states of enteric inflammation can disrupt BBB integrity via the increased presence of circulating pro-inflammatory cytokines that favour the activation of CNS endothelial cells, and TNF $\alpha$  was shown to increase CNS-derived endothelial permeability *in vitro* [308].

Metabolization of amino acids by the microbiota is responsible for the production of approximately 90% of the serotonin and 50% of the dopamine produced in the gut [309]. Further, SCFA-induced activation of enteroendocrine cells can stimulate the expression of the enzymes necessary for serotonin synthesis [310]. Sustained inflammation of the gut was shown to increase secondary messengers in enteric primary afferent neurons, altering their excitability [218]. Changes in local enteric innervation can afferently affect the CNS via the vagus nerve (discussed in the next section), creating a link between these gut-specific alterations and CNS health. It is known that germ-free mice have altered movement, stress, and learning disabilities [311];

however, more research is needed to fully elucidate the mechanisms and extent by which gut physiology can alter CNS activity.

#### **2.1.4 – The enteric nervous system**

The ENS is the most complex division of the autonomic nervous system [223]. It possesses intrinsic innervation that can function autonomously if separated from the rest of the body but is also extrinsically connected to the CNS via vagal and pelvic nerves [312]. The ENS comprises both enteric neurons and enteric glial cells that regulate intestinal motility, local blood flow, gut hormone secretion, and fluid exchange [223, 313]. Along the intestinal tract the ENS is organized into two main plexuses: the submucosal plexus that lies beneath the mucosa, and the myenteric plexus that lies in between the smooth muscular layers surrounding the intestines [223]. Being autonomous, the ENS consists of primary afferent neurons that intake information, relay that information through interneurons, which can trigger effector neurons to perform their functions.

Primary afferent neurons are capable of sensing mechanical distortions and chemical changes in the gut including pH, osmolarity, and glucose levels indirectly via glucagon-like peptides secreted by enteroendocrine cells [314]. Dopamine and serotonin secreted locally by enteroendocrine cells and the microbiota can also affect enteric afferent and effector neurons [315, 316]. These neurotransmitters are unable to cross the blood brain barrier and primarily act locally to promote smooth muscle contraction. Activation of smooth muscle cells by effector neurons is primarily responsible for peristaltic movement of the gut [223]. Research has shown that, in addition to SCFA-mediated activity on enteroendocrine cells and direct synthesis of neurotransmitters, activation of TLR2 and 4 can modulate ENS activity [317, 318]. Indeed, TLR2

knockout mice were shown to have altered ENS architecture and dysmotility [319], and TLR4 knockout mice were shown to have decreased numbers of inhibitory neurons also leading to altered motility [318]. Enteric neurons were also shown to be closely associated with the immune system, directly promoting the anti-inflammatory and wound-healing properties of CX3CR1+ macrophages [320]. Reciprocally, enteric neurons were shown to be altered by CX3CR1+ macrophages to regulate gut motility and protect from colonic hypermotility and diarrhea. Interestingly, this crosstalk was also shown to be dependent on the microbiota, as antibiotic treated mice showed decreased signalling between enteric neurons and CX3CR1+ macrophages.

Although the gut can function autonomously, it is intertwined with the CNS via several extrinsic connections including the vagus nerve. The vagus nerve originates from parasympathetic ganglia in the brain and efferently innervates the gut and afferently relays information back to the brain via the dorsal motor nucleus [321]. Afferent vagus nerve connections can detect mechanical changes in the gut musculature and efferently help regulate with satiety responses [322]. Vagal activation of local enteric neurons has also been shown to help induce anti-inflammatory CX3CR1+ macrophages, as previously described [323]. Further, the vagus nerve can directly detect hormones and cytokines in the mucosa, responding to inflammation by efferently inducing cortisol release in the CNS [324]. Prolonged exposure to inflammation, however, is believed to result in an altered state of vagus nerve sensitization and be responsible for the psychological symptoms associated with inflammatory bowel disease and irritable bowel syndrome including anxiety and depression [321, 325, 326]. In these cases, vagal nerve stimulation was shown to improve disease scores and maintain anti-inflammatory responses [321, 327].



## 2.2 – Intestinal infection

Microbial infections are capable of disrupting intestinal homeostasis, leading to breakdown of the intestinal barrier, decreased nutrient absorption, and diarrhea [328]. Infectious diarrhea is a significant cause of morbidity and mortality in low- and middle-income countries [220]. In children below the age of five, infectious diarrhea can prevent efficient nutrient uptake during key developmental time periods, leading to stunted growth, impaired cognition, and in severe cases death [329]. Enteric pathogens utilize multiple mechanisms to induce diarrhea including inhibiting ion and water intake, disrupting tight junctions, and induction of local inflammation [330-332]. Disruption of the absorptive and secretory abilities of enterocytes leads to an accumulation of water within the lumen causing diarrhea and spread of the enteric pathogen back into the environment to the microbe's own benefit. Dehydration of the host poses the most immediate threat to health during diarrhea, and rehydration therapy has been shown to be completely protective in fatal animal models of infectious colitis [333].

Attaching and effacing (A/E) pathogens are a group of Gram-negative enteric pathogens capable of intimately adhering to intestinal epithelial cells and effacing the cell's microvilli structures. Members of A/E pathogens include enteropathogenic and enterohemorrhagic *Escherichia coli* (EPEC and EHEC) and the closely related mouse pathogen *Citrobacter rodentium*. A/E pathogens first loosely attach to differentiated epithelial cells via mechanisms that are still not fully understood but have been shown for EPEC to be mediated via bundle-forming pili *in vitro* [334]. Intimate attachment to the host cell requires the formation of a type-three secretion system (T3SS), a needle like structure that inserts into the host cell membrane creating a continuous channel from the bacterial cytoplasm to the host cell cytoplasm. The T3SS is encoded

on a pathogenicity island called the locus of enterocyte effacement (LEE) and is shared between EPEC, EHEC, and *C. rodentium* [335]. A number of effector proteins, encoded both within the LEE and from other genetic elements, are injected into the host cytoplasm through the T3SS to mediate disruption of the host cell. One of the first effectors injected is the translocated intimin receptor (Tir), which embeds itself into the host cell membrane where its extracellular domain can act as a receptor for the bacterial protein intimin, allowing the bacterium to intimately attach to the host cell [336]. The intracellular domain of Tir has been shown to instigate significant remodelling of host cell actin via activation of Neural Wiskott-Aldrich syndrome protein (N-WASP) and actin-related protein 2/3 (Arp2/3) [337]. This actin remodelling leads to the effacement of the epithelial microvilli and the accumulation of actin filaments where the bacterium has attached, raising the membrane into a pedestal shape with the bacterium on top and forming the characteristic A/E lesion. Knockout of Tir, intimin, or any vital component of the T3SS apparatus results in avirulence [338, 339].

### **2.2.1 – Enteropathogenic and enterohemorrhagic *Escherichia coli***

EPEC and EHEC are foodborne human pathogens that are transmitted via the fecal-oral route. EPEC outbreaks are most common in developing nations and its associated diarrheal disease manifests primarily in young children [340]. Human trials have shown that EPEC infection in healthy adults, although resulting in diarrhea, led to weak immune responses and a complete lack of fever in 90% of volunteers [341]. No specific reservoir has been identified for EPEC in nature and transmission is believed to occur primarily through direct contamination between people [342]. EHEC, contrary to EPEC, is found primarily in developed nations. EHEC persists in nature

in several animals, the most prominent of which are cattle, and can infect humans via ingestion of improperly cooked beef [340]. EHEC has also been observed to cause outbreaks from raw fruits, vegetables, lettuce, as well as community water sources [340]. EHEC is primarily distinguished from EPEC by the production of Shiga-toxin. Shiga-toxin is a proteinaceous toxin able to bind to globotriaosylceramide (GB3) receptors found on Paneth cells and endothelial cells – once inside the cell it is able to disrupt protein synthesis by modifying ribosomal RNA, leading to cell death [343, 344]. Notably, renal microvascular endothelial cells were shown to be particularly vulnerable to Shiga-toxin [345]. In humans, Shiga-toxin can induce hemorrhagic colitis and, if it enters circulation, hemolytic uremic syndrome resulting in kidney failure [346]. EPEC and EHEC also differ in their tissue tropism in humans, with EPEC primarily colonizing the small intestine and EHEC primarily colonizing the colon. The reason for this difference remains unknown; however, a recent study has suggested that EHEC possesses a transcriptional regulator for the LEE that is inhibited by the high biotin levels found in the small intestine, making the colon a more favourable environment [347].

Both EPEC and EHEC possess a LEE-encoded T3SS used to induce A/E lesions. Tir mediated actin reassembly, however, slightly differs between the two, and Tir from EHEC is not able to complement a Tir-deficient EPEC mutant [348]. EHEC's Tir protein is unable to initiate N-WASP and Arp2/3 mediated actin reorganization directly and requires the help of the non-Lee encoded effector *E. coli* secreted protein F from prophage U (EspFu) [349]. EspFu is recruited to the cytoplasmic side of Tir to mediate actin rearrangement.

Aside from A/E lesion formation, effector proteins injected into the host cytoplasm through the T3SS are able to induce cell death and diarrheal disease via multiple mechanisms. Disruption of tight junctions is a major mechanism by which EPEC and EHEC can instigate diarrhea and is

accomplished by a number of effectors including *E. coli* secreted proteins F (EspF, homologous but unique from EspFu and encoded by the LEE), G (EspG), and non-LEE encoded effector A (NleA) [350]. EspF in particular was shown to further promote actin pedestal formation by its ability to activate N-WASP and Arp2/3, recruiting the actin and occludin proteins directly from tight junctions [351, 352]. NleA was shown to disrupt protein trafficking from the Golgi, preventing new tight junctions from being formed [353, 354]. EspG acts in a similar manner by inhibiting GTPases and disrupting protein trafficking through the Golgi [355]. Further, EspG has been shown to disrupt microtubule formation that results in the internalization of claudin and occludin proteins from tight junctions [356]. EspF and EspG also inhibit glucose uptake transporters, ion transporters, and aquaporins, further leading to the accumulation of water and ions within the lumen and favouring diarrhea formation [357]. Disruption of mitochondrial function by EspF and mitochondria-associated protein (Map) helps result in death of intestinal epithelial cells to further promote intestinal barrier dysfunction. Both EspF and Map were shown to disrupt mitochondrial membrane potential, resulting in the leakage of cytochrome C and the activation of cellular apoptosis [358]. EspF interacts with and depletes the host protein Abcf2, an anti-apoptotic regulator [359]. In yeast cells, Map was shown to promote mitochondrial fission and disruption of the mitochondrial membrane potential [360]. Interestingly, it is known that EspF can interact with Snx9 [361]. While it is believed this interaction's primary function is membrane remodelling, how EspF might affect the Snx9-dependent MitAP pathway previously discussed remains unknown.

### **2.2.2 – *Citrobacter rodentium***

*C. rodentium* is an A/E murine pathogen that was first discovered in the 1970's when both Boston and Tokyo research centers experienced outbreaks within their mouse colonies. Upon identification, *C. rodentium* was recognized as the aetiologic agent of transmissible colonic crypt hyperplasia [362]. The usefulness of *C. rodentium*, however, was not recognized until the 1990's when *C. rodentium* was observed to cause A/E lesions similar to human EPEC and EHEC infections [363, 364]. Since then, genetic analyses have shown striking similarities between *C. rodentium* and EPEC/EHEC with over two thirds of the genes being conserved. The LEE of *C. rodentium*'s was also discovered to be nearly identical to EPEC's [339, 365]. Importantly, mice are naturally resistant to EPEC and EHEC infection, showing no signs of colon pathology and overall poor colonization [366]; hence, *C. rodentium* provided an ideal murine model to study the pathological mechanisms of EPEC and EHEC infections. While the LEE components of *C. rodentium* are more conserved with EPEC, *C. rodentium* was shown to colonize the cecum and eventually move to the distal colon [367], which is more akin to EHEC infections. Shiga-toxin producing *C. rodentium* has been created in an effort to make *C. rodentium* more comparable to EHEC and was able to recapitulate EHEC's more severe diarrhea and renal failure [368]. *C. rodentium* infection is now routinely used to study A/E pathogen virulence mechanisms in mice.

Murine infection with *C. rodentium* is routinely done via oral gavage directly into the GI tract. Most of the inoculum dies within the stomach, and the remaining microbes primarily establish in the cecum within a few hours [367]. Colonization moves towards the distal colon within two to three days [367]. Infection with *C. rodentium*, in general, results in thickening of the intestinal mucosa, lengthening of the colonic crypts, epithelial cell hyperplasia, and an inflammatory immune response (discussed in a later section) [364]. The severity of *C. rodentium* infection largely depends on the mouse genetic background with resistant C57BL/6 and Swiss

mice developing mild self-limiting colitis, while susceptible C3H and FVB mice eventually succumb to diarrheal dehydration around 10 days post infection [369]. Fecal loads of *C. rodentium* peak within two weeks and is no longer detectable in feces within three to four weeks in resistant mice [370].

The *CriI* locus has been identified as a major locus of susceptibility in mice. Notably, the *CriI* locus from C57BL/6 mice was able to completely rescue susceptible C3H mice [369]. The *CriI* locus was shown to regulate *R-spondin 2* expression (*Rspo2*); the *Rspo2* protein is uncontrollably expressed during *C. rodentium* infection in C3H mice, resulting in overt  $\beta$ -catenin activation via the Wnt pathway [369]. Under homeostatic conditions, Wnt signalling maintains the undifferentiated nature of the stem cell niche at the base of crypts. In C57BL/6 mice, this pathway is induced in a controlled manner during infection to increase the proliferation of undifferentiated cells up the colonic crypts, leading to increased epithelial cell sloughing and clearance of the pathogen [371, 372]. In cases of overt activation, as in C3H mice, the rapid and uncontrolled loss of differentiated epithelia leads to decreased absorption, diarrhea, and eventually mortality [369, 371, 372].

*C. rodentium* infection can alter host cell bioenergetics within the colon by both increasing the number of undifferentiated epithelial cells and disrupting mitochondrial function via EspF and Map [364]. Most prominently, these changes have been shown to result in decreased oxidative phosphorylation and consequently decreased oxygen consumption by epithelial cells, leading to a more aerobic environment within the intestinal lumen [373, 374]. This change leads to an expansion of *Enterobacteriaceae* at the mucosal surface [375]. Other changes to the microbiota and microbiota-derived products as a result of *C. rodentium* infection are less known. It is known, however, that the microbiota is capable of regulating susceptibility to *C. rodentium*. Notably,

bacteria capable of metabolizing monosaccharides were shown to outcompete *C. rodentium* and provide colonization resistance [376]. A pool of different SCFAs was also shown to enhance mucous production from goblet cells, further enhancing the mucous barrier and prevent invasion [377]. Segmented filamentous bacteria have been shown to prevent *C. rodentium* by enhancing protective Th17 immune responses [302].

## **2.3 – Host response to intestinal infection**

In order to initiate disease, A/E pathogens must first be able to circumvent the chemical and physical barriers comprised of mucous and antimicrobials. In the colon, while the loose outer mucous layer is freely navigable, it is unclear how A/E pathogens are able to penetrate the more compact inner mucous layer and establish on epithelial cells. A recent study has shown that a diet lacking fibre will result in degradation of the mucous layer by the microbiota for nutrients, providing a mechanism that would make the mucous layer more permeable to invading microbes [378]. Once infection is established, the host is able to recognize the pathogen via pattern recognition receptors (PRRs), resulting in cytokine release and the initiation of immune responses. The type of response induced is highly dependent on the microorganism involved and can result in the activation of a wide array of distinct immune cell populations. In this regard, the *C. rodentium* infection model has proven invaluable in establishing the importance of both the innate and adaptive immune systems within the gut to protect against A/E pathogens [370].

### **2.3.1 – Innate immunity**

Recognition of *C. rodentium* is accomplished via PRRs on epithelial cells and immune cells within the GALT and lamina propria. Signalling through TLRs results in the activation of myeloid differentiation primary response 88 (MyD88) and subsequently nuclear factor  $\kappa$ B (NF- $\kappa$ B), resulting in an early cytokine response involving IL-6, IL-22, IL-1 $\beta$ , IL-23, and CCL2 [379]. Activation of TLR2 was shown to not be necessary for the clearance of *C. rodentium*, but mice lacking TLR2 were shown to have disrupted intestinal barrier integrity and increased weight loss [380]. TLR4 induction was shown to be protective in C3H mice, as TLR4 knockout mice were shown to have decreased colon pathology and inflammation, but also lowered survival [381]. Abolishment of all NF- $\kappa$ B signalling via knockout of MyD88 resulted in significantly increased mortality in C57BL/6 mice challenged with *C. rodentium*, accompanied with increased epithelial damage, increased barrier permeability, and loss of early cytokine responses [382].

ILC3 cells have been discovered to be instrumental players in the protection against *C. rodentium*. Lymphotoxin on ILC3 can activate the lymphotoxin receptor on antigen presenting cells and intestinal epithelial cells, inducing IL-23 secretion. IL-23 can then in return act on ILC3s to induce IL-22 production [383]. IL-22 was shown to be protective against *C. rodentium* by inducing RegIII $\gamma$  secretion via engagement of the IL-22 receptor on epithelial cells [384]. Impairing the activation of ILC3 cells was shown to cause 100% mortality in C57BL/6 mice [384]. ILC3 cells also have the capacity to secrete IL-17, aiding in the activation of endothelial cells and the recruitment of neutrophils via CXCL1/2/5 induction [385]. Early and rapid neutrophil recruitment has also been shown to protect against *C. rodentium*-induced diarrhea. Indeed, knocking out the neutrophil receptor CXCR2 which recognizes CXCL1/2/5 prevents neutrophil influx, results in increased bacterial load, delayed bacterial clearing, and increased water content in feces [385].



CX3CR1<sup>+</sup> macrophages and CD103<sup>+</sup> DCs both perform functions locally within the gut to sense invading *C. rodentium* and orchestrate immune responses. Notably, CX3CR1<sup>+</sup> macrophages were shown to be the key antigen presenting cell responsible for the activation of ILC3 cells, as depletion of these macrophages resulted in significant ILC3 impairment, decreased IL-22, and overall decreased survival [386]. CD103<sup>+</sup> DCs are primarily responsible for presenting antigens to T cells in mesenteric lymph nodes, commencing the adaptive immune response [387]. Knockout of either of these cell types results in reduced survival and increased pathology upon *C. rodentium* challenge [387]. Within the gut, these cells help restimulate T and B cells to further propagate adaptive immune responses.

### **2.3.2 – Adaptive immunity**

Adaptive immune cells, including T and B cells, were observed to be necessary for resistance to *C. rodentium*. Indeed, halting the production of all recombinant antigen receptors via knockout of recombinant activating gene 2 (RAG2) leads to 100% mortality in C57BL/6 mice challenged with *C. rodentium* [388]. Further research into this field demonstrated that specifically CD4<sup>+</sup> T cells and B cells, but not CD8<sup>+</sup> T cells, were necessary for protection against *C. rodentium* [389]. It is known that *C. rodentium* infection triggers IL-17 and IL-22 producing T cells in the form of IL-17<sup>+</sup>IL-22<sup>+</sup> Th17 cells and IL-22<sup>+</sup> Th22 cells. IL-17 aids in initiating neutrophil responses and defensin production [390]. Notably, Th22 cells were shown to be more important long-term sources of IL-22 than Th17 cells [391]. Indeed, transfer of Th22 cells into hypersusceptible IL-22 deficient mice was able to completely rescue the mice from *C. rodentium* infection, while transfer of Th17 cells only provided partial protection [391]. *C. rodentium*

infection does result in the production of IgA and IgG antibodies from B cells; however, only IgG was shown to be protective [388, 392]. In particular, it was shown that IgG fractions from infected resistant mice provided full protection to *C. rodentium* in CD4-deficient susceptible mice [388].

### **3. The gut-brain axis in Parkinson's disease**

The gut requires highly coordinated responses between the immune system, the microbiota, and the complexly innervated network of the ENS to serve its digestive and absorptive function while also protecting from pathogenic microorganisms. A disruption to these systems can lead to systemic alterations throughout the body and affect distal organ sites such as the brain. For example, altering the microbiota can alter the types of SCFAs produced, leading to changes in intestinal permeability, BBB permeability, and promote systemic inflammatory immune responses [393]. Prolonged intestinal inflammation can lead to alterations to both ENS and vagal nerve signalling, providing a direct link between intestinal inflammation and CNS neuronal responses [218]. Conversely, the brain is able to exert control over the GI tract via the autonomic nervous system [223]. This intertwined physiology has been coined the gut-brain axis and is believed to be the foundational mechanism by which the gut may influence neurological diseases.

GI dysfunction is a common feature in PD, manifesting in some fashion in over half of all cases. As previously discussed, constipation caused by reduced gastric motility is one of the most prominent prodromal symptoms of PD and can begin occurring more than a decade before motor phenotypes appear in patients [172]. Recently, a growing body of evidence has begun elucidating links between gastrointestinal disorders and increased PD risk [394]. Further, Lewy pathology has also been proposed to originate within the gut and propagate retrogradely via the vagus nerve to

the dorsal motor nucleus of the CNS as seen by Braak and associates [56, 57]. Dysbiosis of the intestinal microbiota, accompanied by alterations in SCFA levels and intestinal permeability, is also routinely found in PD patients [395]. The following sections will aim to discuss and summarize the current evidence implicating the gut-brain axis in PD.

### **3.1 – Gastrointestinal dysfunction and Parkinson’s disease**

The prodromal nature of intestinal dysfunction in PD patients has led to notion that GI disease may play a causal role in PD initiation. Although correlative, a broad survey of German patients showed an association between gastrointestinal infection exposure and PD risk [396]. Further, intestinal transepithelial permeability is observed to be higher in PD patients, and one study noted decreased occludin protein compared healthy patients from colon biopsies [397]. This study also noted increased intestinal inflammatory cytokine expression profiles, increased T cell presence in the lamina propria, and increased TLR4 staining. Knocking out TLR4 in mice reduced colonic inflammation, restored tight junction integrity, and showed overall less PD-like symptoms in an orally administered rotenone mouse model of PD, suggesting that TLR4 signalling may mediate intestinal permeability and exacerbate PD pathology [397]. Stress-induced intestinal permeability in mice was shown to increase the severity of orally administered rotenone-induced PD-like pathology [206].

Studies involving serum analyses of PD patients indicated decreased LPS-binding protein levels, a hallmark of intestinal permeability [398]. A separate study noted increased colonic permeability in PD patients to sucralose and increased presence of Gram-negative microbes, including *E. coli*, in the lamina propria [399]. Increased exposure to luminal bacteria and LPS can

increase reactive oxygen species production by local macrophages, seeding aSyn misfolding in the ENS (explored further in the next section) [399, 400]. Human immunological studies have found increased inflammatory cytokines including TNF $\alpha$  and IL-6 in the ascending colon from PD patients [401], suggesting an overall increased inflammatory environment that has the potential to affect the vagus nerve, influence BBB permeability, and alter the composition of the microbiota. Correlative studies have also noted an association between constipation and increased Th17 T cells in PD patients, although this data remains strictly correlative [402].

Genome-wide association studies have discovered several genetic loci linked with both inflammatory bowel disease (IBD) and PD [394, 403]. Further, at least five independent epidemiological studies have associated IBD with an increased risk of PD [404-408]. One of these studies based on an American population also noted that patients on anti-TNF $\alpha$  therapy to treat IBD had decreased PD risk [407], suggesting a causality between IBD-induced inflammation and PD risk. Intestinal dopamine levels have been observed to decrease approximately 200-fold during both ulcerative colitis and Crohn's disease [409]; the mechanism behind this is unknown but believed to be a combination of loss of functional epithelial cells, loss of dopaminergic neurons caused by aSyn aggregation in the ENS, and changes to the gut microbiota [400]. Consequently, dopamine receptor D3 (a D2 family receptor) is expressed on T cells and activated in environments with low levels of dopamine [410]. Activation of dopamine receptor D3 was shown to promote pro-inflammatory Th1 and Th17 expansion [411], suggesting a possible feedback loop where inflammation can cause a drop in dopamine, which further exacerbates an inflammatory environment. Animal models have been used to show that experimentally induced colitis can exacerbate neurodegeneration in the LPS-injection rat model [412]. One study also noted that

chronic experimentally induced colitis can lead to aSyn aggregation in the colon that spreads to the brain in the human aSyn overexpression murine model [413].

### **3.2 – $\alpha$ -Synuclein spread along the gut-brain axis**

The staging done by Braak and associates had shown that Lewy pathology spreads in a predictable manner that originated from the olfactory bulb and the dorsal motor nucleus of the vagus nerve [57]. This observation led to the hypothesis that Lewy pathology may originate in tissues exposed to the environment – such as the nose and gut – and propagate to the CNS in a retrograde fashion. In this sense, the direct vagal connection to the ENS provided an ideal candidate for aSyn aggregates to propagate from the gut to brain. Braak and colleagues later did observe aSyn inclusions in both the myenteric and submucosal plexuses from sporadic PD [414], and it was postulated that insult to the intestinal environment in the form of a microbial infection could seed initial aSyn misfolding. Indeed, ENS neuronal cells have been shown to produce aSyn monomers under homeostatic conditions [45], and correlative associations have been drawn between increased intestinal permeability, increased exposure to colonic *E. coli*, increased oxidative stress, and increased insoluble aSyn staining in the colon [399]. Given the ability for oxidative stress to alter aSyn and seed misfolding [63], oxidative stress induced via immune cells upon exposure to microbes or microbial components provides a plausible mechanism by which a microbe could initiate disease. The *E. coli* protein Curli, which itself possesses an amyloid structure, was shown to be able to induce aSyn misfolding directly [60], providing a mechanism linking intestinal infection and Lewy pathology.

Despite the evidence showing Lewy pathology in the ENS, it remains debated whether misfolded aSyn can propagate retrogradely through the vagus nerve to the CNS. One study noted that patients who had undergone full truncal vagotomy, in which all the main branches of the vagus nerve were resected, were shown to have a decreased PD incidence rate [415]. Interestingly, patients who had undergone super-selective vagotomy, in which only the innervations to the upper stomach were resected, did not show any reduction in PD risk, suggesting that the connections to the lower GI tract are responsible for the associated PD risk [415]. Mouse studies have shown that injection of aSyn pre-formed fibrils into the GI tract can induce Lewy pathology within the dorsal motor nucleus of the vagus nerve [56, 416]. Knocking out the aSyn gene in this model prevented the spread of aSyn aggregation, suggesting that the pre-formed fibrils were indeed seeding the misfolding of endogenous aSyn [56]. Importantly, these studies also noted that a full truncal vagotomy was able to prevent spread to the dorsal motor nucleus, suggesting that retrograde spread via the vagus nerve is indeed possible [56, 416].

The vermiform appendix was recently discovered to be an abundant source of enteric aSyn in oligomeric and truncated forms [417]. Appendix lysates were also observed to rapidly produce aSyn aggregates *in vitro* [417]. Analysis of a Swedish registry showed that patients who had an appendectomy had reduced incidence of PD, and this effect was more prominent in the rural population [417]. Appendectomy was also associated with delayed PD onset. The authors of this study noted that patients with familial PD mutations did not benefit from appendectomy, further suggesting that familial PD is influenced solely by genetic factors. Importantly, a more recent follow-up meta-analysis of appendectomies and PD revealed no significant effect [418]; further research is needed to fully elucidate the importance of the appendix in the initiation of PD pathology.

### 3.3 – The microbiota in Parkinson’s disease

The observation that the microbiota can influence distal organ sites such as the brain has made it a target of investigation in PD research. Several studies have noted broad structural changes to the composition of the gut microbiota in PD patients, the most prominent and reproducible findings being a significant increase in Gram-negative *Enterobacteriaceae* and a significant decrease in SCFA-producing bacteria from the taxa *Prevotellaceae* and *Bacteroidetes* [419-424]. One study noted that *Bacteroidetes* were specifically less abundant in PD patients with the tremor motor phenotype [425]. *Prevotellaceae* in particular were shown to be prominent producers of mucin and SCFAs [426, 427], and thus their absence from PD patients would promote increased intestinal permeability. Indeed, PD patients were also observed to have markedly decreased levels of SCFAs in their feces including butyrate, propionate, and acetate [420]. Decreased butyrate production contributes to intestinal barrier permeability and the promotion of pro-inflammatory Th17 over Treg responses [305, 428]. Further, it is speculated that the decreased level of SCFAs would contribute to decreased oxidative phosphorylation by intestinal epithelial cells and an overall increase in oxygen within the colon, which favours *Enterobacteriaceae* growth [429].

These mechanisms are hypothesized to contribute to the increased state of colonic inflammation observed in PD patients. As previously discussed, chronic intestinal inflammation and decreased levels of SCFAs can also alter BBB permeability and vagal nerve sensitization [86, 97, 218, 307], all of which may help contribute to PD pathology. Alterations to the ENS and vagus nerve in PD also leads to reduced peristaltic movement and increased intestinal transit time,

leading expansion of the colonic microbiota to the small intestine (small intestinal bacterial overgrowth; SIBO), a condition observed in over half of all PD patients [430, 431]. SIBO further promotes intestinal inflammation and thought to also contribute to increasing intestinal permeability.

Several studies have also noted changes to the abundance of specific microbes in PD patients including microbes in the Gram-negative phylum *Proteobacteria* which contains the genus *Escherichia* [432]. The shift towards Gram-negative bacteria is believed to further contribute to TLR activation and promote the pro-inflammatory milieu observed in the gut of PD patients. One of the most striking and significant differences noted in at least two independent studies was the increase in the microbe *Akkermansia muciniphila* in PD patients [420, 425, 433], a Gram-negative mucin-degrading microbe. Contradictorily, *A. muciniphila*, despite possessing LPS and degrading mucin, is associated with anti-inflammatory states in humans and have been shown to promote thickening of the colonic mucous layers in both humans and mice; however, the mechanism by which this occurs is unknown [421, 434].

Mouse studies attempting to determine the causal effect of the microbiota in PD progression has shown conflicting evidence, further highlighting the limitation of PD murine models. In the human aSyn overexpressing murine model it was shown that the microbiota and microbiota-derived SCFAs were necessary for PD-like symptom development [435], contradicting the evidence that decreased SCFAs are associated with PD in humans. A fecal microbiota transplant from a PD patient was shown to exacerbate pathology in this model compared to a microbiota from a healthy patient. A separate study using the MPTP murine model showed that PD-like motor symptoms were accompanied by a decrease in Gram-positive *Firmicutes*, an increase in Gram-negative *Proteobacteria*, and significant activation of CNS microglia [436]. In



accordance with the previous study, this model was associated with an increase in the SCFAs butyrate, propionate, and acetate. Performing a fecal microbiota transplant from control mice reverted all motor phenotypes, decreased the level of activated microglia, and restored the level of SCFAs to baseline. Mice subjected to oral administration of rotenone showed a shift towards Gram-negative bacteria accompanied with PD-like motor phenotypes but, contrarily, showed little effect on overall SCFA production [206]. This model also showed a significant increase in the genus *Akkermansia*, akin to humans. The effect of *A. muciniphila* on intestinal inflammation is debated in the literature; both colitis and PD models have shown that *A. muciniphila* is associated with disease [206, 437], while obesity models have suggested that *A. muciniphila* has anti-inflammatory properties [438]. Different strains of *A. muciniphila* may account for some of this variability [439].

Currently there is no model that consolidates the varying information observed between humans and mouse models of PD. As a result, the direction of causality between PD and an altered microbiota in humans remains unknown. Disease timing may be an important factor – microbiota sampling done from patients diagnosed with PD are usually late in disease development as motor symptoms don't arise until approximately 70-80% of dopaminergic neurons are destroyed, while mouse sampling may be done earlier. Regardless, further research in this field is required to elucidate any potential mechanisms linking the microbiota-gut-brain axis to PD development.

## PREFACE TO CHAPTER 2

Familial forms of Parkinson's disease are believed to be caused solely by the inheritance of a mutation in a single gene such as *PINK1*. *Pink1*<sup>-/-</sup> mice are unable to recapitulate aspects of Parkinson's disease including neurodegeneration and distinctive motor phenotypes, putting into question the relevance of these mice as a model. However, the recent discovery that bacterial lipopolysaccharide can induce the presentation of mitochondrial antigens on MHC I in the absence of PINK1 has suggested that a second, environmental trigger may be necessary for symptom development, and that Parkinson's disease may be immunological in nature. In this chapter we show that a live Gram-negative intestinal infection – the attaching and effacing mouse pathogen *Citrobacter rodentium* – can induce mitochondrial antigen presentation in *Pink1*<sup>-/-</sup> mice. Repeated exposure to infection induced several key features of Parkinson's disease including motor symptoms that were reversed with L-DOPA treatment and the loss of tyrosine hydroxylase-positive axonal varicosities in the striatum.

## CHAPTER 2: Intestinal infection triggers Parkinson's disease-like symptoms in *Pink1*<sup>-/-</sup> mice

### Abstract

Parkinson's disease is a neurodegenerative disorder with motor symptoms linked to the loss of dopaminergic neurons in the substantia nigra compacta. Although the mechanisms triggering the loss of dopaminergic neurons are unclear, mitochondrial dysfunction and inflammation are thought to have key roles [440, 441]. An early-onset form of Parkinson's disease is associated with mutations in the *PINK1* kinase and *PRKN* ubiquitin ligase genes [442]. While PINK1 and Parkin (encoded by *PRKN*) are involved in the clearance of damaged mitochondria [443], but recent evidence obtained using knock-out and knock-in mouse models have led to contradictory results regarding the contribution of PINK1 and Parkin to mitophagy *in vivo* [83, 444-446]. It has previously been shown that PINK1 and Parkin have a key role in adaptive immunity by repressing presentation of mitochondrial antigens [84], which suggests that autoimmune mechanisms participate in the aetiology of Parkinson's disease. Here, we show that intestinal infection with Gram-negative bacteria in *Pink1*<sup>-/-</sup> mice engages mitochondrial antigen presentation and autoimmune mechanisms that elicit the establishment of cytotoxic mitochondria-specific CD8<sup>+</sup> T cells in the periphery and in the brain. Notably, these mice show a sharp decrease in the density of dopaminergic axonal varicosities in the striatum and are affected by motor impairment that is reversed after treatment with L-DOPA. These data support the idea that PINK1 is a repressor of the immune system and provide a pathophysiological model in which intestinal infection acts as a

triggering event in Parkinson's disease, which highlights the relevance of the gut-brain axis in the disease.

## Main Text

Although mutations in PINK1 and Parkin in patients with Parkinson's disease lead to disease progression with near 100% penetrance, *Pink1*<sup>-/-</sup> and *Parkin*<sup>-/-</sup> mice are generally healthy and display little – if any – motor impairment reminiscent of Parkinson's disease [447]. Thus, factors other than the loss of function of these proteins are likely to be required to trigger Parkinson's disease pathophysiology. We showed that in the absence of PINK1 and/or Parkin, the bacterial endotoxin lipopolysaccharide (LPS) activates the formation of mitochondria-derived vesicles and the presentation of mitochondrial antigens on major histocompatibility complex (MHC) class I molecules at the surface of antigen-presenting cells [84]. We hypothesized that bacterial infection with Gram-negative bacteria (LPS+) could trigger MitAP and elicit the establishment of mitochondria-specific autoreactive CD8<sup>+</sup> T cells.

To test this hypothesis, we used the macrophage-like cell line RAW 264.7, which was transfected to express the antigenic reporter protein glycoprotein B (gB) from Herpes virus in the mitochondrial matrix, and infected the cells with a panel of bacteria to identify activators of MitAP. In this assay, a gB-specific CD8<sup>+</sup> T cell hybridoma detects the presentation of the peptide gB<sub>498-505</sub> [448] on MHC I molecules at the surface of antigen presenting cells. All Gram-negative – but not Gram-positive – bacteria we tested induced MitAP (Fig. 1a), with the highest level obtained with enteropathogenic *Escherichia coli* (EPEC) and *Novosphingobium aromaticivorans*. The latter is suspected to be the causative agent of primary biliary cholangitis, a liver autoimmune disease

associated with the presentation of mitochondrial antigens including the matrix protein 2-oxoglutarate dehydrogenase (OGDH) [449]. To study how bacteria triggers MitAP, we focused on EPEC, a human pathogen for which a mouse model of infection exists [366]. As seen with LPS [84], EPEC infection in RAW macrophages induced MitAP within 8 h (Fig. 1b), and this was dependent on the sorting nexin Snx9 and repressed by Parkin (Fig. 1c). By contrast, the presentation of gB expressed in the cytoplasm was not inhibited in absence of Snx9 or the presence of Parkin (Fig. 1d). Exposure to heat-killed EPEC also induced MitAP, which rules out the possibility that bacterial effectors injected in host cells through the type III secretion system are required to trigger this pathway (Fig. 1e). EPEC infection induced the release of gB from mitochondria in vesicular-like structures within a 60-120 min time period (Fig. 1f, g). PINK1 also repressed the presentation of a mitochondria-derived peptide from OGDH in primary dendritic cells (Fig. 1h). EPEC infection of RAW macrophages did not induced marked degradation of mitochondrial proteins or alter the levels of the autophagy protein LC3, which suggests that mitophagy is not involved in presentation (Extended Data 1).

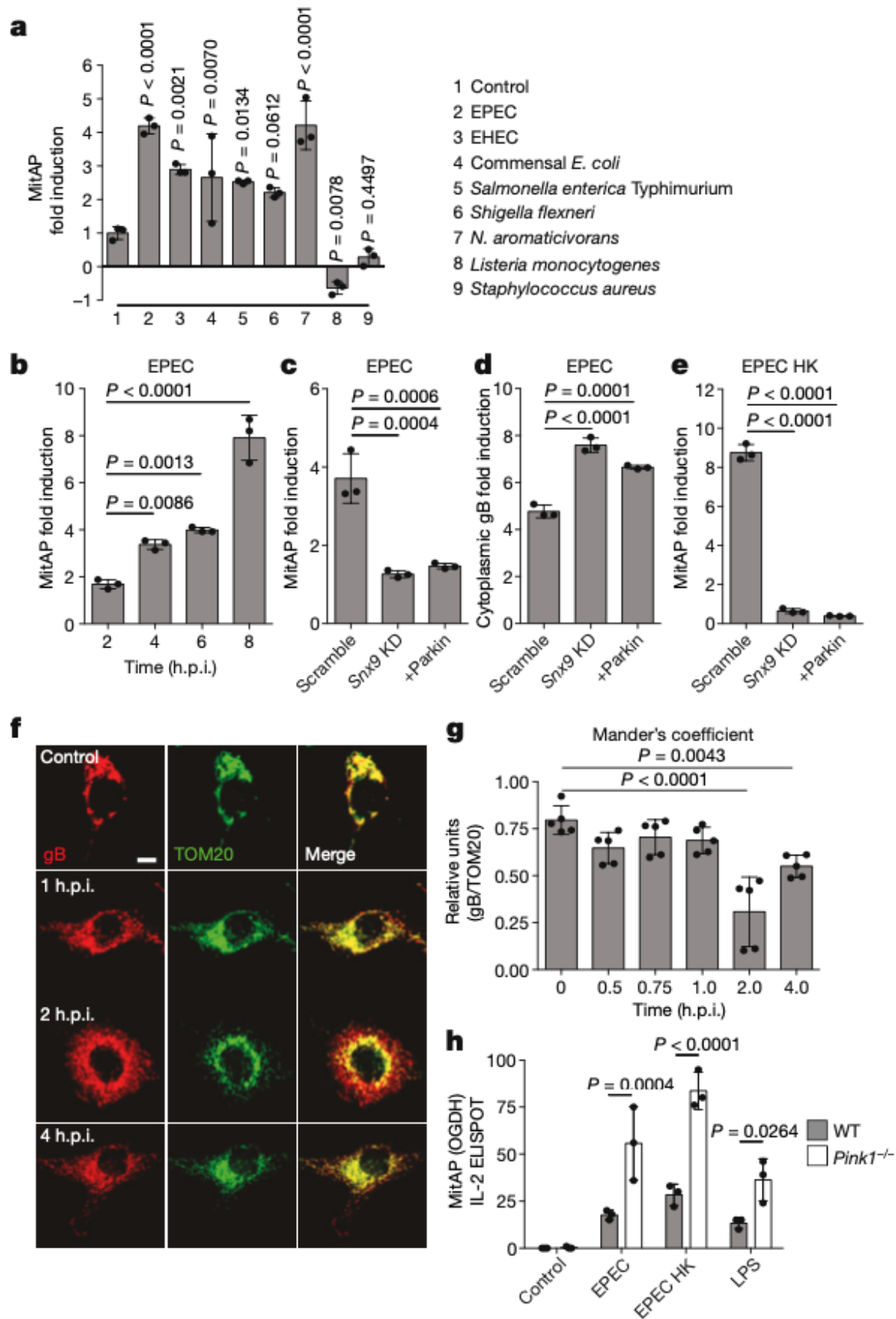


**Fig. 1 Gram-negative infection induces MitAP in vitro.** **a**, MitAP was measured as the fold induction compared with uninfected controls in RAW cells expressing the *Herpes simplex* glycoprotein B (gB) in the mitochondrial matrix (RAW-mito-gB), infected with Gram-negative (2–7) or Gram-positive (8 and 9) bacteria for 8 h. *P* values are compared with the control condition (1). **b**, MitAP in RAW cells expressing gB in the mitochondrial matrix infected with EPEC. **c**, MitAP in RAW cells expressing gB in the mitochondrial matrix ectopically expressing non-specific scrambled short hairpin RNA (shRNA), *Snx9* shRNA or Parkin, and infected with EPEC. KD, knockdown. **d**, RAW cells expressing gB in the cytoplasm were infected with EPEC and the presentation of cytoplasmic gB was measured. **e**, MitAP in RAW cells expressing gB in the mitochondrial matrix after exposure to heat-killed (HK) EPEC (1:1 ratio) after 8 h. **f**, Representative images of cells in **e** stained for gB (red) and the outer membrane protein TOM20 (green). Scale bar, 10  $\mu$ m. **g**, Quantification of co-localization between TOM20 and gB determined by Mander's coefficient at the indicated time points ( $n = 5$  cells imaged). **h**, MitAP in bone marrow-derived dendritic cells isolated from wild-type or *Pink1*<sup>-/-</sup> mice, infected in vitro with EPEC or heat-killed EPEC, or treated with LPS for 8 h. *P* values were determined by analysis of variance (ANOVA) at a 95% confidence interval followed by Dunnett's multiple comparison's test (**a–e**), or two-way ANOVA at a 95% confidence interval followed by Sidak's multiple comparison's test (**f**). Data in **a–e**, **h** are mean  $\pm$  s.d. from a representative experiment performed three times.

To determine whether *Citrobacter rodentium* – a mouse intestinal pathogen that is used as a model of EPEC infection [366] – triggers MitAP *in vivo*, we infected WT and *Pink1*<sup>-/-</sup> mice by oral gavage. Monitoring of *C. rodentium* in the stool indicated that the infection was resolved by 20 days post-infection (p.i.) (Fig. 2a). At the peak of infection (13 days p.i.), WT and *Pink1*<sup>-/-</sup> colons displayed similar levels of *C. rodentium* colonization, histopathological scores, and epithelial hyperplasia (Extended Data 2a-c). Analysis of fecal markers of intestinal inflammation (Lipocalin-2 and Calprotectin) also revealed no difference between the two genotypes (Extended Data 2d and e), and only a mild increase in circulating pro-inflammatory cytokines was detected in both mouse groups (Extended Data 3). This indicates that the loss of PINK1 did not alter the physiological response to infection nor lead to sustained, high levels of circulating cytokines, such as found recently during exhaustive exercise [450]. WT and *Pink1*<sup>-/-</sup> mice displayed a higher spleen (Fig. 2b) and colon (Extended Data 4) index than uninfected controls without noticeable weight loss (Extended Data 4), which confirmed that *C. rodentium* causes only mild symptoms in mice with a C57BL/6 background [366]. At 13 days p.i., a comparable T cell immune response was triggered in WT and *Pink1*<sup>-/-</sup> mice, consistent with the fact that both groups resolved the infection and developed an efficient protective immunity (Extended Data 5). Superinfection for three additional rounds at one-month intervals (arrows in Fig. 2a) showed no colonization of the gut, which indicates that WT and *Pink1*<sup>-/-</sup> mice were effectively immunized after the first infection [451].

We next asked whether MitAP occurred within antigen presenting cells isolated from the spleen, as seen previously upon LPS injection into *Pink1*<sup>-/-</sup> mice [84]. We observed an increase in MitAP only in *Pink1*<sup>-/-</sup> infected mice (Fig. 2c), a process that led to the establishment of a clonally selected CD8<sup>+</sup> T cell population specific for mitochondrial OGDH (Fig 2d). OGDH-specific



CD8<sup>+</sup> T cells were also observed in mice treated with LPS (Extended Data 6). The elicited IFN $\gamma$  + OGDH-specific CD8<sup>+</sup> T cells displayed markers of cytotoxicity including the cytokine receptor CX3CR1 [452], the marker of T cell degranulation CD107a, and the cytotoxic T cell granule-specific serine protease granzyme B (Fig. 2e and f, and Extended Data 7). Notably, the ligand of CX3CR1 is CX3CL1 (fractalkine), a chemoattractant expressed by neurons during inflammation [453].

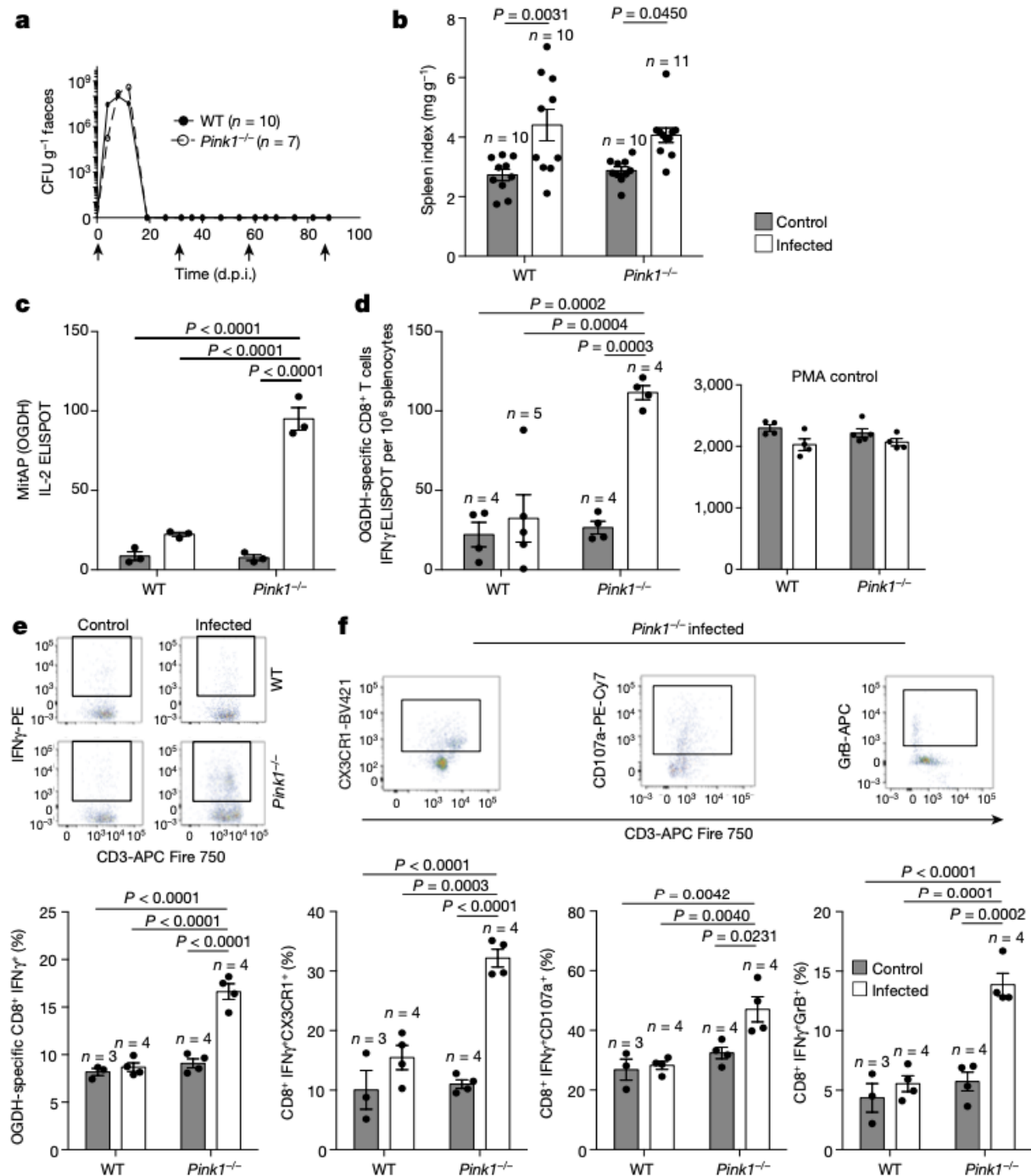


**Fig. 2** *Citrobacter rodentium* infection induces MitAP and the establishment of cytotoxic mitochondria-specific CD8<sup>+</sup> T cells in *Pink1*<sup>-/-</sup> mice. **a**, Faecal burden assessed at 4, 8, 12, 19 and 26 d.p.i. in wild-type (WT; n = 10) and *Pink1*<sup>-/-</sup> (n = 7) mice infected four times with *C. rodentium* at 28-day intervals (arrows). Data are representative of three independent experiments.

**b**, The spleen index at the peak of infection (13 d.p.i.) in control and infected wild-type and *Pink1*<sup>-/-</sup> mice. Data pooled from two independent experiments. **c**, Induction of MitAP in *C. rodentium*-infected mice (13 d.p.i.) in splenic CD11c<sup>+</sup> antigen-presenting cells pooled from three mice. Data from a representative experiment performed three times. **d**, The induction of OGDH-specific CD8<sup>+</sup> T cells in splenocytes from control and infected wild-type and *Pink1*<sup>-/-</sup> mice (13 d.p.i.) incubated with a pool of OGDH peptides. Data are representative of three independent experiments. **e**, Quantification and characterization of OGDH-specific CD8<sup>+</sup> T cells in control and infected wild-type and *Pink1*<sup>-/-</sup> mice (13 d.p.i.). APC, allophycocyanin; PE, phycoerythrin. **f**, Expression of the cytotoxic markers CX3CR1, CD107a and granzyme B (GzB), as assessed in the IFN $\gamma$ <sup>+</sup> OGDH-specific CD8<sup>+</sup> T cells from **c**. BV421, Cy7 and Fire 750 denote fluorochrome markers. Data in **e** and **f** are representative of three independent experiments. *P* values were determined via two-way ANOVA at a 95% confidence interval followed by Tukey's multiple comparison's test (**b–f**). Data in **a** denote median values. Data in **b–f** are mean  $\pm$  s.e.m.

Next, we evaluated whether these T-cells gained access to the brain. Flow cytometry analysis of cell dissociations prepared from perfused brain tissue confirmed that immune cells – including T cells – infiltrated this organ in infected animals within 13-28 days p.i. (Fig. 3a-c), irrespective of their genotype (Extended Data 8). Similar results were observed using ELISPOT analyses (Fig. 3d). However, anti-mitochondrial (OGDH)-specific CD8<sup>+</sup> T cells were observed only in the brains of the *Pink1*<sup>-/-</sup> mice (Fig. 3e). which suggested that autoimmune attacks on the dopaminergic system could occur. For this, dopaminergic neurons (DNs) would have to express MHC I molecules and present the appropriate mitochondrial antigens. Recent work reported that LPS or IFN $\gamma$  induced the expression of MHC I molecules at the surface of DNs, rendering them susceptible to CD8<sup>+</sup> T cell attack *in vitro* [115]. We observed that LPS and IFN $\gamma$  treatment strongly induced the expression of MHC class I molecules at the surface of cultured neurons and glial cells (mostly astrocytes) present in mixed preparations isolated from the substantia nigra (Fig. 3f). In co-culture experiments, mixed neuronal preparations from *Pink1*<sup>-/-</sup> mice stimulated an OGDH-specific CD8<sup>+</sup> T cell hybridoma, indicating MitAP induction (Fig. 3g). We then sorted the LPS- and IFN $\gamma$ -treated neurons and astrocytes using magnetic beads coated with the astrocyte marker GLAST and found that only the GLAST-negative fraction (neurons) effectively stimulated the OGDH hybridoma (Fig. 3h). Next, we developed a cytotoxic assay to test whether MitAP induction in DNs would render them susceptible to T cell attack. For this, we used CD8<sup>+</sup> T cells isolated from transgenic 2C mice, which all recognize OGDH peptides loaded on MHC I molecules, including the LSPFPFDL (p2Ca) peptide used in our study [454]. Within two days of co-culture, we observed a marked swelling of DN cell bodies and a shortening of neuronal processes in the somatodendritic compartment (Extended Data 9). At five days, we observed that approximately 40% (p<0.0001) of the TH-positive DNs from *Pink1*<sup>-/-</sup> mice were killed, with no

significant decrease in non-dopaminergic neurons (Fig. 3i). Wild type DNs were not significantly targeted by the OGDH specific CD8<sup>+</sup> T cells. Direct loading of the OGDH peptide onto MHC class I at the neuron surface was used as a positive control, and led to robust neuron death (Fig. 3i), which confirms that T cell attack in our assay was driven by the presentation of this peptide. Together, these data suggest that infection in a genetically susceptible background (*Pink1*<sup>-/-</sup>) engages a pathophysiological process that is accompanied by the infiltration of mitochondria-specific CD8<sup>+</sup> T cells in the brain, potentially exposing DNs to T cell attack.

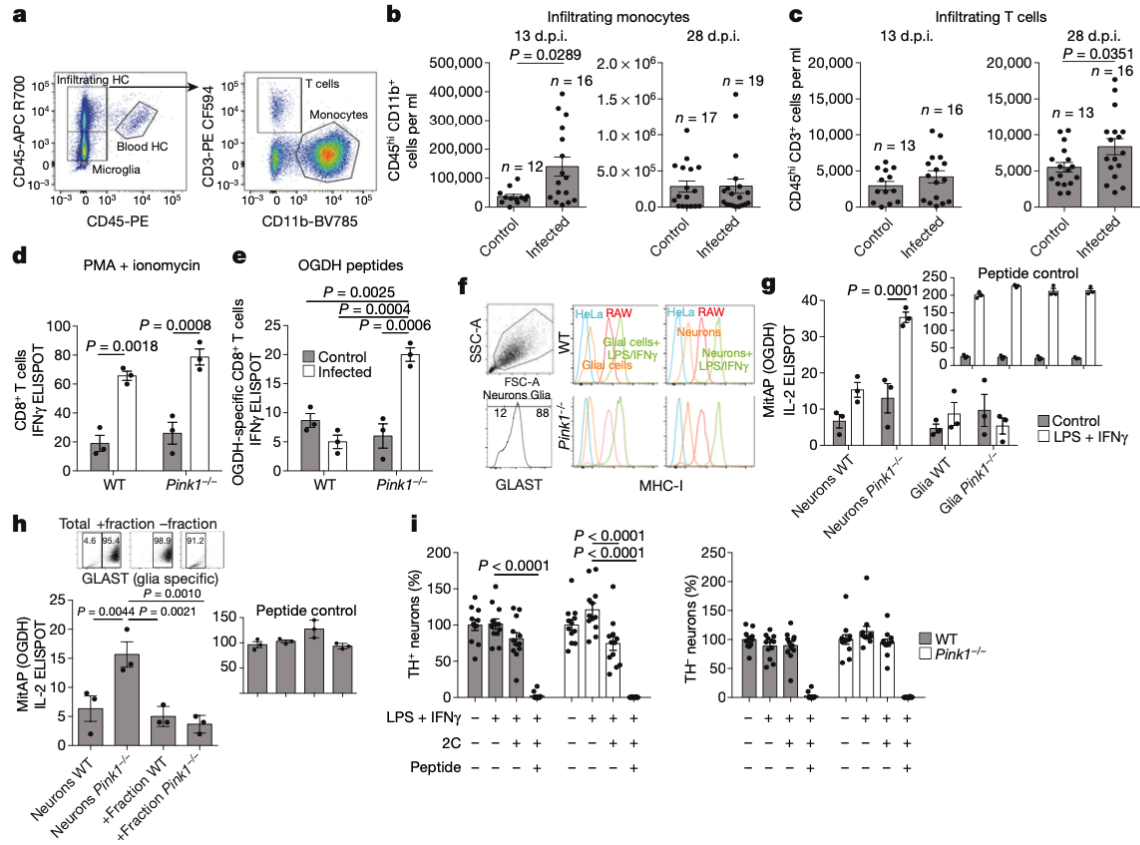


**Fig. 3** *Citrobacter rodentium* infection induces anti-OGDH T cell infiltration into the central nervous system. **a**, Representative gating on haematopoietic cells (HC) from brain and spinal cord at 13 and 28 d.p.i. **b**, **c**, Absolute numbers of monocytes (**b**) and T cells (**c**) at 13 and 28 d.p.i. Data pooled from three independent experiments (b and c). **d**, **e**, Total number of IFN $\gamma$ -producing T cells determined by PMA + ionomycin stimulation (**d**) and number of IFN $\gamma$ -producing T cells specific for OGDH peptides (**e**). (d, e) Data pooled from five mice. PMA, phorbol 12-myristate 13-acetate. Data in **d** and **e** are from a representative experiment performed three times. **f**, Neurons from the substantia nigra compacta cultured on glial cells gated with anti-MHC-I and anti-GLAST antibodies. The expression of MHC class I in neurons and glial cells with or without LPS and IFN $\gamma$  treatment, HeLa cells (negative control) and RAW cells (positive MitAP control) is shown. **g**, The induction of MitAP was assessed in LPS/IFN $\gamma$ -treated neurons, control neurons, and glial cells by

IL-2 ELISPOT. Data from a representative experiment performed three times. **h**, MitAP was measured in GLAST<sup>-</sup> neuronal and GLAST<sup>+</sup> glial cell populations. Enrichment is shown in the top panels. Data from a representative experiment performed three times. **i**, Percentage of neuron killing after five days of co-incubation with conditions indicated. Data pooled from four independent experiments ( $n = 12$  replicates).  $P$  values were determined by two-tailed Mann–Whitney unpaired  $t$ -test at a 95% confidence interval (**b**, **c**), two-way ANOVA at a 95% confidence interval with Tukey’s multiple comparison’s test (**d**, **e**, **g**, **i**), one-way ANOVA at a 95% confidence interval with uncorrected Fischer’s least significant difference test (**h**). Data are as mean  $\pm$  s.e.m.

We observed the emergence of motor impairment in the infected *Pink1*<sup>-/-</sup> mice (Fig. 2a) as early as 4 months p.i. This included limited hind leg activity – a feature also reported in a rat model of Parkinson’s disease [455] – as well as slower general movement and a decrease in head lifting (Supp. Video 1). Quantitative behavioural tests performed at 6 months p.i. indicated that infected *Pink1*<sup>-/-</sup> mice had reduced total movement time, reduced total distance travelled and reduced vertical movement episodes, but similar strength in the grip test, compared to infected WT littermates (Fig. 4a). Infected *Pink1*<sup>-/-</sup> mice performed poorly in the pole test – a sensitive measure of motor impairment in rodent Parkinson’s disease models associated with dopamine loss in the striatum [456] (Fig. 4b). Acute administration of the dopamine precursor L-DOPA reversed the pole test deficit within 60 min, linking the observed phenotypes with loss of dopamine (Fig. 4b and Supp. Video 2). Motor impairments were not detected in uninfected *Pink1*<sup>-/-</sup> mice, confirming previous studies reporting little, if any, Parkinson’s disease-like symptoms in these mice [447, 457, 458]. Behavioural tests at 12 months p.i. showed that a reversal of the PD-like symptoms had occurred (Extended Data 10a, and Fig 4c).

To understand the mechanisms underlying the transient emergence of motor impairment in infected *Pink1*<sup>-/-</sup> mice, we performed unbiased stereological counting of the number of DNs in the ventral mesencephalon. No significant difference between the various groups of mice was observed in both the substantia nigra compacta (Fig. 4d) and ventral tegmental area (Extended Data 10b) at 6 months p.i. However, we observed that the density of tyrosine hydroxylase (TH)-positive axonal varicosities in the DN axon terminals was reduced by more than 40% in both the dorsal and ventral striatum of *Pink1*<sup>-/-</sup> mice at 6 months p.i. (Figs. 4e and f). Consistent with the reversed behavioural phenotype, the density of TH signal returned to normal in the striatum of infected *Pink1*<sup>-/-</sup> mice 12 months p.i. (Extended Data 10c, d). The density of dopamine transporter-



positive axon terminals was also significantly reduced at 6 months p.i. (Extended Data 10e), indicating that the alterations observed were not simply the result of downregulation of TH. The recovery of striatal TH reversal occurred concomitantly with a decrease in the levels of autoreactive OGDH-specific CD8<sup>+</sup> T cells detected in infected *Pink1*<sup>-/-</sup> mice with aging (Extended Data 10f), further supporting the involvement of autoimmune mechanisms in the disease process. Although the mechanisms responsible for the destruction of DNs in Parkinson's disease are unknown, it is generally assumed that motor impairments in patients emerge only after considerable loss of dopaminergic neurons. Our data suggest that impairment of terminals may precede death of DNs, providing a window of opportunity for therapeutic intervention. How the transient impairment of motor functions observed here relates to the progression of human Parkinson's disease is not clear. This could be related to the fact that experimental mice are kept in pathogen-free conditions whereas humans are exposed to numerous pathogens throughout their lives. Further experiments are needed to determine whether consecutive infections with various pathogens in *Pink1*<sup>-/-</sup> mice will lead to non-reversible motor dysfunctions and death of DNs.

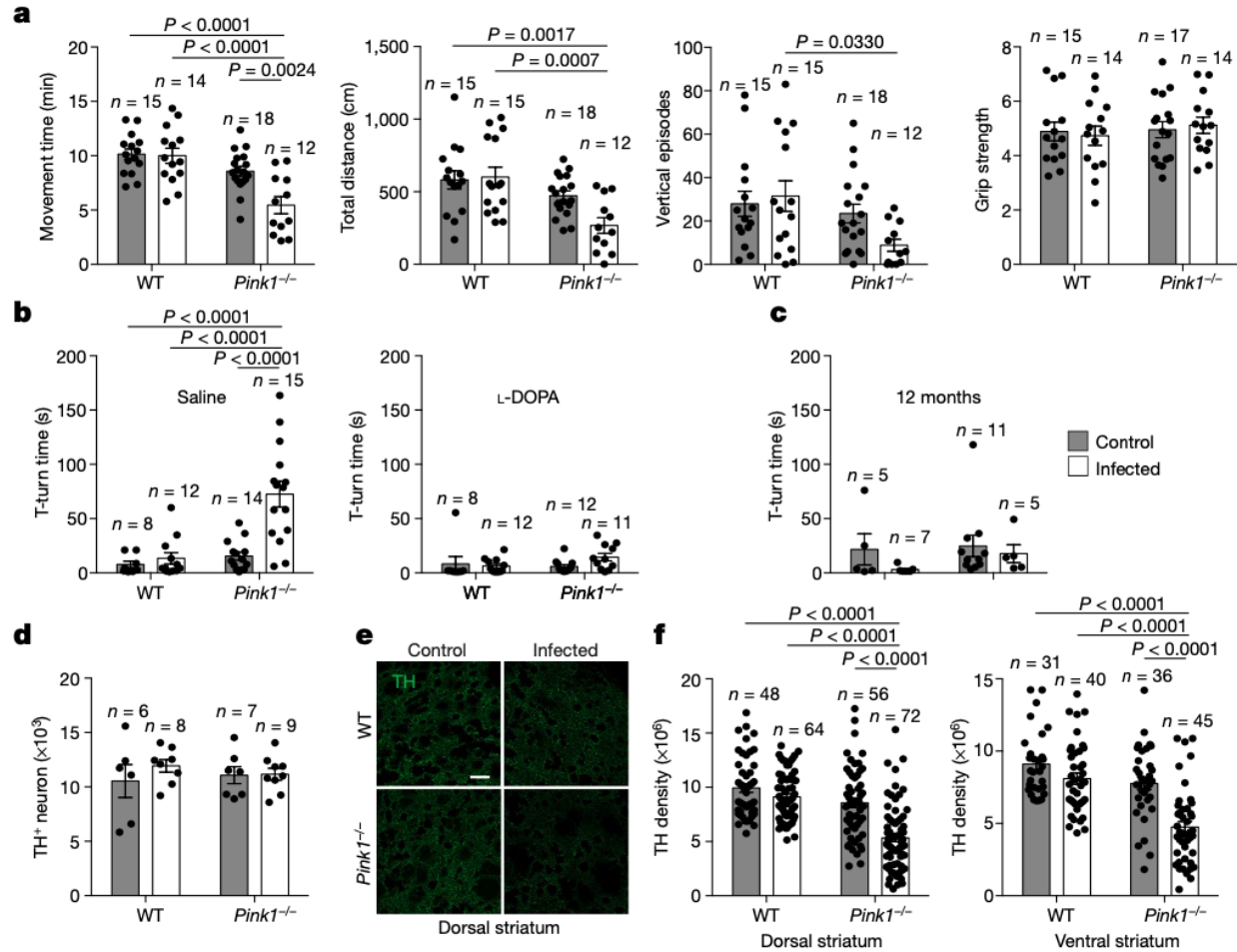


**Fig. 4** *Citrobacter rodentium* infection induces motor impairment and a loss of dopaminergic axonal varicosities in the striatum of *Pink1*<sup>-/-</sup> mice. **a**, Mice were tested at 6 m.p.i. for movement time, distance travelled, the number of vertical episodes, and grip strength. Data pooled from three independent experiments. **b**, Pole test in mice at 6 m.p.i. treated with L-DOPA or saline. Data pooled from three independent experiments. **c**, Pole test on a single cohort of mice at 12 m.p.i. **d**, Stereological analyses of TH<sup>+</sup> neurons in the substantia nigra. Data pooled from two independent experiments. **e**, Representative images of TH staining in the dorsal striatum at 6 m.p.i. Data representative of two independent experiments. Scale bar, 100 μm. **f**, Quantification of TH signal density in the dorsal and ventral striatum from the mice in **d**, determined by measuring

signal strength per unit of area. *P* values determined by two-way ANOVA at a 95% confidence interval with Tukey's multiple comparison's test. Data are mean  $\pm$  s.e.m.

While additional research is needed to fully unravel the mechanism at play and understand the relevance and implications of these findings for human disease, our data provide evidence that an autoimmune response engaged in the absence of PINK1 during intestinal infection may participate in the etiology of Parkinson's disease. We observed mitochondria-specific CD8<sup>+</sup> T cells within the brains of infected *Pink1*<sup>-/-</sup> mice and demonstrated their capacity to kill DNs *in vitro*. The extent of the involvement of T cells in the destruction of DNs *in vivo* remains to be established. Previous work has addressed the role of adaptive immunity in Parkinson's disease. It was shown that Th17 CD4<sup>+</sup> T cells target and attack DNs in a human induced pluripotent stem-cell model of sporadic Parkinson's disease [113], and CD4<sup>+</sup> and CD8<sup>+</sup> helper and cytotoxic T cells selective for  $\alpha$ -synuclein have been found in the blood and brains of Parkinson's disease patients [114]. Our work points to a role for PINK1 and MitAP in the initiation of autoimmune mechanisms leading to dopaminergic dysfunction after infection, but it does not exclude additional contributions of PINK1 in mitochondrial quality control pathways. The discovery that intestinal infection transforms asymptomatic *Pink1*<sup>-/-</sup> mice into a fully penetrant model, presenting with acute motor symptoms that are reversed after treatment with L-DOPA, adds to the growing body of evidence that implicates the gut-brain axis in Parkinson's disease [440, 459, 460]. This also provides a model to characterize the onset of Parkinson's disease and develop therapeutic approaches.

## Methods

### Animals and cells

2C, *Pink1*<sup>-/-</sup> [84] and littermate control mice were handled in strict accordance with good animal practice as defined by the Canadian Council on Animal care and according to protocols approved by the Comité de déontologie animale of the Université de Montréal and the McGill University animal care facility. Mito-gB and Cyto-gB cell lines were established from RAW 264.7 macrophage cell lines expressing H-2K<sup>b</sup> and the glycoprotein gB from HSV-1 in the mitochondria or in the cytoplasm<sup>2</sup>. Snx9 KD and +Parkin GFP cells were generated as previously described [84]. They were cultured in DMEM (10% (vol/vol)) fetal calf serum (FCS), penicillin (100 units/ml) and streptomycin (100 µg/ml). The β-galactosidase-inducible HSV gB/K<sup>b</sup>-restricted HSV-2.3.2E2 CD8<sup>+</sup> T cell hybridoma (2E2) was kindly provided by Dr. Frank Carbone (University of Melbourne). The OGDH/L<sup>d</sup> and OGDH/K<sup>b</sup>-restricted 2CZ CD8T<sup>+</sup> cell hybridoma was kindly provided by Dr. Nilabh Shastri, (University of California). Hybridomas were maintained in RPMI-1640 medium supplemented with 5% (vol/vol) FCS, glutamine (2 mM), penicillin (100 units/ml) and streptomycin (100 µg/ml).

#### Primary Neuronal Cultures

Postnatal day 0–3 (P0–P3) mice were cryoanesthetized and decapitated for tissue collection. Primary cultures of substantia nigra neurons were prepared from wild type (WT) and *Pink1*<sup>-/-</sup> mice and plated onto pre-established monolayers of astrocytes as previously described [461].

#### Preparation of bacterial cultures and heat-killed EPEC for *in vitro* experiments

Enteropathogenic *Escherichia coli* (strain E2348/69), Enterohemorrhagic *Escherichia coli* (strain EDL933), *Shigella flexneri* (strain M90T), *Salmonella enterica* serovar Typhimurium (strain SL1344), Commensal *Escherichia coli* isolated from mouse, *Listeria monocytogenes* (strain EGD), and *Staphylococcus aureus* (strain Newman) were prepared in overnight cultures of LB

broth and incubated at 37°C while shaking. *Novosphingobium aromaticivorans* (strain ATCC700278) was prepared in LB broth and incubated at 30°C standing for 48 hours. All bacterial strains were diluted to a final concentration of  $1 \times 10^5$  CFU/ $\mu$ l in DMEM+10%FBS before being used to infect cells an MOI of 1. Heat-killed EPEC was prepared by placing the diluted culture of EPEC at 95°C for 10 min before being applied to cells at a dose of 1:1 heat-killed EPEC to cells.

#### MHC class I Antigen Presentation Assay

$2 \times 10^5$  antigen presenting cells were infected with EPEC or with the indicated bacteria at MOI 1 for the indicated times. Cells were then fixed with 1% PFA for 10 min at RT and extensively washed with RPMI, 10% fetal bovine serum (FBS) and 0.1 M glycine. Finally,  $10^5$  2E2 T cells were added for 16 h and  $\beta$ -galactosidase activity measured at 595 nm after the addition of CPRG substrate.

For OGDH antigen presentation using the OGDH/K<sup>b</sup> restricted hybridoma 2CZ, we used an IL-2 ELISPOT assay (Mabtech, 3441-4APW) to measure OGDH antigen presentation by H2-K<sup>b</sup> expressing cells (*Pink1*<sup>-/-</sup> and littermate control derived cells). For experiments with neurons, cells cultured for 10 days were treated or not with LPS (1  $\mu$ g/ml) and IFN $\gamma$  (100U/ml) for 3 days. Cells were then trypsinised and immediately fixed with 1% PFA.  $10^5$  cells from the neuron culture were incubated with  $5 \times 10^4$  2CZ hybridoma cells in an IL-2 ELISPOT plate. Alternatively, neurons were negatively sorted using GLAST magnetic beads (Miltenyi, 130-095-826). Briefly, cultured cells were treated with LPS (1  $\mu$ g/ml) and IFN $\gamma$  (100U/ml) for 3 days. Cells were then trypsinised, washed and immediately incubated with GLAST magnetic beads for 15 min at 4°C. Cells were then magnetically separated and a negative fraction (neurons) and positive fraction (glial cells) were collected. Cells were then counted and fixed with 1% PFA and the IL-2 ELISPOT assay was performed using  $10^3$  cells (neurons or glial cells) and  $5 \times 10^4$  2CZ cells.

## Immunofluorescence

RAW cells were fixed with pre-warmed (37°C) 5% PFA that was directly added to cells after removal of the culture medium. After incubation at 37°C for 15 min, PFA was quenched with 50 mM NH<sub>4</sub>Cl/PBS for 10 min at RT. Cells were permeabilized with 0.1% Triton X- 100/PBS (v/v) for 10 min at RT and blocked with 5% FBS/PBS for 10 min at RT. Cells were incubated with the indicated primary antibodies (anti-gB SantaCruz, 1:100, anti-Tom20 SantaCruz, 1:1000) for 16h. After the wash with PBS, cells were incubated with the appropriate secondary antibodies (anti-rabbit-A488 Life Technologies, 1:1000, anti-mouse-A568 Life Technologies, 1:1000) for 1h. Cells were observed with an Andor/Yokogawa spinning disk confocal system (CSU-X) attached to an Olympus IX81 inverted microscope and 100X or 60X objectives (NA1.4). For the quantification of mitochondria-derived vesicular structures, stacks of images were acquired with 0.4 µm steps were analyzed by ImageJ. Quantification was based on at least 3 independent experiments (10-15 cells/experiment). Measurement of the Mander's colocalization coefficient was made using JACoP plugin from ImageJ.

For neuronal cultures, after PFA (4%) fixation, cells were permeabilized (Triton X-100 0.1%) and non-specific binding sites blocked with BSA (50 mg/ml). To identify TH neurons and quantify their survival, a rabbit anti-TH antibody was used (rabbit-anti-TH Millipore, 1:2000). This antibody was used in combination with a monoclonal mouse anti-microtubule associated protein 2 antibody (mouse-anti-MAP2 Sigma, 1:1000) to distinguish dopaminergic neurons from other neurons. TH positive neurons as well as MAP2 positive neurons were counted using an epifluorescence microscope (Nikon TE200).

To prepare brain sections, WT and *Pink1*<sup>-/-</sup> mice were deeply anesthetized with pentobarbital (0.07 mg/g, i.p.) before intracardiac perfusion with PBS 1M followed by 100 ml of

4% PFA. The brain was removed, post-fixed by immersion for 24h in PFA solution at 4°C, and then placed in sucrose solution for 48h. Serial coronal free-floating sections (40 µm thickness) sections were cut using a cryostat and collected in an antifreeze solution. Coronal sections were permeabilized (Triton X-100 0,1%), nonspecific binding sites blocked (BSA, 105 mg/ml) and incubated overnight with rabbit anti-TH antibody (1:2000) or rat anti-DAT antibody (rat-anti-DAT Millipore, 1:2000). Fluorescence imaging quantification analyses on brain slices were performed on images captured using a Fluoview FV1000 confocal microscope (Olympus). Images acquired using 488 nm laser excitation were scanned sequentially to prevent nonspecific bleed-through signal. Brain slices images were captured using a 60x oil-immersion objective from fields in the dorsal and ventral striatum, SNc and VTA. The striatal compartment located superior to the plane of the anterior commissure and inferior to the corpus callosum was considered dorsal striatum, while the ventral striatum included the shell and core of the nucleus accumbens. For image acquisition in the dorsal striatum, four random fields on each side were taken from the left and the right hemisphere in each section. For acquisition in the ventral striatum, SNc and VTA, two fields were selected per hemisphere in each section. All images quantification was performed using ImageJ (National Institutes of Health) software. A threshold was first applied at the same level for every image analyzed before performing further analyses. This threshold was determined by measuring the average background signal intensity and subtracted from the raw image. Quantification of TH-positive axon terminals in dorsal striatal sections was performed by averaging eight fields per section and eight different sections were independently quantified for each mouse. For ventral striatum sections, the analysis was performed by averaging four fields per section and five different sections were independently quantified for each mouse.

#### Stereological Analysis



Sections were first rinsed in 0.01 M PBS, then in 0.01 M PBS + 30% H<sub>2</sub>O<sub>2</sub> and again three times in 0.01 M PBS. Sections were then incubated in rabbit anti-TH antibody at a 1:1000 dilution (all dilutions made in 0.3% Triton X-100/0.01 M PBS) for 48 h at 4°C. After rinses in 0.01 M PBS (3 × 10 min), they were incubated for 12h at 4°C in biotin-streptavidin conjugated AffiniPure IgG (anti-rabbit-streptavidin Jackson Immunoresearch, 1:200), washed three times with 0.01 M PBS and then incubated for 3h at RT in streptavidin HRP conjugate (GE Healthcare, 1:200). Sections were visualized after 5 min 3,3'-diaminobenzidine tetrahydrochloride (Sigma-Aldrich)/glucose oxidase reaction, mounted on charged microscope slides in 0.1 M acetate buffer, counterstained with cresyl violet, defatted using a series of ethanol and xylene baths and finally coverslipped using permount. The number of TH neurons in both SNc and VTA was analyzed by unbiased stereological counting. The total number of TH neurons was obtained by applying the optical fractionator method [462] using Stereo Investigator (version 6; MicroBrightField). In brief, TH-immunoreactive neurons were counted in every sixth section at 100× magnification using a 60 × 60 μm<sup>2</sup> counting frame. A 10 μm optical dissector was used with two 1 μm guard zones, and counting sites were located at 100 μm intervals after a random start.

#### Infection with *Citrobacter rodentium*

For the short-term experiments, mice were infected with chloramphenicol resistant *Citrobacter rodentium* (4x10<sup>8</sup> CFU) by oral gavage. To monitor bacterial burden, faeces were collected from each mouse, weighed, dissociated in PBS, serial-diluted, and plated on chloramphenicol MacConkey agar Petri plates. To determine colon-associated *C. rodentium*, the last centimeter of distal colon was harvested, weighed, dissociated in PBS, diluted, and plated on chloramphenicol MacConkey agar Petri plates. Petri plates were incubated at 37°C overnight to allow colony growth, which were counted the following day. Final counts were measured as

CFU/g of feces and plotted on a log-scale in Prism. Fecal collection occurred on days 4, 8 and 12 days post infection (p.i.). Mice were sacrificed at day-13 p.i. For the long-term experiments, mice were infected 4 times, 28 days apart. Feces were collected after each infection on days 4, 8, 12, 19, and 26 p.i.

#### Dendritic cell purification

*Pink1*<sup>-/-</sup> and littermate control mice were infected or not with *C. rodentium* and sacrificed at day-13 p.i. Spleens were collected, and CD11c<sup>+</sup> DC were purified using a pan dendritic cells isolation kit (Miltenyi) followed by a positive selection using CD11c magnetic beads (Miltenyi). DC purity and activation level was assessed by FACS (BD FACS Canto II).

#### IFN $\gamma$ ELISPOT

*Pink1*<sup>-/-</sup> and littermate control mice were either infected with *C. rodentium* and sacrificed at day-13 p.i., or injected 4 times intraperitoneally with 1 mg/kg LPS 1 week apart prior to sacrifice. Spleens were collected, and 10<sup>6</sup> cells were stimulated with a pool of 6 OGDH peptides in pre-coated IFN $\gamma$  ELISPOT plates (from Mabtech kit, 3321-4APT) for 16h: the well-known p2Ca peptide (H2-K<sup>b</sup> restricted [463]) and 5 other peptides that were designed using the online epitope prediction software SYFPEITHI. These peptides are: IVYETFHL (H2-K<sup>b</sup>-restricted), STPGNFFHVL (H2-D<sup>b</sup>-restricted), IVFTPKSL (H2-K<sup>b</sup>-restricted), MSSANGVDYV (H2-D<sup>b</sup>-restricted) and SAPVAAEPFL (H2-D<sup>b</sup>-restricted). Peptides were added at 0.5  $\mu$ mol/ml each. Plates were washed with PBS and incubated 2h at RT with detection antibody (clone R4-6A2-biotin, 1  $\mu$ g/ml), following which plates were washed again with PBS and incubated 1h at RT with streptavidin-ALP (1:1000). Plates were then washed a final time and exposed to substrate (BCIP/NBT) until spots emerged. For the CNS-infiltrating T cells, irradiated splenocytes (20Gy)

from control littermates were used as antigen presenting cells.  $10^6$  splenocytes were added per well.

#### FACS analysis

*Pink1*<sup>-/-</sup> and littermate control mice were infected or not with *C. rodentium* and sacrificed at day-13 p.i. Spleens were collected, and  $10^7$  cells were stimulated with a pool of 6 OGDH peptides (see section ELISPOT IFN $\gamma$ ) for 24h. In the last 6h of stimulation, Golgi Stop (BD, 1:1000) and Golgi Plug (BD, 1:1000) were added to inhibit cytokine secretion. Live-dead (BD) staining was performed by adding the dye (1:2000) for 20min at 37°C. Cells were blocked with PBS, 2% FBS and 1% CD16/CD32 for 15min at 4°C with agitation, and the surface markers stained by adding the appropriate antibodies for 20min at 4°C with agitation. Cells were fixed and permeabilized using a kit from BD (Fixation/Permeabilization solution kit, 554714): the cytofix/cytoperm solution was added for 20 min at 4°C with agitation. Cells were blocked with the perm wash solution and 1% CD16/CD32 for 15 min at 4°C with agitation and stained for intracellular cytokines or markers for 16h at 4°C with agitation. Cells were analyzed using the BD FACS Aria II SORP. For experiments with neurons, cells kept for 10 days *in vitro* were treated or not with LPS (1 $\mu$ g/ml) and IFN $\gamma$  (100U/ml) for 3 days. Cells were then trypsinized and stained with GLAST-APC (1:500) and H2-K<sup>b</sup>-PE (1:100) for 15 min at 4°C. Cells were finally fixed and analyzed by FACS Canto II. Absolute numbers were enumerated with true count beads (BioLegend). Antibody details can be found in the reporting summary.

#### Neuron cytotoxicity experiments

Cells kept for 10 days *in vitro* were treated or not with LPS (1 $\mu$ g/ml) and IFN $\gamma$  (100U/ml) for 3 days. Cells were then exposed to  $5 \times 10^5$  2C purified CD8T cells (using the EasySep mouse CD8<sup>+</sup> T cell isolation kit from Stemcell) that were previously activated for 2 days with anti-

CD3/anti-CD28 beads. After a total of 15 and 18 days in culture cells were fixed with 4% PFA and stained for TH, MAP-2 and DAPI. The number of TH+ and MAP-2+ neurons was counted.

#### Cytokine quantification

Serum was obtained by allowing the blood to clot at RT for a minimum of 30 min and centrifuged at 2000 x g for 10 min at +4°C. The supernatant was transferred to a fresh tube and stored at -70°C until the analysis. Cytokines were quantified by Eve Technologies (Calgary, Alberta).

#### Behavioural tests

All the behavioral experiments were performed during the light cycle (10 a.m. to 5 p.m.), on male and female mice of both genotypes. The investigator was blinded to the treatment group during experimental procedures. Mice housed 2–5 in a cage were tested at 6 or 12 months p.i. On the test day, mice were transferred to the testing room and allowed a resting time of 60 min before testing.

#### Grip Strength test

Grip strength tests were performed with a grip strength meter (model Bio-GS3, BioSeb, France). Mice were tested three times and the results were averaged for each mouse. The muscular strength (N) of mice was quantified by testing either the front paws or the 4 paws. Each mouse was weighed before the grip strength test.

#### Basal locomotor activity

Open Field automated activity chambers (Omnitech Electronics Inc., Columbus, USA) were used to quantify horizontal activity and rearing. All experiments were performed between 2 PM and 5 PM using animals maintained on a 12h light/dark cycle from 7 AM to 7 PM. Mice were placed individually in activity boxes (20 x 20 cm) where their horizontal and vertical activity was

measured by photocell beams. Spontaneous locomotor activity was measured in 10 min intervals during 30 min. Primary experimenter was blinded to both genotype and infection status.

#### Pole test

The pole was made with a 48 cm metal rod of 1cm diameter covered with adhesive tape to facilitate traction, placed in the home cage. Mice were positioned head-up at the top of the pole and the time required to turn (t-turn) and climb down completely was recorded. They were either given 6.5 mg/kg benserazide (Sigma, B7283) + 25 mg/kg L-DOPA (Sigma, D1507), or an equal volume of saline. Failure to descend the pole was given a maximum time of 180s before exclusion. Primary experimenter was blinded to both genotype and infection status.

#### Western Blotting:

Total cell lysates were collected in Pierce lysis buffer + cOmplete EDTA-free protease inhibitor (1 tablet / 50 ml) (Roche), quantified and normalized via the BCA Pierce Quantification Kit (Thermo Fischer), and 20 µg was used for immunoblotting. Proteins were separated on mini-Protean precast gels (BioRad) at 200V for 40 min and transferred electrophoretically at 100V for 90 min onto an activated PVDF membrane. Membranes were blocked in phosphate buffered saline + 0.4% tween20 (PBST) + 5% milk for 30 min at room temperature, followed by incubation in primary antibody (diluted in PBS + 1% bovine serum albumin) overnight at 4°C. The following day the membranes were washed 3 times in PBST, incubated in secondary antibody (diluted in PBST + 5% milk) for 30 min at room temperature, and washed 3 more times in PBST. Membranes were visualized by developing in Clarity Western ECL substrate (BioRad). Antibody details can be found in the reporting summary

#### Isolation of infiltrating lymphocytes:

Control and *C. rodentium*-infected WT and *Pink1*<sup>-/-</sup> littermates were anesthetized by isoflurane induction at either day 13 or 28 post infection and cardiac-perfused with PBS prior to collection of brain and spinal cord tissue (CNS, central nervous system). To dissociate the CNS tissue, all samples were minced via scalpel and digested in RPMI + 0.5 mg/ml Collagenase D + 0.01 mg/ml DNase I for 25 min at 37°C prior to filtration through a 70 µm filter. To isolate lymphocytes, samples were centrifuged at 1500 RPM at 4°C for 8 min, resuspended in a 33% percoll solution diluted in RPMI, and centrifuged again at 2000 RPM without brake at 25°C for 30 min to pellet lymphocytes. The pellet was then resuspended in 300µl of PBS + 2% FBS + 2 mM EDTA before proceeding with FACS staining. To discriminate infiltrating hematopoietic cells (HC) from blood HC, mice were anesthetized, injected i.v. with CD45-PE (BD) for 3min and then cardiac-perfused with PBS prior to collection of brain and spinal cord tissues.

#### T cell purification

*Pink1*<sup>-/-</sup> and littermate control mice were infected with *C. rodentium* and sacrificed at day-28 p.i. Mice were perfused with PBS and CNS tissue was collected. T cells were then purified using a Pan T cell isolation kit (Miltenyi) and tested for the frequency of OGDH-specific CD8 T cells using IFN $\gamma$  ELISPOT.

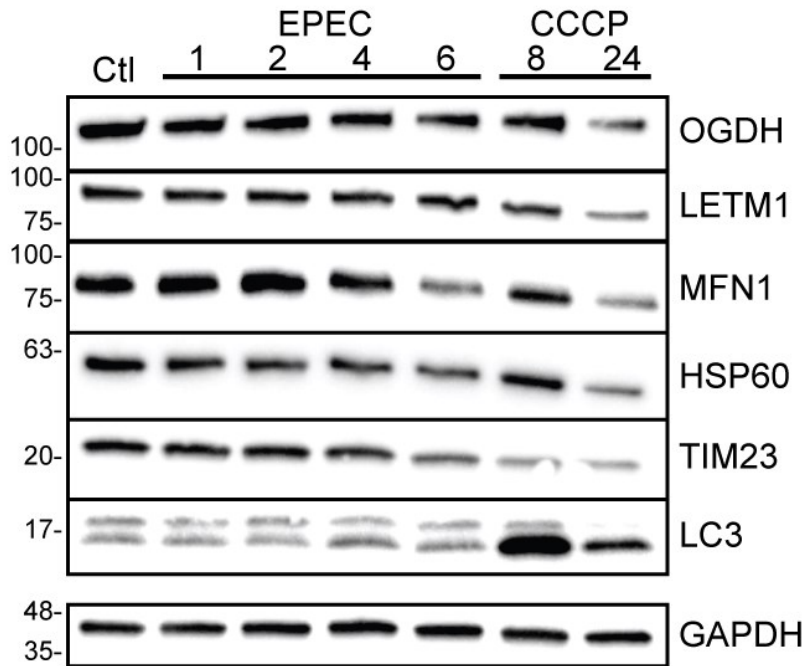
#### Histopathology:

Control and *C. rodentium*-infected WT and *Pink1*<sup>-/-</sup> littermates were euthanized at day 13 post infection and their distal colon sections were harvested. Tissue was fixed in 10% buffered formalin, paraffin embedded, sectioned at 5 µm and stained with hematoxylin and eosin (H&E). H&E sections were blindly scored by an expert board-certified pathologist for both pathology and crypt heights. Slides were imaged on a Zeiss Axiovert 1 using Zen 2 software.

#### ELISA:

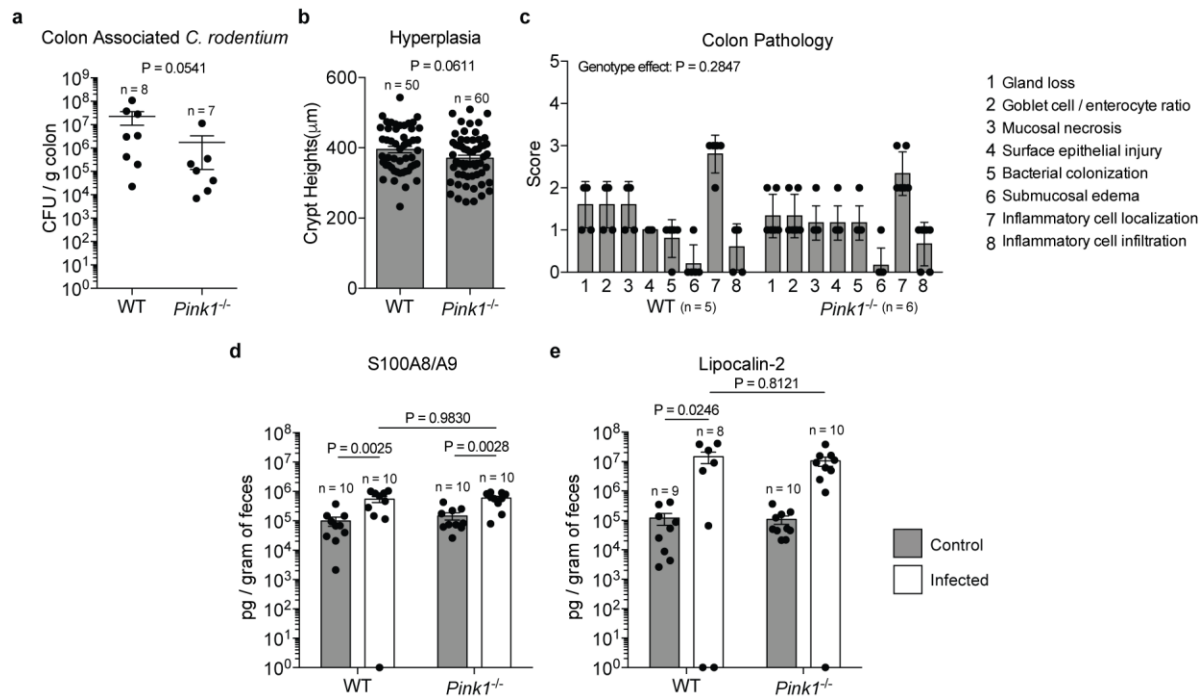
Fecal samples were suspended in PBS + 0.1% Tween20 at a ratio of 100 mg of feces / ml. Samples were vortexed for 20 min prior to centrifugation at 13000 rpm and to isolate the supernatants, which were stored at -80°C. ELISAs were performed using the mouse Lipocalin-2/NGAL DuoSet and the mouse S100A8/A9 DuoSet kits (R&D Systems). Samples were applied to a 96-well plate pre-coated with either Lipocalin-2 or S100A8/A9 capture antibody, washed three times with PBS + 0.05% Tween20, treated with the respective detection antibody, washed three times, treated with streptavidin-HRP, washed three more times, and developed with a 1:1 ratio of hydrogen peroxide and tetramethylbenzidine. The optical density of the plates was read at 450 nm.

## Extended Data

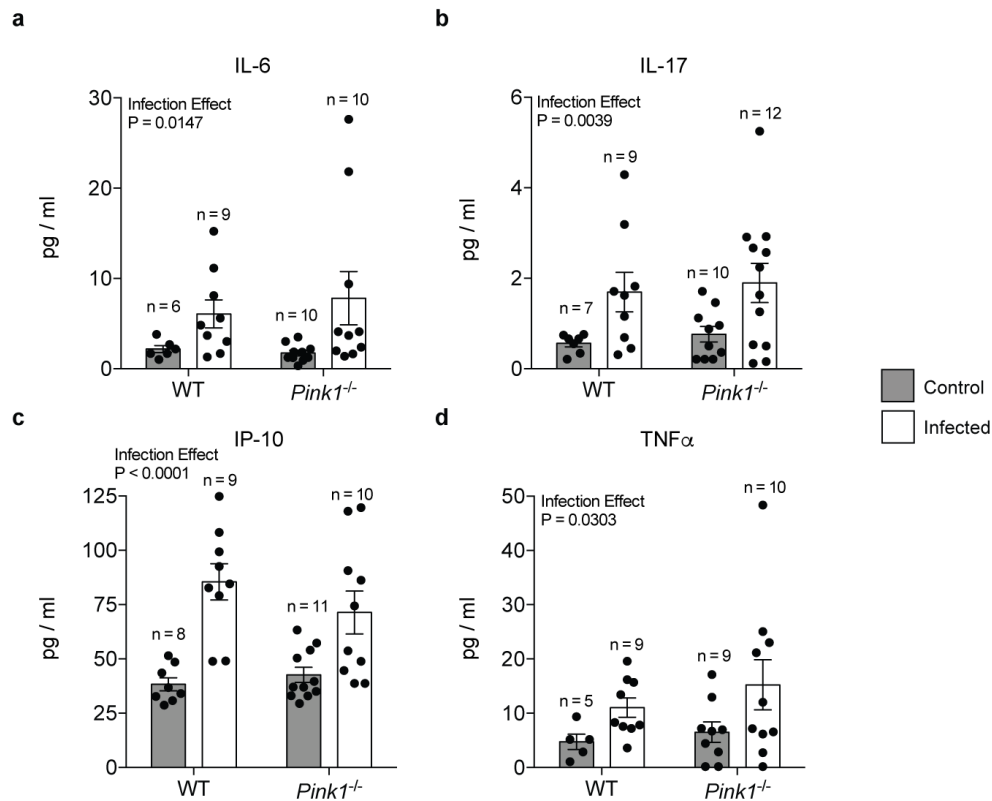


**Extended Data Fig. 1 EPEC infection results in the selective degradation of mitochondrial proteins.** RAW 264.7 macrophages were either infected with EPEC at a multiplicity of infection of 1 for 1, 2, 4 or 6 h or treated with 20  $\mu$ M CCCP for 8 or 24 h alongside control (Ctl) cells. Total cell lysates were collected for all conditions, quantified, separated via SDS-PAGE, and probed for mitochondrial markers via western blot. Data are representative of two independent experiments.

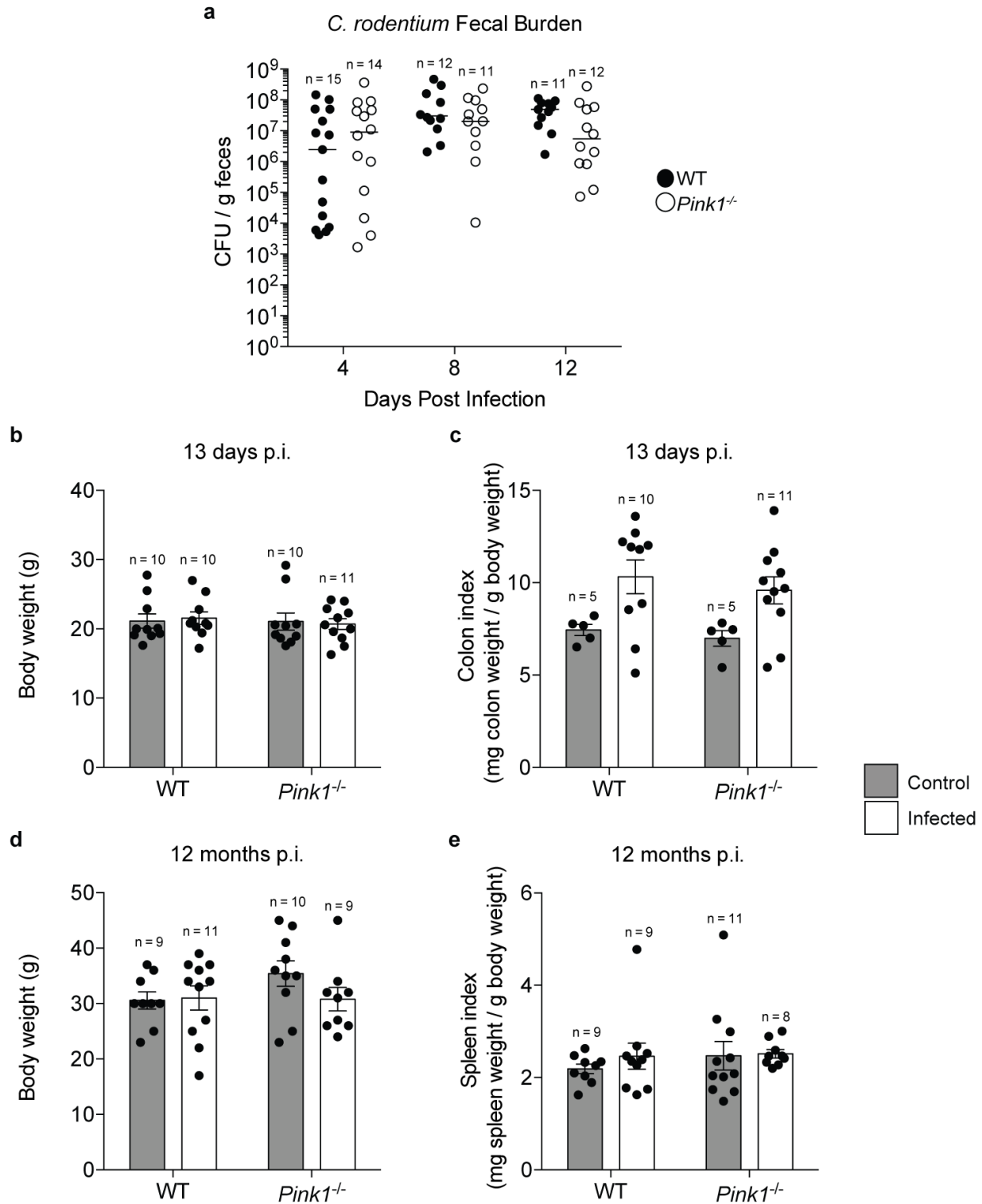




**Extended Data Fig. 2** *Citrobacter rodentium* induces mild colonic pathology and inflammation in both wild-type and *Pink1*<sup>-/-</sup> mice. **a**, The distal colon was collected at 13 d.p.i. and assessed for colon-associated *C. rodentium* in infected wild-type and *Pink1*<sup>-/-</sup> mice via serial dilution and plating on MacConkey agar. Data representative of two independent experiments. **b**, Analysis of colonic epithelial hyperplasia via measurement of crypt heights from haematoxylin and eosin (H&E)-stained colon sections. Data represents individual crypt measurements from five wild-type mice and six *Pink1*<sup>-/-</sup> mice. Data representative of two independent experiments. **c**, Tissue pathology scores from H&E-stained distal colon sections from infected wild-type and *Pink1*<sup>-/-</sup> mice. **d**, **e**, Protein quantification of faecal lipocalin-2 (**d**) and S100A8/A9 (**e**) from control and infected wild-type and *Pink1*<sup>-/-</sup> mice. Data pooled from two independent experiments. *P* values were determined by two-tailed Mann–Whitney unpaired *t*-test at a 95% confidence interval (**a**, **b**), two-way ANOVA at a 95% confidence interval (**c**), or two-way ANOVA at a 95% confidence interval with Tukey’s multiple comparison’s test. Data are mean  $\pm$  s.e.m.

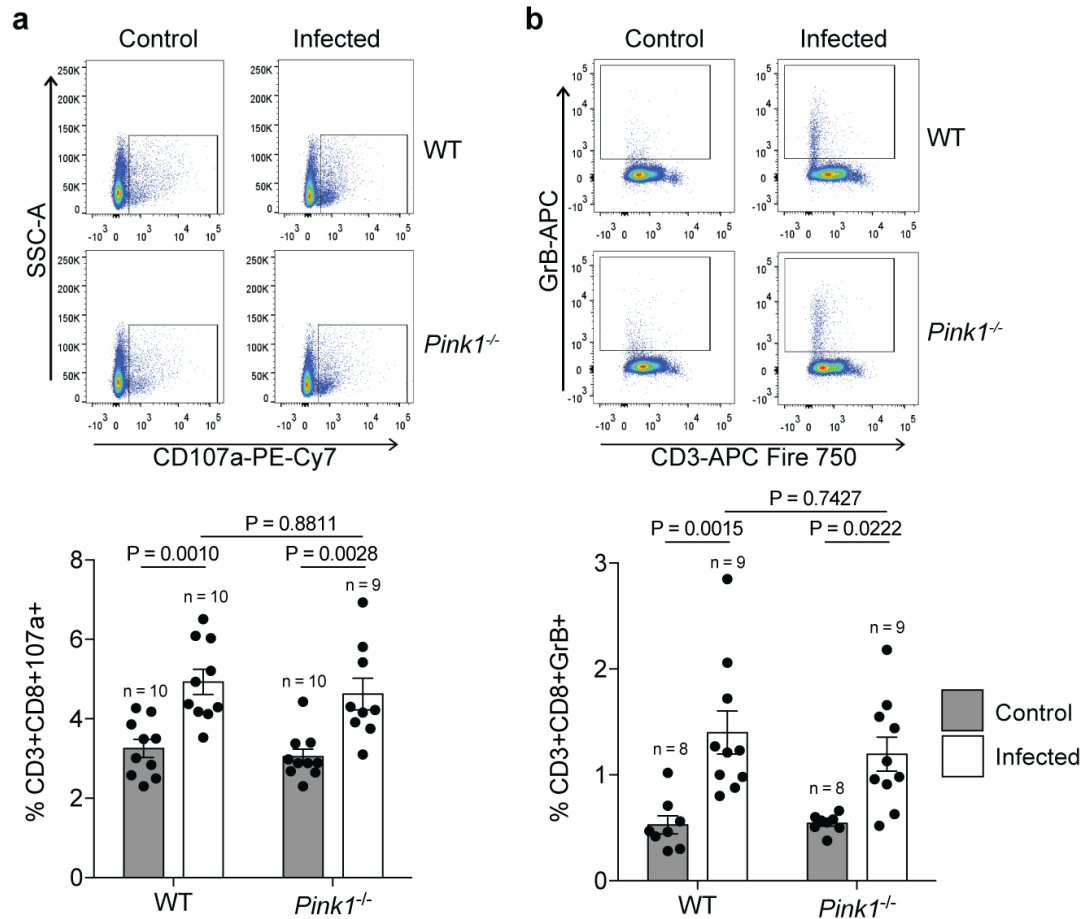


**Extended Data Fig. 3** *Citrobacter rodentium* infection induces a mild increase in systemic pro-inflammatory cytokines in both wild-type and *Pink1*<sup>-/-</sup> mice. **a–d**, Mice were infected with *C. rodentium* and serum was collected at 13 d.p.i. for ELISA analysis of the pro-inflammatory cytokines IL-6 (**a**), IL-17 (**b**), IP-10 (**c**) and TNF (**d**). All data pooled from two independent experiments. *P* values were determined by two-way ANOVA at a 95% confidence interval. Data are mean  $\pm$  s.e.m.

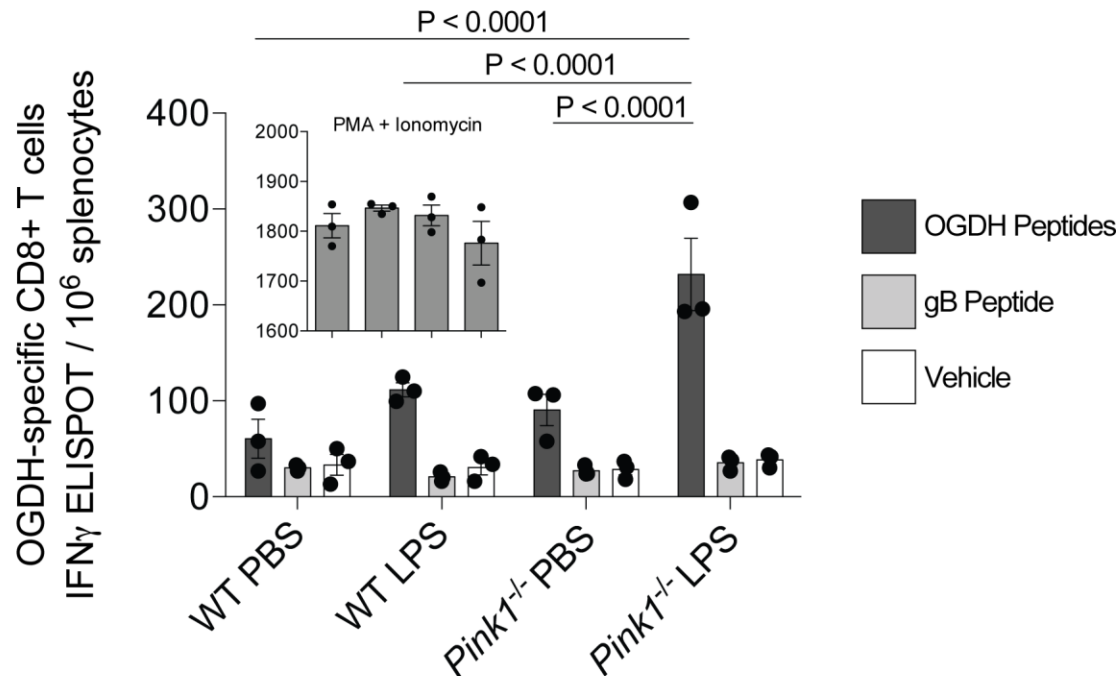


**Extended Data Fig. 4** *Citrobacter rodentium* infection parameters are similar in wild-type and *Pink1*<sup>-/-</sup> mice. **a**, *Citrobacter rodentium* faecal burden in wild-type and *Pink1*<sup>-/-</sup> mice at 4, 8 and

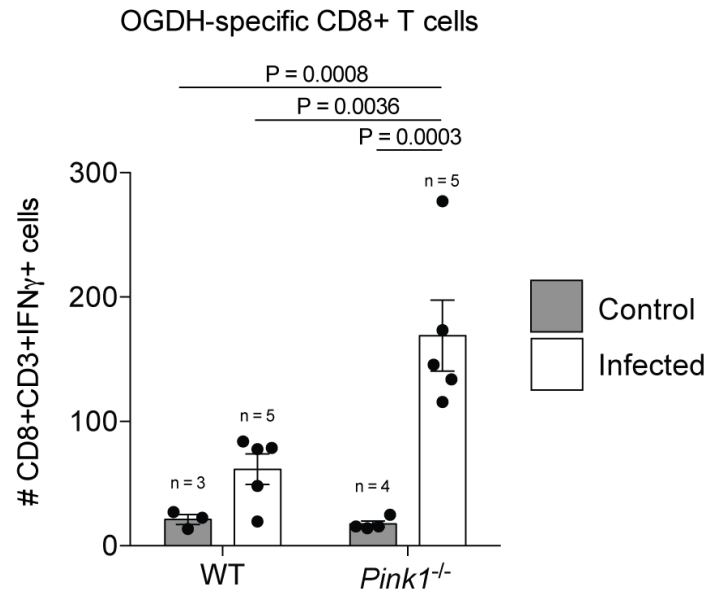
12 d.p.i. Data pooled from three independent experiments. **b**, **c**, Body weight (**b**) and colon index (**c**) of control and infected wild-type *Pink1*<sup>-/-</sup> mice at 13 d.p.i. Data pooled from two independent experiments. **d**, **e**, Body weight (**d**) and spleen index (**e**) of uninfected and infected wild-type and *Pink1*<sup>-/-</sup> mice serially infected four times, 28 days apart, measured at 12 months after initial infection in a single cohort of animals. Data in **a** denote median values; data in **b–d** are mean ± s.e.m.



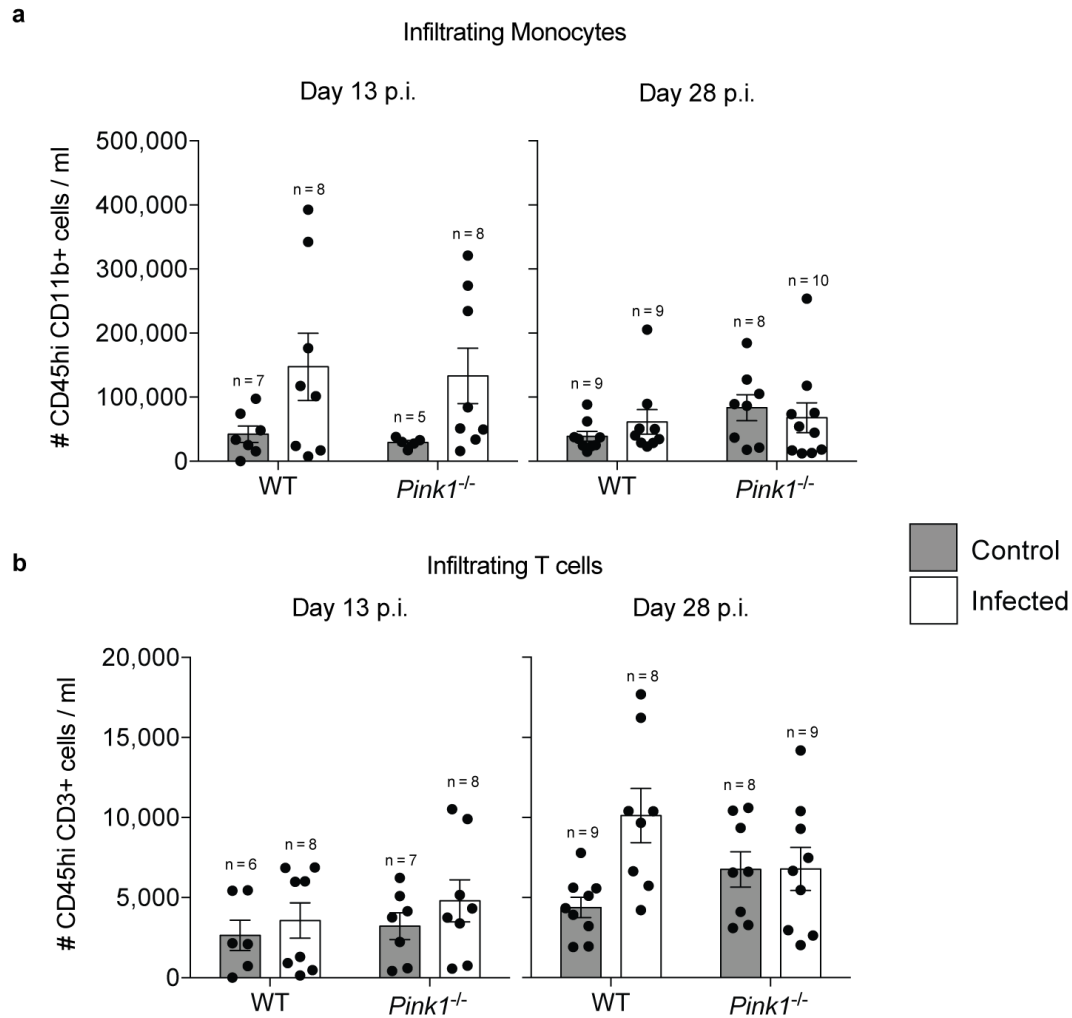
**Extended Data Fig. 5** *Citrobacter rodentium* infection induces a similar CD8<sup>+</sup> T cell immune response in both wild-type and *Pink1*<sup>-/-</sup> mice. Mice were infected with *C. rodentium* and CD8<sup>+</sup> T cell markers were assessed at 13 d.p.i. in the spleen. **a**, **b**, Flow cytometry was used to quantify the frequency of CD3<sup>+</sup>CD8<sup>+</sup>CD107a<sup>+</sup> (**a**) and CD3<sup>+</sup>CD8<sup>+</sup>GrB<sup>+</sup> (cytotoxic CD8<sup>+</sup> T cells) (**b**) in control and infected wild-type and *Pink1*<sup>-/-</sup> mice. *P* values determined by two-way ANOVA at a 95% confidence interval with Tukey's multiple comparison's test. Data are mean ± s.e.m.



**Extended Data Fig. 6 Intraperitoneal injection of LPS induces anti-OGDH CD8<sup>+</sup> T cells in *Pink1*<sup>-/-</sup> mice.** Wild-type and *Pink1*<sup>-/-</sup> littermates were injected with 1 mg kg<sup>-1</sup> of LPS intraperitoneally four times, once a week starting at 6 weeks of age. Spleens were obtained 7 days after the last treatment. The presence of anti-OGDH CD8<sup>+</sup> T cells was tested for via IFN $\gamma$  ELISPOT by replacement of peptides in MHC class I complexes on splenocytes with OGDH peptides, control gB peptides, or vehicle (water), and plated with splenic T cells on IFN $\gamma$  detection plates. PMA peptide-loading controls to assess the levels of MHC class I expression in each group are shown in the inset. Data are representative of three independent experiments performed in triplicate. Significance was determined by two-way ANOVA at a 95% confidence interval with Tukey's multiple comparison's test. Data are mean  $\pm$  s.e.m.

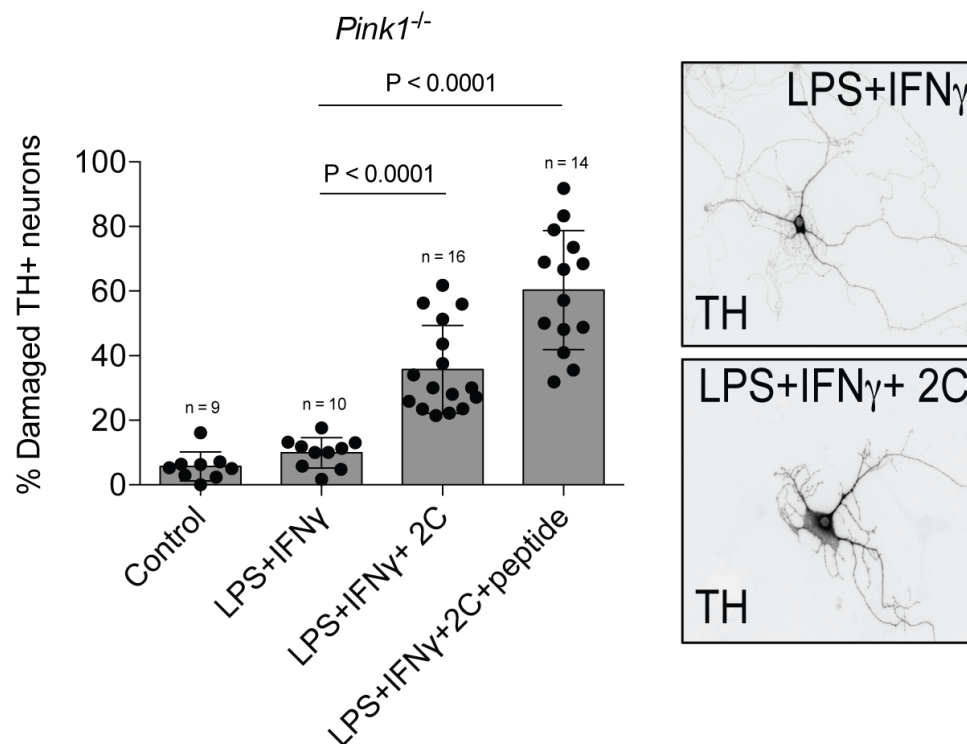


**Extended Data Fig. 7 *Citrobacter rodentium* infection induces OGDH-specific CD8<sup>+</sup> T cells in *Pink1*<sup>-/-</sup> mice.** Flow cytometry and spleen numeration were used to quantify OGDH-specific CD8<sup>+</sup> T cells previously identified by their expression of IFN $\gamma$  after stimulation with OGDH peptides. Analysis was done on both control and infected wild-type and *Pink1*<sup>-/-</sup> mice. Data are representative of three independent experiments. *P* values were determined by two-way ANOVA at a 95% confidence interval with Tukey's multiple comparison's test. Data are mean  $\pm$  s.e.m.

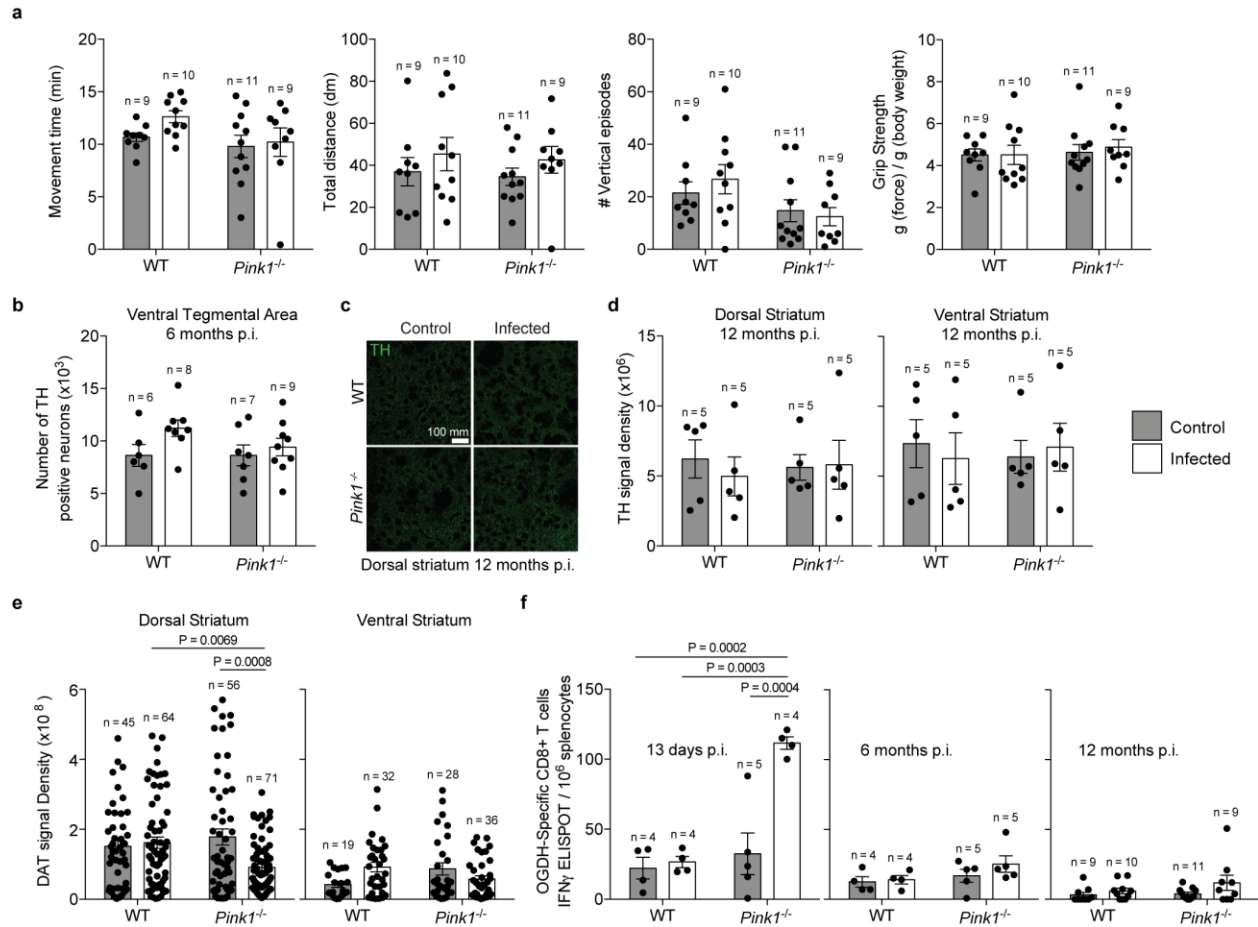


**Extended Data Fig. 8** *Citrobacter rodentium*-induced monocyte and T cell infiltration into the central nervous system occurs in both wild-type and *Pink1*<sup>-/-</sup> mice. Brain and spinal cord tissue were assessed for haematopoietic cells in both control and infected wild-type and *Pink1*<sup>-/-</sup>. **a**, **b**, Absolute number of monocytes (**a**) or T cells (**b**) at 13 and 28 d.p.i. were calculated using true count beads. Data pooled from two independent experiments. Data are mean ± s.e.m.





**Extended Data Fig. 9 TH<sup>+</sup> neurons are susceptible to damage from 2C cells after treatment with LPS and IFN $\gamma$ .** Quantification (left) and representative images (right) of the cytotoxic assay in which neurons from *Pink1*<sup>-/-</sup> mice were treated with LPS, IFN $\gamma$  or left untreated (control) and co-cultured with or without OGDH-specific CD8<sup>+</sup> T cells isolated from 2C mice for 2 days. Exogenous addition of OGDH peptides (last column) was used as a positive control. Dopaminergic neurons were identified by TH staining, and damage was determined by the presence of swollen cell bodies and the shortening of dendrites. Data represents measures from individual coverslips and are representative of three independent experiments. *P* values were determined by one-way ANOVA at a 95% confidence interval with Tukey's multiple comparison's test. Data are mean  $\pm$  s.e.m.

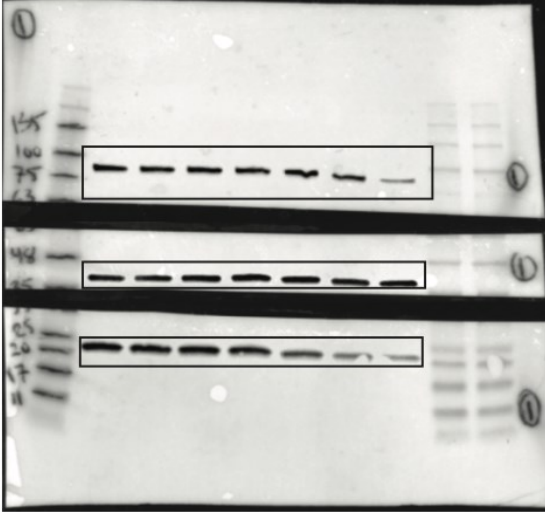


**Extended Data Fig. 10 *Citrobacter-rodentium*-induced anti-mitochondrial CD8<sup>+</sup> T cells and loss of locomotor function is transient.** **a**, Actimetry tests and grip strength of mice at 12 m.p.i. Data are from a single cohort of mice. **b**, Quantification of TH<sup>+</sup> neurons in the ventral tegmental area after stereological analyses. Data pooled from two independent experiments. **c**, Representative images of TH staining in the dorsal striatum at 12 m.p.i. Data are from a single cohort. **d**, Quantification of TH<sup>+</sup> neurons in the dorsal and ventral striatum after stereological analyses. Representative of a single cohort. **e**, Quantification of dopamine transporter (DAT) signal density in the dorsal and ventral striatum at 6 m.p.i. Data accumulated from mice from **b**. Data pooled from two independent experiments. **f**, Quantification of OGDH-specific T cells from wild-type and *Pink1*<sup>-/-</sup> mice at 13 d.p.i., 6 m.p.i. and 12 m.p.i. Data at 13 d.p.i. are representative of

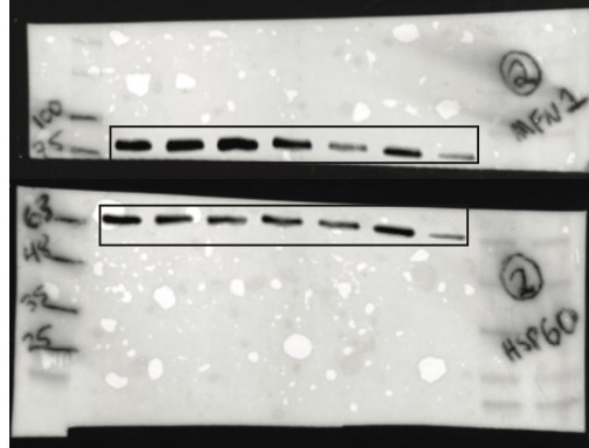
three independent experiments; data at 6 m.p.i. are representative of two independent experiments; data at 12 m.p.i. are from a single cohort of mice. *P* values determined by two-way ANOVA at a 95% confidence interval with Tukey's multiple comparison's test. Data are mean  $\pm$  s.e.m.

## Supplementary Information and Videos

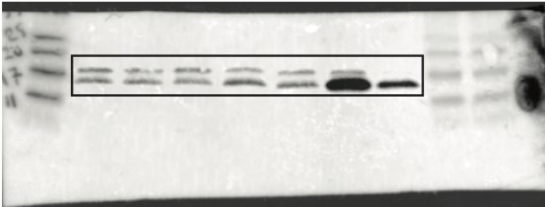
Gel 1: LETM1 (top), GAPDH (middle), TIM23 (bottom)



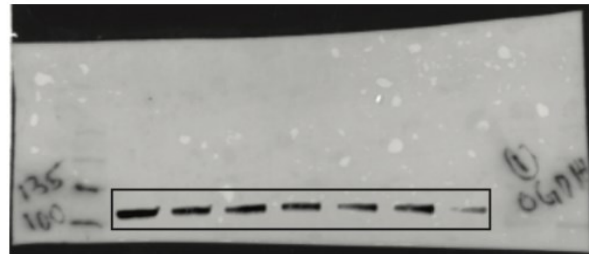
Gel 2: MFN1 (top), HSP60 (bottom)



Gel 3: LC3



Gel 4: OGDH



**Supplementary Figure 1: Source western blot images.** Samples were quantified and normalized prior to loading onto 4 separate gels. All 4 gels were loaded from the same tube simultaneously with 20  $\mu$ g of protein. Ladder was loaded on the left of the samples once and twice on the right of the samples, and molecular weights indicated with a pen. Boxes indicate where the image was cropped for manuscript.

<https://youtu.be/UEdUToE6S0U>

**Supplementary Video 1: *Pink1*<sup>-/-</sup> mice develop an observable motor impairment during serial infection with *C. rodentium*.** WT and *Pink1*<sup>-/-</sup> mice were serially infected with *C. rodentium* four times over the course of four months and monitored for the development of a motor impairment. Four months after the initial infection, *Pink1*<sup>-/-</sup> mice (right video panel) developed an observable motor impairment compared to WT mice (left video panel) with regards to movement speed, splayed legs, decreased

<https://youtu.be/hyaFIMKsuxM>

**Supplementary Video 2: L-DOPA treatment rescues the T-turn impairment observed in *Pink1*<sup>-/-</sup> mice serially infected with *C. rodentium*.** *Pink1*<sup>-/-</sup> mice serially infected with *C. rodentium* showed a decreased ability to T-turn (invert 180° when placed upright on a pole) (left video panel). Treatment of these mice with L-DOPA reverted the T-turn impairment (right video panel).

## **Acknowledgements**

MD and HM received a grant from the Michael J. Fox Foundation. The authors thank Mélanie Guérin for technical support. LET was supported by a grant from the Brain Canada Foundation, the Krembil Foundation and by the CIHR (grant MOP106556). AMP was supported by the Finnish Parkinson's Disease Foundation. CD was supported by a studentship from Parkinson Canada. SG was supported by CIHR grants (MOP 133580 and PJT-162406) and NSERC (RGPIN-2014-05119). TC was supported by studentships from CIHR and Healthy Brains for Healthy Lives initiative.

## **Data Availability Statement**

The authors declare that data supporting the findings of this study are available within the paper and its supplementary information files.

## PREFACE TO CHAPTER 3

Our work above suggests a two-hit model for familial forms of Parkinson's disease: genetic susceptibility (knockout of *Pink1*) and an environmental trigger (intestinal infection with *Citrobacter rodentium*). A growing body of literature has highlighted differences in the microbiota between Parkinson's disease patients and healthy controls. In chapter 3, we sought to compare the bacterial microbiota in *Pink1*<sup>-/-</sup> and wild-type mice over the course of *C. rodentium* infection. Bioinformatic analysis on bacterial 16s rRNA genes was used to determine differences in overall community diversity and individual microbe abundances. Short-chain fatty acids have also been shown to influence the gut-brain axis and be altered in Parkinson's disease patients and was also investigated in this study. Comparison of this data not only allowed for inferences between genotypes, but also how infection can disrupt the intestinal environment. The divergent results observed between human studies and mouse models is further explored and compared to our own data.



## **CHAPTER 3: Characterization of the intestinal microbiota during *Citrobacter rodentium* infection in a mouse model of infection-triggered Parkinson's disease**

### **Abstract**

Parkinson's disease (PD) is a neurodegenerative disorder that has been shown to be influenced by the intestinal milieu. The gut microbiota is altered in PD patients, and murine studies have begun suggesting a causative role for the gut microbiota in progression of PD. We have previously shown that repeated infection with the intestinal murine pathogen *Citrobacter rodentium* resulted in the development of PD-like pathology in *Pink1*<sup>-/-</sup> mice compared to wild-type littermates. This addendum aims to expand this work by characterizing the gut microbiota during *C. rodentium* infection in our *Pink1*<sup>-/-</sup> PD model. We observed little disturbance to the fecal microbiota diversity both between infection timepoints and between *Pink1*<sup>-/-</sup> and wild-type control littermates. However, the level of short-chain fatty acids appeared to be altered over the course of infection with butyric acid significantly increasing in *Pink1*<sup>-/-</sup> mice and isobutyric acid increasing in wild-type mice.

### **Introduction**

Parkinson's disease (PD) is the second most common neurodegenerative disease in the world, affecting more than 10 million people worldwide [464, 465]. PD is associated with a range of symptoms including movement deficits caused by the destruction of dopaminergic neurons. In humans, motor symptoms manifest as tremors, slowness of movement (bradykinesia), muscle

rigidity, and altered gait and balance [116, 117, 466]. The molecular mechanisms underlying the death of the dopaminergic neurons in PD remain poorly understood [464, 467, 468]. Although the majority of PD cases (>85%) are idiopathic in nature with no known cause, familial forms of the disease are thought to be strongly linked to inheritance of mutations within one of many PD-associated causative genes including *PINK1*[4]. Inheritance of biallelic *PINK1* mutations is associated with early-onset PD [4, 469].

The PINK1 protein is largely known for its role in mitochondrial quality control [73, 79]. PINK1 is a kinase that is stabilized on the outer mitochondrial membrane when the mitochondrion loses its membrane potential, initiating a pathway resulting in mitophagy [470]. The lack of functional PINK1 in familial forms of PD was thus thought to promote the accumulation of dysfunctional mitochondria causing dopaminergic neuronal death; however, this has proven difficult to validate. Notably, *Pink1*<sup>-/-</sup> mice, although having dysfunctional mitochondria, fail to experience neurodegeneration or significant motor impairment [80]. An alternative function for PINK1 was recently discovered whereby it suppresses the presentation of mitochondrial peptides on MHC I to the immune system in response to bacterial lipopolysaccharide (LPS) [84], suggesting that PINK1's role in PD may be immunological and influenced by external factors.

Indeed, despite the strong association between *PINK1* mutations and PD, recent epidemiological evidence has noted that the manifestation of familial forms of PD may not be reliant solely on genetics but can also be influenced by external factors [471, 472]. A growing body of research has begun to reveal the importance of peripheral organs like the gut in PD. At least five independent studies have now demonstrated that patients with inflammatory bowel diseases (IBD) have an increased PD incidence rate [404-408]. Further, treatment for IBD with anti-TNF therapy has been documented in one study to reduce PD incidence rates in IBD patients

by over 75% [407]. A recent report also correlated appendectomies to decreased PD incidence rates [417]. In animal studies, chronic stress-induced intestinal dysfunction was shown to correlate with exacerbated PD-like symptoms in a rotenone-induced mouse model of PD [206]. Considerable research on the intestinal microbiota has also been carried out in both humans and animal models to examine whether a PD-specific microbiota exists and whether it is a causative factor in PD progression (reviewed in Cryan et al. [393], Sun et al. [395], Tremlett et al. [473]). It is still unclear how the gut microbiota may affect brain physiology, although a number of studies have now highlighted how an altered microbiota can lead to enhanced TLR4 signalling that results in changes in glial cell function [397, 474], while others have noted how the microbiota can affect blood brain barrier permeability [306]. Notably, a human PD-patient derived gut microbiota was also shown to exacerbate PD-like pathology in an  $\alpha$ -synuclein overexpressing mouse model of PD, and this was proposed to be mediated by the altered production of short-chain fatty acids (SCFAs) [435].

Given this evidence, intestinal inflammation a plausible mechanism by which the gut-brain axis may be aggravated. Our recently published work sought to test the hypothesis that inflammatory signaling in the intestine could influence the development of PD phenotypes in *Pink1*<sup>-/-</sup> mice [475]. To do so, we used *Citrobacter rodentium*, a murine intestinal pathogen modeling pathogenic *Escherichia coli* infection of humans. In this work, we showed that *C. rodentium* infection of *Pink1*<sup>-/-</sup> mice, but not their WT littermates, induced the presentation of mitochondrial antigens on MHC I and the subsequent formation of anti-mitochondrial CD8<sup>+</sup> T cells. Further analysis revealed that these anti-mitochondrial CD8<sup>+</sup> T cells were detectable within the central nervous system. Following three additional exposures to *C. rodentium* over four months, *Pink1*<sup>-/-</sup> mice displayed reduced spontaneous locomotion in an open field chamber and

motor deficits as measured by decreased ability to descend a pole, a deficit that was reversed by treatment with L-DOPA, a dopamine synthesis precursor. Together, this data led us to hypothesize a two-hit model proposing that the onset of PD-like pathology is dependent on both an external factor (intestinal infection) and a genetic component (the *Pink1*<sup>-/-</sup> background).

The model put forward in our previous paper is that anti-mitochondrial CD8 T cells induced by infection in the *Pink1*<sup>-/-</sup> mice enter the CNS, causing damage to dopaminergic neurons and leading to motor symptoms. However, this does not rule out the possibility that other features of *C. rodentium* infection may also contribute to the development of PD-like symptoms in *Pink1*<sup>-/-</sup> mice. *C. rodentium* infection induces temporal shifts in the mouse intestinal microbiota including an expansion of *Enterobacteriaceae* [375, 476]. As described above, gut microbiota alterations, such as an expansion in *Enterobacteriaceae* and *Verrucomicrobia*, have been implicated in PD [395]. This raises the possibility that microbiota differences between wild-type (WT) and *Pink1*<sup>-/-</sup> mice, either before, during, or after infection could be implicated in the infection-induced PD-like phenotypes observed. To gain insight into the role of the microbiota in our model, this addendum aims to characterize changes in the gut bacterial microbiota and SCFA production during *C. rodentium* infection and compare these changes between *Pink1*<sup>-/-</sup> mice and their WT littermates.

## **Gut Bacterial Diversity**

Susceptibility to *C. rodentium* varies depending on genetic background, with resistant C57BL/6 and 129S1 mouse lines experiencing only mild self-limiting colitis compared to the severe colitis, diarrhea, and weight loss observed in susceptible backgrounds [364, 369, 477]. Infection kinetics of *C. rodentium* also vary between mouse backgrounds, although the loads

generally peak between 9 and 13 days post infection (PI) with a fecal burden reaching upwards of  $10^9$  colony forming units per gram of feces [367]. In our previous study, we used WT and *Pink1*<sup>-/-</sup> littermate mice that had been previously generated and used for PD studies on a B6.129 mixed background [475]. Both WT and *Pink1*<sup>-/-</sup> mice presented with similar and mild self-limiting colitis. We also reported that both WT and *Pink1*<sup>-/-</sup> mice become colonized to a similar degree, with the infection peaking at day 13 PI with between  $10^8$  and  $10^9$  fecal colony forming units per gram of feces. The infection was completely cleared in all mice by day 26 PI. This kinetic allowed us to compare the influence of *C. rodentium* infection on the microbiota by collecting fecal samples prior to infection (pre), at day 13 (peak), and at day 26 (post) for 16S rRNA gene sequencing. To do this, we used the Illumina MiSeq sequencing platform and amplified the V4 region of the gene using the 515F and 806R primers. The sequencing data was analyzed using QIIME2 version 2019.7 [478].

To determine how the *Pink1*<sup>-/-</sup> genetic background might affect fecal microbial diversity during *C. rodentium* infection, we rarefied our sequences to a depth of 20,000 reads and compared the number of unique amplicon sequencing variants (ASVs) across time points and genotypes. The number of ASVs in both WT and *Pink1*<sup>-/-</sup> mice largely remained stable and comparable throughout the infection (Figure 1A). Although not significant, there was a trend for the number of ASVs to decrease at the peak of infection in both genotypes. To measure microbial diversity between time points and genotypes, we next compared the Shannon index. Consistent with the number of ASVs, the Shannon index also remained largely unchanged, with a small, non-significant decrease at the peak of infection (Figure 1B).

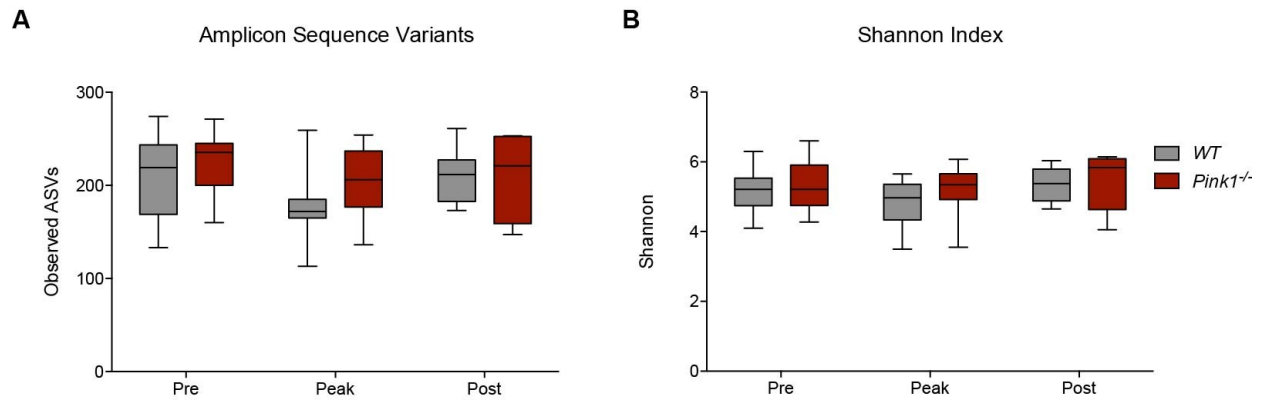


**Figure 1: The  $\alpha$ -diversity within the intestinal microbiota remains steady and comparable between WT and *Pink1*<sup>-/-</sup> mice during *Citrobacter rodentium* infection.** A) Comparison of the number of unique amplicon sequence variants observed upon rarefaction of the sequencing results to a depth of 20,000 reads. B) Comparison of the Shannon index. Statistics determined via pairwise Kruskal-Wallis test. (WT: Pre N=16, Peak N = 15, Post N = 6. *Pink1*<sup>-/-</sup>: Pre N = 18, Peak N = 16, Post N = 5). Data represented as quartile box and whisker blots.

We next sought to compare the bacterial communities between genotypes and time points by assessing  $\beta$ -diversity. To do so, we generated principle coordinate analysis (PCoA) plots using weighted UniFrac. The weighted UniFrac PCoA plot, which considers relative abundance and evolutionary relatedness, revealed no distinct clustering based on genotype or timepoint (Figure 2A). This was also confirmed by PERMANOVA analysis (Figure 2B). Combined with the data highlighting the number of ASVs and the Shannon index, our results suggest that *C. rodentium* infection does not significantly impact the diversity of the fecal microbiota in our model system over the course of infection. Further, the infection does not appear to interact with the *Pink1*<sup>-/-</sup> genotype to result in a distinct fecal microbial community. These results are compatible with other studies that have suggested that *C. rodentium* does not greatly disturb the bacterial communities present within the intestinal lumen or feces of mice [375, 476].

### **Taxonomic Analysis of the Gut Bacterial Microbiota**

The composition of the murine intestinal microbiota, which is primarily comprised of species from the phyla *Bacteroidetes* and *Firmicutes*, can influence both *C. rodentium* colonization rates and infection susceptibility [302, 479]. Studies have now highlighted that ablation of the gut microbiota via antibiotic treatment can increase susceptibility to *C. rodentium* [364, 479]. Further, transfer of the microbiota from a resistant mouse strain can confer resistance to a susceptible mouse strain [480]. Both an increased diversity within the phylum *Firmicutes* and a higher ratio of *Bacteroidetes* to *Firmicutes* have been associated with decreased susceptibility to *C. rodentium* [481]. Segmented filamentous bacteria have also been shown to inhibit *C. rodentium* colonization at the mucosal surface, likely through immune mechanisms [302].

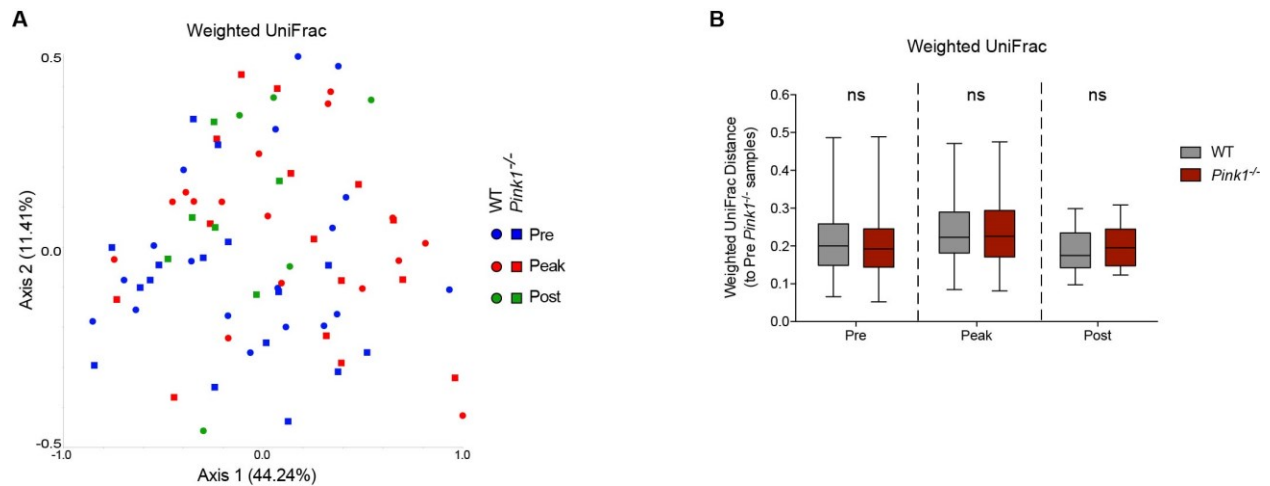


**Figure 2: The gut microbiota bacterial communities are similar between WT and *Pink1*<sup>-/-</sup> mice during *C. rodentium* infection.** A) Principle coordinate analysis between timepoints during the course of *C. rodentium* infection within WT mice and within *Pink1*<sup>-/-</sup> mice, determined using the weighted UniFrac diversity metric. B) Graphical analysis of the weighted UniFrac diversity metric. Statistics determined via PERMANOVA analysis, ns = not significant. Data represented as quartile box and whisker blots.



Conversely, *C. rodentium* is also able to alter the intestinal environment by causing an expansion of undifferentiated epithelial cells, altering the expression profile of host cells to favour oxidative phosphorylation, and increasing oxygen levels at the mucosal surface [375, 429]. Notably, this can result in decreased *Bacteroidetes* and *Firmicutes* and a significant expansion of *Enterobacteriaceae* [375]. At the peak of infection, *C. rodentium* comprises approximately 10% of luminal bacteria and between 40-90% of mucosal bacteria [375, 476]. It has been shown that as a result of PINK1's role in mitochondrial maintenance, cells in *Pink1*<sup>-/-</sup> mice experience a deficit of ATP production, loss of mitochondrial membrane potential, and overall lower mitochondrial respiratory potential [80]. Thus, we considered the possibility that, during *C. rodentium* infection, *Pink1*<sup>-/-</sup> mice might have decreased mucosal oxygen levels that would subsequently lead to alterations in microbiota compared to WT mice.

To determine the taxonomic composition of the microbiota within our sample groups, we generated bar plots at the phylum level and compared between time points and genotypes. In accordance with previous reports [375, 476], the major phyla present in both the WT and *Pink1*<sup>-/-</sup> mice at steady state were *Bacteroidetes* and *Firmicutes* (Figure 3A). We also observed the presence of *Verrucomicrobia*, *Epsilonbacteraeota*, *Proteobacteria*, *Cyanobacteria*, and *Actinobacteria* at low proportions. Prior to infection, no significant differences in composition were observable between WT and *Pink1*<sup>-/-</sup> mice at the genus level. This was further confirmed using an Analysis of the Composition of the Microbiota (ANCOM), a statistical test which determined no significance between genotypes at any time point. Notably, the ratio of *Bacteroidetes* to *Firmicutes* in our mice was high, consistent with the resistant phenotype we observed [475]. No segmented filamentous bacteria were detected. At the peak of infection, we observed an expansion in the phylum *Proteobacteria*, which increased to approximately 6-10% in both WT and *Pink1*<sup>-/-</sup> mice, which is

likely a direct reflection of the increase in *C. rodentium* loads during infection (Figure 3B). The ANCOM analysis showed no significant differences between genotypes at this time point, providing further evidence that the *C. rodentium* colonization levels in WT and *Pink1*<sup>-/-</sup> mice are comparable, as we have previously reported [475]. The relative percent abundance of *C. rodentium* also corroborates previous 16S analyses of luminal contents [375]. Post infection, we observed that the relative percent abundance of *Proteobacteria* reverted to pre-infection levels in both genotypes, likely reflecting that the infection has been cleared by this time point (Figure 3C).

We also noted a modest increase in the phylum *Verrucomicrobia* in both WT and *Pink1*<sup>-/-</sup> mice at the peak of infection and, although not significant (Figure 3C), WT mice demonstrated a trend towards an elevated percentage of *Verrucomicrobia* compared to *Pink1*<sup>-/-</sup> mice post infection (Figure 3D). It is interesting to note that *Verrucomicrobia*, which is increased at the peak of infection, is largely dominated by the genus *Akkermansia*. *Akkermansia muciniphila* is a Gram-negative mucin-degrading microbe associated with anti-inflammatory immune signatures in humans [482]. It has been reported to be a signature in PD patient fecal microbiotas compared to healthy controls [425, 483], an observation that we were not able to model in our mice. A higher proportion of *Akkermansia*, a similar finding to our own, has however been observed in a chronic stress-induced gut dysfunction mouse model of PD [206], suggesting this difference might be consistent in mouse models. Overall, the lack of significant compositional changes between genotypes at any time point combined with the diversity metrics suggests that the fecal microbiota of WT and *Pink1*<sup>-/-</sup> mice remains largely comparable throughout infection with *C. rodentium*.

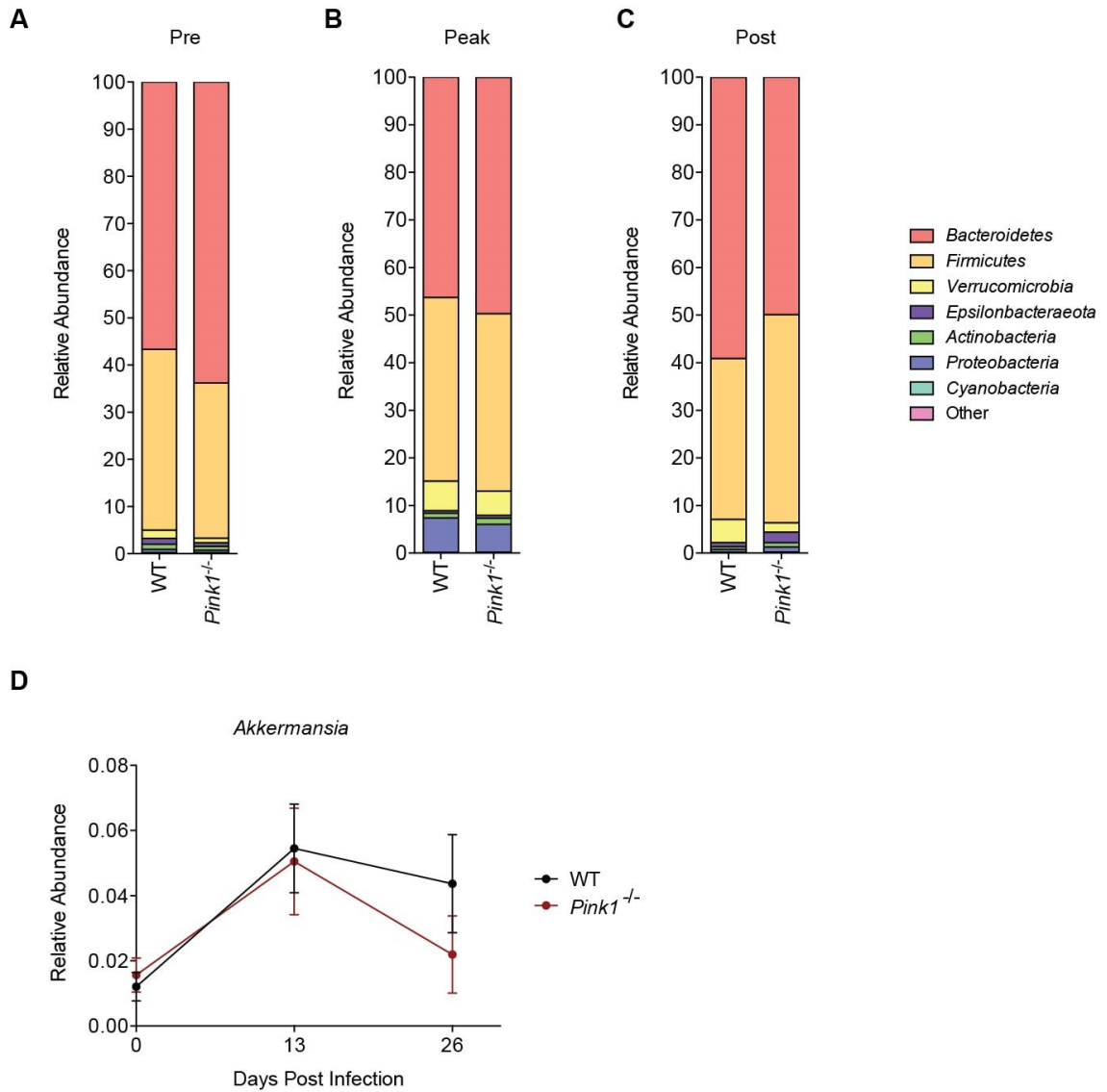


**Figure 3: Taxonomic analysis and comparison of the intestinal bacterial microbiota at the phylum and genus level during *Citrobacter rodentium* infection between WT and *Pink1<sup>-/-</sup>* mice.** A) Average relative abundance of major phyla present in WT and *Pink1<sup>-/-</sup>* mice A) pre-, B) peak-, and C) post-infection with *C. rodentium*. D) Relative abundance of the genus *Akkermansia* over the course of *C. rodentium* infection. Data represented as mean +/- SEM.

## Short-Chain Fatty Acid Analysis

A growing body of evidence has highlighted the potential implication of bacterially generated short-chain fatty acids (SCFAs) in PD. In humans, decreased levels of the fecal SCFAs butyrate, propionate, and acetate have been observed in PD patient fecal samples compared to matched controls [420]. In a chemically induced mouse model of PD, a fecal microbiota transfer leading to increased propionic and isobutyric acid levels correlated with increased dopamine levels [484]. Conversely, a recent study from Sampson et al. demonstrated that transferring a human PD-derived microbiota into a mouse alpha-synuclein overexpression PD model resulted in increased butyric acid and propionic acid levels, followed by an increase in PD-like symptoms, and administration of a mix of SCFAs into germ-free mice recapitulated some of the observed effects [435].

SCFAs are highly implicated in intestinal barrier integrity and immunological responses. Butyric acid functions as a histone deacetylase inhibitor and is instrumental in maintenance of intestinal barrier integrity [485, 486]. Notably, a deficit in butyric acid has been associated with intestinal disorders in humans [487, 488]. Changes in SCFAs within our model system might therefore provide a plausible mechanism by which intestinal permeability is altered, allowing bacteria and/or bacterial molecules such as LPS to initiate and exacerbate pathological immune responses in the lamina propria. Indeed, we have also previously shown that LPS is likely a key player in the induction of mitochondrial antigen presentation. Additionally, butyric acid promotes the differentiation and genesis of regulatory T cells by increasing the acetylation of the *foxp3* locus [428], and acetate has been shown to increase the suppressive potential of regulatory T cells [489]

providing another possible mechanism by which differences in SCFAs between WT and *Pink1*<sup>-/-</sup> mice might impact the host response to *Citrobacter* infection.

To determine the levels of various SCFAs, we analyzed fecal samples from the WT and *Pink1*<sup>-/-</sup> mice before, during, and after infection with *C. rodentium* via gas chromatography (Microbiome Insights). Acetic acid levels were comparable between genotypes at all time points, but significantly decreased at the peak of infection and remained low post infection (Figure 4A). Propionic acid levels remained steady and comparable at all time points (Figure 4B). There was a trend for the level of isovaleric acid to decrease with infection, but it remained low and comparable between genotypes at all time points (Figure 4C). Notably, butyric acid levels significantly increased at the peak of infection selectively in *Pink1*<sup>-/-</sup> mice and remained high post infection (Figure 4D). Contrarily, isobutyric acid significantly increased with infection only in WT mice (Figure 4E). Valeric acid and hexanoic acid were below the limit of detection for all sample groups (data not shown).

The increased level of butyric acid in infected *Pink1*<sup>-/-</sup> mice (Figure 4D) is notable in light of the results observed in the study by Sampson et al. in which SCFA treatments alone were sufficient to induce some PD-like symptoms in germ-free  $\alpha$ -synuclein over-expressing mice [435]. Both results remain contradictory to human studies where butyric acid levels are consistently observed to be lower in PD patients - it is still unclear how to consolidate this data. It is possible that the elevated levels of butyric acid observed in mouse studies reflect early time points in PD pathology, while lower butyric acid levels observed in humans reflect end points.

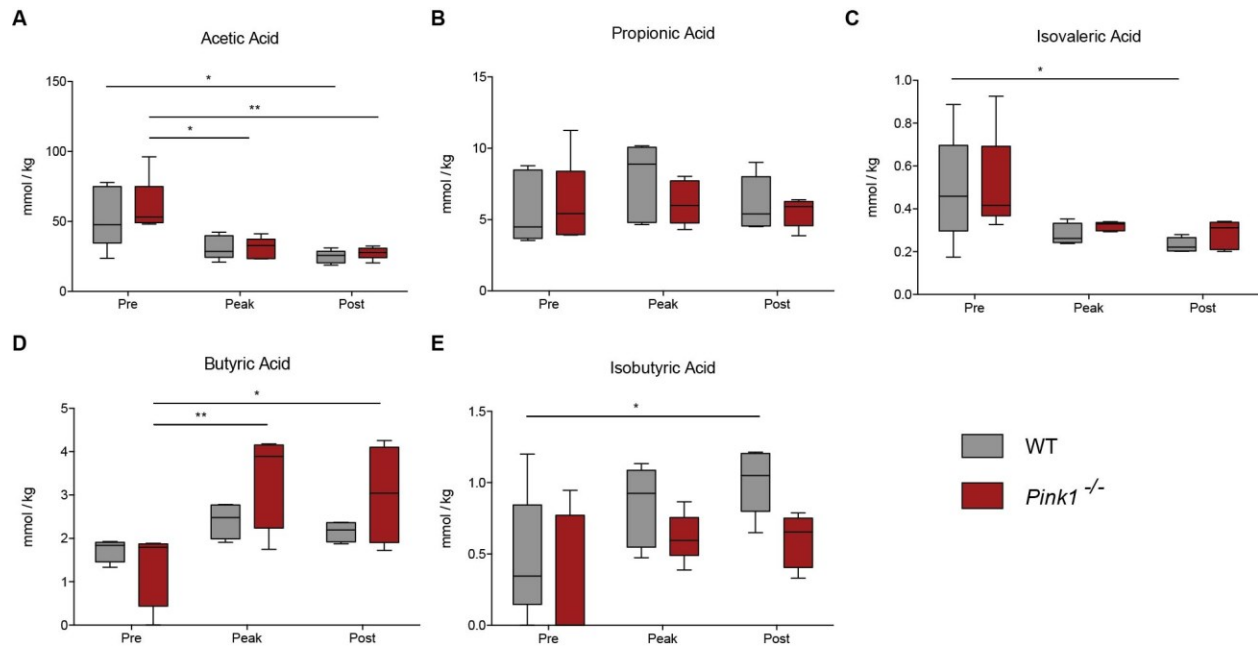


**Figure 4: Comparison of fecal short-chain fatty acid concentrations between WT and *Pink1*<sup>-/-</sup> mice during *Citrobacter rodentium* infection.** Analysis of A) acetic acid, B) propionic acid, C) isovaleric acid, D) butyric acid, and E) isobutyric acid fecal concentrations via gas chromatography. \*P<0.05, \*\*P<0.01 Significance determined via two-way ANOVA with a Tukey post-hoc test. (N = 5 per group). Data represented as quartile box and whisker plots.

Based on the effects of butyric acid's actions as a histone deacetylase inhibitor in enterocytes, higher butyric acid levels would be predicted to improve barrier function rather than induce intestinal dysfunction or aggravate the gut-brain axis. Further, butyric acid's effects on regulatory T cells [428] would be predicted to dampen rather than exacerbate immune pathology. An increase in butyric acid in response to infection in *Pink1*<sup>-/-</sup> mice could therefore potentially represent a compensatory response to protect intestinal integrity. Rectal administration of butyrate also ameliorates *C. rodentium* induced cell injury [490], suggesting that the increased level of butyrate we observe can represent a protective response in our model. In our previous work, we showed that *C. rodentium* infection in *Pink1*<sup>-/-</sup> mice leads to the production of autoreactive CD8<sup>+</sup> T cells and an increased expression of the pro-inflammatory marker IFN $\gamma$  [475]. While CD4<sup>+</sup> T cells were not analyzed in this paper directly, no evidence was suggestive of increased immune regulation via regulatory T cells; however, a more thorough study would be needed to confirm this. Little is known about the functions of isovaleric and isobutyric acid; both were observed at similar levels between PD patients and healthy matched controls [420].

One important caveat of the studies described here is that the microbiome and SCFA analyses were performed during the course of a single *C. rodentium* infection. Our original study demonstrated that anti-mitochondrial CD8 cells were generated at the peak of a single infection. However, the mice that developed motor symptoms had been exposed to *C. rodentium* four times over the course of four consecutive months. Since *C. rodentium* only colonized the mice to detectable levels during the first infection, suggesting that *C. rodentium*-induced changes to the intestinal environment are likely to occur during the first infection, we chose to focus our analysis within this time frame. It remains to be determined whether subsequent exposures to *C. rodentium* might lead to other changes in microbiome or SCFA composition between WT and *Pink1*<sup>-/-</sup> mice.

## Concluding Remarks

Currently the literature regarding the relationship between intestinal microbiota and PD remains largely correlative in humans. The complex nature of PD, in that there are multiple suspected pathological mechanisms in idiopathic and familial forms, further adds to the complexity of studying the role of the gut and the microbiota within a population. The current murine model systems that exist for PD also tend to be limited to specific features of the disease and generally fail to encompass the multiple aspects and symptoms of PD. Nevertheless, regulation of the immune system via the intestinal milieu provides a plausible mechanism by which the gut-brain axis might drive PD.

Here we looked at how the host-microbe interactions in our previously published two-hit murine model system for PD may impact the microbiota. Notably, the lack of significant differences in diversity metrics and in compositional analyses between WT and *Pink1*<sup>-/-</sup> mice at each time point during *C. rodentium* infection further serves as evidence that these mice are processing the infection similarly and have minimal intestinal disturbance. This suggests that other features of *C. rodentium* infection, such as immune activation, may be more directly involved in the development of the observed motor phenotypes. The role of SCFAs in *C. rodentium* infection, intestinal inflammation, and the gut-brain axis also need to be further elucidated. Although exogenous treatment with SCFAs has been noted to affect *C. rodentium* infection[490], to our knowledge, this is the first study to look at how *C. rodentium* affects the levels of various gut microbiota-derived SCFAs. The difference we observed in the levels of butyric acid between WT and *Pink1*<sup>-/-</sup> mice may provide a possible source by which the intestinal milieu can alter immune



responses in *Pink1*<sup>-/-</sup> mice; however, more in-depth studies are needed to fully elucidate its role in PD and in various PD model systems.

### **Acknowledgements and Funding**

This work was supported by a CIHR Project Grant (PJT 162406) awarded to SG and LET. TC was supported by the Healthy Brains for Healthy Lives initiative: this research was undertaken thanks in part to funding from the Canada First Research Excellence Fund, awarded to McGill University for the Healthy Brains, Healthy Lives initiative. AS was supported by Frederick Banting and Charles Best Canada Graduate Scholarships (434615). Research in the Maurice lab was supported by the Canada Research Chair Program, the Montreal General Hospital Foundation, and the Kenneth Rainin Foundation (2016-1280). Research in the Trudeau laboratory was funded by grants from the CIHR, Brain Canada and Krembil Foundations, as well as by the Henry and Berenice Kaufmann Foundation. Sequencing was performed at the Genome Quebec Innovation Centre.

### **Disclosure Statement**

The authors report no conflict of interest.

## CHAPTER 4: Discussion

### 4 – Overview

Parkinson's disease (PD) is a neurodegenerative movement disorder caused by the specific destruction of dopaminergic neurons in the substantia nigra pars compacta (SNc) [6]. Although considered a complex disorder with influences from both genetic and environmental factors, familial forms of PD are caused by inheriting a mutation in one of several PD-related genes, such as *PINK1*, that results in a nearly 100% penetrance of the disease [4]. The PINK1 protein is responsible for orchestrating the process of mitophagy [78], leading to the hypothesis that the death of dopaminergic neurons is caused by an accumulation of dysfunctional mitochondria and reactive oxygen species. The particular vulnerability of the dopaminergic neurons is believed to be a consequence of their significant energy demand to maintain signal propagation along their highly arborized axons [35]. The PINK1 protein also plays a role in inhibiting the release of proteins from the mitochondria to be loaded on MHC I [84]. Mice lacking PINK1, without further manipulation, fail to experience neurodegeneration [80].

Enteropathogenic and enterohemorrhagic *Escherichia coli* (EPEC and EHEC) infections are transmitted via the fecal oral route and are responsible for diarrheal disease in the developing and developed world [340]. The murine model of these pathogens, *Citrobacter rodentium*, causes fatal diarrheal disease in susceptible mice and self-limiting colitis in resistant mice [364]. Infection with *C. rodentium* induces intestinal epithelial cell damage and mitochondrial disruption [364]. Interestingly, intestinal dysfunction – including loss of barrier integrity, slowed colonic motility, inflammatory profiles, and an altered microbiota – are non-motor symptoms associated with PD

[130]. Constipation can precede PD development by over a decade, and inflammatory bowel disease (IBD) increases the risk of PD onset [172].

In this thesis we explored the potential implication of the gut brain axis in *Pink1*<sup>-/-</sup> mice using the *C. rodentium* infection model. We showed that infection with *C. rodentium* induced mitochondrial antigen presentation (MitAP) and the concomitant formation of anti-mitochondrial CD8<sup>+</sup> T cells exclusively in *Pink1*<sup>-/-</sup> mice. Flow cytometric analysis of these CD8<sup>+</sup> T cells revealed that they produced the cytolytic enzyme granzyme B, IFN $\gamma$ , and the receptor CX3CR1 – whose cognate ligand CX3CL1 is expressed by neurons – at higher levels compared to controls. Infection with *C. rodentium* induced the infiltration of immune cells into the central nervous system (CNS) regardless of mouse genotype, but anti-mitochondrial CD8<sup>+</sup> T cells were found in the CNS exclusively in *Pink1*<sup>-/-</sup> mice. Co-culture of anti-mitochondrial T cells with SNc neurons exposed to lipopolysaccharide (LPS) and IFN $\gamma$  resulted in neuronal death. Repeated infection with *C. rodentium* resulted in motor impairment that was reversed with L-DOPA treatment and the loss of tyrosine hydroxylase (TH) + axonal varicosities in striatal tissue. Overall disturbance to the intestinal environment was minimal: pathological scoring and fecal inflammatory markers were all increased with infection but comparable between genotypes. This result was also mirrored in an analysis of the fecal microbiota, which showed little change to structural diversity over the course of infection regardless of genotype. Taxonomic analysis revealed little change, with the exception of an increase in *Verrucomicrobia* in wild-type mice post infection. Despite minimal effects to the bacterial composition, we did observe alterations to the levels of short-chain fatty acids (SCFAs) including a significant rise in butyric acid uniquely in *Pink1*<sup>-/-</sup> mice. Combined, these results suggest that infection can alter the intestinal environment, induce immunological

changes systemically, and promote the onset of PD-like pathology in *Pink1*<sup>-/-</sup> mice. Infection may therefore play an etiological function in the onset of familial PD.

#### **4.1 – A two-hit model for familial Parkinson’s disease**

The significant penetrance of familial PD-related mutations (near 100%) has led to the idea that familial PD is completely genetic in nature [4]. Epidemiological studies investigating loss-of-function *PINK1* mutations has supported this idea in humans [140, 148]. However, a growing body of evidence has had difficulty replicating these findings in both drosophila and mouse genetic models [79, 80]. The work presented in this thesis has also shown that *Pink1*<sup>-/-</sup> mice, if left untreated, do not develop any classical PD-like pathology. The addition of an environmental insult to this model – infection with the Gram-negative intestinal microbe *C. rodentium* – was sufficient to induce the development of motor impairment and signs of dopaminergic neurodegeneration. This information led us to believe that familial PD may not be solely genetic in nature. Instead, we put forward the hypothesis of a two-hit model for familial PD that requires both genetic susceptibility in the form of a PD-related mutation, and an environmental trigger such as an infection.

Other studies involving genetic models of PD have also generally required a second environmental stress to induce or exacerbate a PD-like phenotype. One study noted that exhaustive exercise or an accumulation of mutated mitochondrial DNA resulted in substantial STING-mediated inflammation and eventually a motor defect in usually healthy *Prkn*<sup>-/-</sup> mice [450]. Although not a genetic model, MPTP-treated mice were shown to have exacerbated PD-like pathology when treated orally with the Gram-negative intestinal pathogen *Proteus mirabilis* [491],

further highlighting how a second hit with an intestinal infection may be vital for the etiology of PD. Chronic stress-induced gut dysfunction also exacerbated PD-like pathology in rotenone treated mice [206]. The observation that PD patients also reported higher exposure to gastrointestinal infections also corroborates our work; however, the patients used in this study were above the age of 50 and thus likely represented idiopathic and not familial PD [396]. Similarly, the correlation between PD and other infections such as *Helicobacter pylori* has mostly been established in idiopathic cases [184]. More work is needed to determine whether similar trends exist in familial PD.

The disparity in disease penetrance between humans and murine genetic models could be explained by a difference in environments: humans are constantly exposed to environmental challenges including infections, while mice are kept in specific pathogen-free facilities where they are not normally exposed to forms of external stress. This difference could mean that humans who have familial PD-related mutations are constantly being exposed to factors that might trigger the onset of PD pathology, making it appear as if the penetrance of such mutations is nearly 100%. We also showed that *C. rodentium* infection resulted in only brief self-limiting colitis before being cleared in our *Pink1*<sup>-/-</sup> mice. This implies exposure to infection does not need to be severe, but instead could simply be repeated transient exposure to common microbes. The concern has been raised that mutations in certain genes only appear as nearly 100% penetrant due to the fact that only patients who develop signs of PD would be tested; however, GWAS studies have yet to suggest otherwise.

In chapter 2 we showed that MitAP was induced by Gram-negative, but not Gram-positive, bacteria. Despite this implying that this process is initiated via the LPS-TLR4 pathway, it was also previously shown that heat shock at 42°C was sufficient to induce MitAP in Parkin deficient RAW

264.7 cells. Although this data is solely *in vitro*, it suggests that perhaps a bacterial infection is not needed to initiate MitAP. The TLR4 pathways are capable of inducing the secretion of various cytokines, which may themselves act as the inducer of MitAP (explored further in the next section) – it is unclear if heat shock could induce similar cytokine secretion. As previously discussed, inflammatory bowel disease is associated with an increased risk of developing PD [394]. It is thus possible that PD-like symptom development in *Pink1*<sup>-/-</sup> mice may also not be restricted to bacterial infection, but instead could be induced by any form of intestinal inflammation. Human studies investigating the correlation between *Helicobacter pylori* infection and have found that the infection does not need to be present during PD onset [178], suggesting that infection may induce immunological sequelae that can pose long-term effects on our health. Future studies should focus on expanding our current model to other forms of inflammation, such as the DSS-induced colitis model commonly used to study inflammatory bowel disease.

Of the Gram-negative pathogens tested *in vitro*, EPEC was shown to be the strongest inducer, justifying the use of its murine model *C. rodentium* *in vivo*. The use of other Gram-negative microbes *in vivo* was not explored. In our study we only examined the effect of four consecutive infections with *C. rodentium*; each subsequent infection resulted in no bacterial colonization beyond the first, suggesting the mice had become immune to *C. rodentium*. The effect of a single infection on long-term PD-like symptom development in *Pink1*<sup>-/-</sup> mice was not evaluated in our study – it thus unclear whether the initial colonization and inflammatory response induced during the first infection is sufficient for disease development, or if subsequent boosts to the immune system are also necessary. Future work should also focus on determining the capacity of different Gram-negative microbes to induce PD-like phenotypes in *Pink1*<sup>-/-</sup> mice and observing whether symptom severity correlates with ability to induce MitAP. We hypothesize that

performing multiple infections with different microbes would lead to a more sustained and pronounced phenotype.

The evidence presented in this thesis currently suggests a simple two-hit model for familial PD; however, the etiological mechanisms underlying PD may be more complex. Indeed, as previously discussed, susceptibility to *C. rodentium* infection has already been shown to be dependent on a number of different factors including genetic background and composition of the gut microbiota [364]. While the microbiota in our model was explored in chapter 3 and showed no major shifts during infection, it is possible that an altered starting microbiota may prevent or worsen symptom development in *Pink1*<sup>-/-</sup> mice. Furthermore, utilizing a more susceptible mouse strain, such as C3H mice which succumb to fatal diarrhea when infected with *C. rodentium* but can be rescued by intensive fluid therapy, may result in a different outcome. Our two-hit model thus may also be dependent on these factors, implying a multi-hit model. The observation that MitAP triggered the formation of anti-mitochondrial CD8<sup>+</sup> T cells led us to hypothesize that the observed neurodegeneration in our model may be caused by immunological mechanisms. However, the PD hallmark of Lewy pathology was not investigated, and pathological spread from the gut via the vagus nerve remains a possibility. *C. rodentium* was documented as having curli fimbria that are homologous to *Escherichia coli*, which was previously shown to be able to seed misfolded aSyn [60]. The absence of Lewy pathology would not be unfounded; research has shown that aSyn aggregates are markedly absent from the majority of familial PD cases [64].

## **4.2 – Mitochondrial antigen presentation**

Previous work had shown that MitAP involves the release of unique mitochondrial-derived vesicles (MDVs) that carry select mitochondrial proteins to be degraded in the lysosome/endosome, and then loaded onto MHC I molecules for presentation [84]. MDV release was dependent on the protein sorting nexin 9 (Snx9) and inhibited by Parkin and PINK1. MitAP did not occur under homeostatic conditions despite the cells expressing low levels of endogenous Parkin – an environmental trigger in the form of LPS or heat shock was required. The cellular pathways leading from the sensing of environmental stress to the release of MDVs remains unknown. The observation in chapter 2 that both LPS and Gram-negative bacteria, but not Gram-positive bacteria, can induce MitAP suggests that TLR4 may be the first step in the pathway. TLR4 signals through two distinct signalling arms; the myeloid differentiation primary response 88 (MyD88)-dependent and -independent pathways [492]. Most other TLRs, including TLR2/6 that recognizes peptidoglycan, signal uniquely through the MyD88-dependent pathway [492]. Given the inability for Gram-positive bacteria to induce MitAP, we believe that the MyD88-independent pathway is likely leading to MDV release, but this remains to be formally proven.

TLR4 signalling results in cytokine secretion including IL-6, TNF $\alpha$ , and the MyD88-independent pathway-produced type I interferons [492]. The MyD88-independent pathway signals through a number of adaptor molecules before reaching the nucleus with the transcription factor interferon regulatory factor 3 (IRF3). One of these adaptor molecules, TANK-binding kinase 1 (TBK1) can regulate stimulator-of-interferon-genes (STING), which mediates the production of pro-inflammatory cytokines like type I interferons and IL-6 [493]. STING-mediated inflammation was shown to be necessary for the development of PD-like pathology in *Prkn*<sup>-/-</sup> mice during exhaustive exercise [450]. STING can also be activated via cyclic guanine/adenosine monophosphate synthase (cGAS), which, as its name suggests, can recognize the circularized



nucleotide molecules AMP/GMP [494]. TLR3, which also recognizes nucleotides in the form of double stranded RNA, also acts in an MyD88-independent pathway to induce IRF3 [492]. As mentioned in chapter 1, infection with the 1918 RNA H1N1 influenza virus has been associated with increased PD prevalence, and is a negative-sense RNA virus that has to go through a double stranded RNA intermediate [178]. It is unclear if H1N1 RNA could induce the TLR3 pathway. The same study that showed STING-induced inflammation is mediated by PINK1 and Parkin also showed that PD-like disease development in *Prkn*<sup>-/-</sup> mice could be mediated by mutated mitochondrial DNA [450]. Together, this data suggests that activation of nucleotide-induced inflammatory pathways may be upstream of MDV release, although what this would be in the case of a Gram-negative bacterial infection is unclear.

The unfolded protein response (UPR) senses stress within the endoplasmic reticulum and can induce inflammatory cytokine production through a number of cellular pathways [495]. Notably, the endoplasmic reticulum is also where STING performs its function [493]. LPS was also shown to be able to induce the UPR in certain cell lines [496], placing LPS-induced TBK1 activation, the STING pathway, the UPR, and cytokine production all mechanistically within close proximity. Misfolded aSyn was shown to induce the UPR, and UPR-dependent pathways were shown to cause neurodegeneration in several models [497]. The UPR was also shown to be activated in nigrostriatal regions of PD patients' brains post-mortem [498]. It is thus possible that the UPR may act as a unifying mechanism that can be induced by several environmental triggers. How the UPR may be related to MDV release and MitAP remains unknown; it is possible that UPR can induce MDV release, or the inverse in which the MitAP pathway triggers the UPR. Within the cell, TBK1 is closely associated with mitochondria and is recruited to ubiquitin chains during PINK1/Parkin mediated mitophagy [499]. Mitophagy also involves the recruitment of

membranes from the endoplasmic reticulum [500], potentially putting the UPR, STING, and mitophagy pathways in close proximity. Nevertheless, significant research is still needed to define the order of these pathways, how they are related, and their relevance to MitAP and PD.

Further work is needed to elucidate whether mitophagy and MitAP are independent pathways or whether they regulate each other. Western blot analysis of several mitochondrial proteins and the autophagy adaptor LC3 in chapter 2 revealed that MitAP appeared to occur independently of mitophagy. However, the *in vitro* work presented in this thesis primarily focuses on MitAP within 2-8 hours of treatment with an external stress. Mitophagy has largely been observed to take longer [501] – it is therefore possible that mitophagy at later time points may act to disrupt the MitAP process.

#### **4.3 – The anti-mitochondrial immune response**

The induction of MitAP *in vivo* following *C. rodentium* infection was followed by the expansion of anti-mitochondrial CD8<sup>+</sup> T cells in *Pink1*<sup>-/-</sup> mice. These T cells expressed higher levels of IFN $\gamma$ , fractalkine receptor CX3CR1, secretory marker CD107, and granzyme B compared to control mice. Central tolerance to self-antigens is usually attained via deletion of self-reactive T cells in the thymus during thymocyte development [502]. The detection of CD8<sup>+</sup> T cells that react to self-oxoglutarate dehydrogenase (OGDH) in our model thus suggests that anti-mitochondrial T cells are able to escape central tolerance. The generation of mice expressing transgenic T cell receptors specific for self-OGDH (2C mice) further supports this, as autoreactive T cells in these mice can be observed in the periphery without need for further genetic modification [503]. It is currently unclear as to why anti-mitochondrial immune cells appear to be exempt from

central tolerance – perhaps, over the course of evolution, it was favourable to instead focus on inhibiting MitAP via PINK1 and Parkin. The relatedness of mitochondria to prokaryotes may have also played a role in this, as it is possible that at one point in history the deletion of anti-mitochondrial immune cells led to enhanced susceptibility to bacterial infections. This notion is supported in the etiology of primary biliary cirrhosis, an autoimmune liver disease caused by immune cells targeting the mitochondrial enzyme pyruvate dehydrogenase complex (PDC) [504]. Notably, both *E. coli* and *Novosphingobium aromaticivorans* infections have been linked to primary biliary cirrhosis, which is believed to be caused by similar epitopes between the mammalian and bacterial PDC genes [504]. In chapter 2 we also showed that both EPEC and *N. aromaticivorans* were two of the strongest inducers of MitAP *in vitro*. Of course, the possibility remains that the origins of the MitAP pathway were not originally intended to affect the adaptive immune system, but instead performed functions regarding the trafficking of mitochondrial proteins and the engagement of alternative cellular pathways. Investigating whether the MitAP pathway exists in *pink1*<sup>-/-</sup> *Drosophila* flies may provide evidence in this regard, as *Drosophila* do not possess an adaptive immune system.

The PINK1 and Parkin proteins, aside from orchestrating the process of mitophagy, are now believed to have immunological functions in the form of preventing anti-mitochondrial immune responses. It is currently unclear whether PINK1 and Parkin have other immunological functions. Evidence from patients with biallelic mutations in either *PINK1* or *PRKN* have shown elevated levels of systemic inflammatory cytokines including IL-6 [505]; however, it is unclear if this is due to direct regulation or an indirect association due to an accumulation of dysfunctional mitochondria. Effector T cell subsets were also shown to undergo shifts in their metabolic activity during activation – CD8<sup>+</sup> T cells in particular are known to shift away from oxidative

phosphorylation to a more glycolytic profile during activation and IFN $\gamma$  production [506]. It is also therefore possible that the absence of PINK1 in our model may influence the immune response by favouring pro-inflammatory IFN $\gamma$ + CD8+ T cell responses, as we've observed via flow cytometry in chapter 2.

It is currently unknown how other cell types – such as B cells – may be influenced in our model. The literature currently linking humoral immune responses to PD is sparse. There is evidence that PD patients do develop anti-aSyn antibodies, but this response tends to decrease with age and appears to not be a major contributor to disease development [507]. Further, although T cells have been observed in the brain of PD patients, there is no evidence of B cell infiltration [108], further suggesting that any immunological effect on SNc dopaminergic neurons are mediated via either T cells or innate immune cells such as microglia.

The exact mechanisms which underlie the unique susceptibility of SNc dopaminergic neurons is currently unknown; although, as discussed in chapter 1, several have been proposed. Immunologically, SNc dopaminergic neurons are believed to be more susceptible to T cell attack due to their propensity to express MHC I at higher levels than other neuronal cell types [115]. Indeed, MHC I levels were observed to increase after treatment with the supernatant from microglia treated with LPS and IFN $\gamma$ , suggesting that microglia-derived cytokines can promote neuronal destruction. In our model we observed that the BBB was compromised regardless of genotype, which may have allowed LPS to enter circulation and promote neuroinflammation. This response could have allowed for the induction of antigen presentation on MHC I on SNc dopaminergic neurons. The observed difference in TH+ axonal varicosities between WT and *Pink1*<sup>-/-</sup> mice can be explained by the ability to undergo MitAP – while both genotypes are presenting more MHC I, only *Pink1*<sup>-/-</sup> mice are presenting mitochondrial peptides via MitAP and

are thus susceptible to attack. While we were able to show that anti-mitochondrial CD8<sup>+</sup> T cells can destroy dopaminergic neurons *ex vivo*, a limitation of our study is that we were unable to effectively demonstrate this *in vivo*. In future work it may prove useful to utilize magnetic resonance imaging to directly measure breakdown of the BBB. Advanced immunofluorescence imaging can also be performed to see upregulation of MHC I on SNc dopaminergic neurons.

Although T cells are able to be observed by immunohistochemistry in the brain of PD patients post-mortem, we did not replicate these results in our studies. Flow cytometric and ELISPOT analysis did reveal the presence of autoreactive CD8<sup>+</sup> T cells in *Pink1*<sup>-/-</sup> mice, albeit in low numbers. This result is consistent with the observation that our mice appeared to be fairly healthy – they did not appear to suffer from encephalitis or any severe immune infiltration. What we thus posit is that immune cell infiltration was limited and led to the slow and gradual decline of SNc dopaminergic axonal varicosities over time, akin to what is observed in the early stages of PD patients. We failed to observe the death of SNc dopaminergic neuronal cell bodies, only axonal degeneration, which eventually led to the axons regenerating and a reversal of phenotype. We hypothesize that if we had continued the infections for a longer period of time that the cell bodies would have also eventually been destroyed and the phenotype would have been permanent.

A major limitation of the work presented in this thesis is the lack of direct evidence linking MitAP to the PD-like phenotype. We have shown independently that firstly MitAP and anti-OGDH CD8<sup>+</sup> T cell responses occur in *Pink1*<sup>-/-</sup> mice post infection, and that secondly after four subsequent infections these *Pink1*<sup>-/-</sup> mice develop a PD-like phenotype. We do provide evidence *ex vivo* that anti-mitochondrial CD8<sup>+</sup> T cells are able to destroy SNc dopaminergic neuronal cultures; however, direct evidence of this occurring *in vivo* has yet to be performed. Modification of the immune system in this model to achieve this is challenging; losing large parts of the immune

system can lead to hyper susceptibility to *C. rodentium* infection [370]. CD8<sup>+</sup> T cells, however, are not vital; thus the generation of a *CD8/Pink1* double knockout mouse could be used to directly determine the necessity of CD8<sup>+</sup> T cells to the development of a PD-like phenotype in our model.

#### **4.4 – The gut microbiota and short-chain fatty acids**

Whether the microbiota plays a causative role in the development of PD remains debated. As previously discussed in chapters 1 and 3, the microbiota is observed to be altered in PD patients with an elevated abundance of *Enterobacteriaceae* and a decreased abundance of SCFA producing bacteria [420]. The mucin-degrading Gram-negative microbe *Akkermansia muciniphila* is also observed to be higher in PD patients [420]. We did not observe any large-scale shifts to the diversity and structure of the microbiota in *Pink1*<sup>-/-</sup> mice compared to WT mice over the course of *C. rodentium* infection. Specifically, we did observe an increase in the abundance of *A. muciniphila* in WT mice post infection; however, the importance and relevance of this finding are unclear. Indeed, *A. muciniphila* is associated with anti-inflammatory signatures *in vivo*, and thus it may be playing a protective role in WT mice [482]. It is unclear how to resolve the discrepancy observed between mice and human PD patients. Timing may play an important factor in this regard: in chapter 3 we performed our fecal sampling during the course of infection before PD-like symptom development, while samples from PD patients are taken at late stages in the disease and thus may represent post-disease anti-inflammatory signatures. Future studies should focus on the development of the microbiota over the entire course of disease development in our model.

The data presented in chapter 3 demonstrated that there was no significant shift to the composition of the microbiota over the course of *C. rodentium* infection, regardless of genotype.

This suggests that the phenotype we observed post-infection in chapter 2 was likely due to the *C. rodentium* infection itself and not due to an indirect mechanism via the microbiota. However, analysis of the levels of SCFAs did reveal discrepancies between genotypes which may affect disease outcome. Questions such as how a completely different starting microbiota – such as you would find in mice bred in a different facility – would affect disease progression in our model should be investigated in the future.

We showed in chapter 3 that butyric acid is significantly increased during infection in *Pink1<sup>-/-</sup>* but not WT mice. Butyric acid is able to perform a number of immunomodulatory properties including promoting the differentiation of regulatory T cells (Treg) and enhancing the formation of tight junctions [305, 428]. Butyric acid can also stimulate enteroendocrine cells to promote the synthesis of serotonin within the gut, aiding in motility [242]. This information is contradictory to what has been observed in PD patients, which includes the increased presence of pro-inflammatory T cells, decreased intestinal barrier integrity, and reduced colonic transit time leading to constipation. As discussed previously, however, our data corroborates what has been observed in other PD mouse studies [206, 435], suggesting that the gut environment in murine models may simply differ too much from humans to properly recapitulate PD-related intestinal dysfunction. In our model, these observations may represent a protective response to *C. rodentium*, as protection against infection relies on a balanced Th17/Treg phenotype and overall maintenance of barrier integrity. Currently the data related to SCFAs in this thesis are strictly correlative – it is therefore also possible that the significant alterations to the level of SCFAs observed are strictly coincidental and have no bearing on PD-like symptom development. Previously published work has shown that SCFAs from a PD-derived microbiota can enhance PD-like symptoms in an aSyn

overexpressing murine model [435]. Thus, future work should focus on elucidating the mechanistic importance of butyric acid in our model.

The observed changes in the level of SCFAs suggests that although the overall composition of the microbiota is not being altered, the genes these microbes are expressing may be different. It is still unclear how the microbiota metagenome impacts human health; however, shifts in the overall metabolic profile of the microbiota has been associated with several diseases including obesity and atherosclerosis [508, 509]. Metagenomic evaluation of the metabolic profiles that dominate in our model was not thoroughly tested in this thesis but may provide evidence of shifts that can alter host susceptibility to PD-like disease development. For example, microbiota-wide expression of carbohydrate-fermentation pathways are associated with increased mucous degradation and susceptibility to enteric pathogens [510]. This information can prove instrumental in guiding future microbiota-related research in our model.

#### **4.5 – Revisiting *Pink1*<sup>-/-</sup> mice as a model for Parkinson’s disease**

The previous failures to observe a significant PD-like phenotype in *Pink1*<sup>-/-</sup> mice has led researchers to question the usefulness of these mice as a model for PD. Indeed, these mice have failed to display signs of SNc dopaminergic neurodegeneration or motor impairment when aged in isolation [80, 81]. One study did note that *Pink1*<sup>-/-</sup> mice do eventually lose some of their olfactory sense, similar to the loss of smell observed as a prodromal symptom in PD patients, and suggested that these mice may be useful as a model for pre-symptomatic PD [81]. What we put forward in this thesis is that these mice require a second hit to become symptomatic and can indeed be useful to model motor impairment and neurodegeneration in PD.



As described in chapter 1, the diagnosis of PD in humans is complicated since the presentation of symptoms is generally unique to the individual [125]. Nonetheless, a PD diagnosis requires bradykinesia, one additional motor symptom, and for the patient to be sensitive to clinical therapy that restores dopaminergic signalling, usually in the form of L-DOPA treatment [125]. In addition to these clinical features, the definitive measure for PD is to show significant SNc dopaminergic neurodegeneration post-mortem. In our mouse model we observed slowness and less overall movement, a phenotype which mirrors the bradykinesia observed in humans. Further the inability to coordinate the T-turn on the pole test signifies an impairment in coordination. Reversal of the pole test phenotype with L-DOPA is also strongly indicative that this phenotype is arising because of a loss of dopamine signalling. The observed loss of TH<sup>+</sup> axon varicosities in the striatum also further verifies this. PD is strictly a human disease and it is impossible to completely recapitulate and compare symptoms across species; nonetheless, our mice appear to meet the requirements in order to refer to their pathology as PD-like.

It is important to note though that discrepancies still exist in our model, the most notable of which is the eventual reversal of phenotype. TH<sup>+</sup> axon varicosities were decreased at the peak of motor symptoms and appeared to regenerate once the motor symptoms were reversed at 12 months post infection. At no point did we observe destruction of the cell bodies within the SNc. This data suggests that the axon terminals were destroyed, akin to the dying back hypothesis, but that the pathology was perhaps not severe enough to regress all the way to the cell soma. In humans, motor impairment is usually only observed once 70-80% of all SNc dopaminergic neurons are destroyed and this phenotype is irreversible [6]. Our model might represent an early point in disease progression where neurodegeneration is just beginning.

The results presented in this thesis suggest that *Pink1*<sup>-/-</sup> mice may yet still be useful in helping model PD. In particular, the inducible nature of our model via infection can be leveraged to investigate the complex interactions between genetics, the immune system, and environmental components. Validating that MitAP and anti-mitochondrial immune responses are present in PD patients will also help draw further comparisons to our model, which will then allow for further correlates of disease to be deduced.

#### **4.6 – Conclusion**

The molecular mechanisms underlying the neurodegeneration of SNc dopaminergic neurons in PD remain elusive. The cause of neuronal death in familial cases of PD is also disputed, as the supposedly causative mutations are unable to cause similar pathology in murine models. A growing body of evidence has indicated that the gut-brain axis likely plays a central role in the etiology of PD. This thesis sought to investigate whether intestinal disruption could induce a PD-like phenotype in usually asymptomatic *Pink1*<sup>-/-</sup> mice via the gut-brain axis and to explore potential causative molecular mechanisms. In chapter 2 we examined the effect of the Gram-negative intestinal infection *C. rodentium* on *Pink1*<sup>-/-</sup> mice and found that infection could induce both MitAP and the formation of pro-inflammatory anti-mitochondrial CD8<sup>+</sup> T cells. Live Gram-negative, but not Gram-positive, infections induced Snx9-dependent MitAP that resulted in MDV release as previously reported with LPS alone. Repeated infection with *C. rodentium* led to the development of PD-like motor impairment that was reversed by L-DOPA treatment and was accompanied by degeneration of TH<sup>+</sup> axonal varicosities in both the dorsal and ventral striatum. Upon examination of the CNS, we noted that infection induced the infiltration of CD8<sup>+</sup> T cells regardless of genotype,

but only in *Pink1*<sup>-/-</sup> mice did we find the presence of anti-mitochondrial CD8<sup>+</sup> T cells. *Ex vivo* analysis of anti-mitochondrial CD8<sup>+</sup> T cells plated in co-culture with SNc neuronal preparations pre-treated with LPS revealed that the T cells could exert their cytolytic functions on the neuronal cells. Although we observed axonal loss in our mice akin to the dying-back hypothesis, we did not observe death of the SNc cell bodies. Letting the mice recover for an additional six months without further infection led to a regeneration of the TH<sup>+</sup> striatal varicosities and a reversal of the PD-like phenotype. In chapter 3 we examined whether *C. rodentium* infection might be altering the gut microbiota in our model via a 16s rRNA gene analysis. Our data indicated that the microbiota was comparable between WT and *Pink1*<sup>-/-</sup> mice at steady state, and that there was little shift to the diversity of microbes present over the course of *C. rodentium* infection. Notably, we detected shifts in the production of SCFAs with butyric acid being significantly increased in *Pink1*<sup>-/-</sup> mice post infection, and isobutyric acid being significantly increased in WT mice post infection. The significance of SCFA alterations in our model remains to be determined. In summary, this thesis provides new insights into the impact of the gut-brain axis in PD development. To our knowledge, this is the first report to suggest a two-hit model for familial cases of PD wherein both a genetic susceptibility (like a mutation in the *PINK1* gene) and an environmental trigger (like a Gram-negative intestinal infection) are both needed for disease progression. Our report also adds to the mounting evidence that PD may have immunological origins that begins in the gut.

## REFERENCES

1. Kalia, L.V. and A.E. Lang, *Parkinson's disease*. Lancet, 2015. **386**(9996): p. 896-912.
2. Dorsey, E.R., et al., *Projected number of people with Parkinson disease in the most populous nations, 2005 through 2030*. Neurology, 2007. **68**(5): p. 384-6.
3. Raza, C., R. Anjum, and N.U.A. Shakeel, *Parkinson's disease: Mechanisms, translational models and management strategies*. Life Sci, 2019. **226**: p. 77-90.
4. Klein, C. and A. Westenberger, *Genetics of Parkinson's disease*. Cold Spring Harb Perspect Med, 2012. **2**(1): p. a008888.
5. Schrag, A. and J.M. Schott, *Epidemiological, clinical, and genetic characteristics of early-onset parkinsonism*. Lancet Neurol, 2006. **5**(4): p. 355-63.
6. Beitz, J.M., *Parkinson's disease: a review*. Front Biosci (Schol Ed), 2014. **6**: p. 65-74.
7. Polymeropoulos, M.H., et al., *Mapping of a gene for Parkinson's disease to chromosome 4q21-q23*. Science, 1996. **274**(5290): p. 1197-9.
8. Tan, M.M.X., et al., *Genetic analysis of Mendelian mutations in a large UK population-based Parkinson's disease study*. Brain, 2019. **142**(9): p. 2828-2844.
9. Braak, H., et al., *Staging of the intracerebral inclusion body pathology associated with idiopathic Parkinson's disease (preclinical and clinical stages)*. J Neurol, 2002. **249** Suppl 3: p. III/1-5.
10. De Virgilio, A., et al., *Parkinson's disease: Autoimmunity and neuroinflammation*. Autoimmun Rev, 2016. **15**(10): p. 1005-11.
11. Kim, H.S., et al., *Nonmotor symptoms more closely related to Parkinson's disease: comparison with normal elderly*. J Neurol Sci, 2013. **324**(1-2): p. 70-3.
12. Carlsson, A., B. Falck, and N.A. Hillarp, *Cellular localization of brain monoamines*. Acta Physiol Scand Suppl, 1962. **56**(196): p. 1-28.
13. Bjorklund, A. and S.B. Dunnett, *Dopamine neuron systems in the brain: an update*. Trends Neurosci, 2007. **30**(5): p. 194-202.
14. Molinoff, P.B. and J. Axelrod, *Biochemistry of catecholamines*. Annu Rev Biochem, 1971. **40**: p. 465-500.
15. Daubner, S.C., T. Le, and S. Wang, *Tyrosine hydroxylase and regulation of dopamine synthesis*. Arch Biochem Biophys, 2011. **508**(1): p. 1-12.
16. Molinoff, P.B., R. Weinshilboum, and J. Axelrod, *A sensitive enzymatic assay for dopamine- $\beta$ -hydroxylase*. J Pharmacol Exp Ther, 1971. **178**(3): p. 425-31.
17. Gaspar, P., et al., *Tyrosine hydroxylase-immunoreactive neurons in the human cerebral cortex: a novel catecholaminergic group?* Neurosci Lett, 1987. **80**(3): p. 257-62.
18. Baker, H., et al., *Cortical and striatal expression of tyrosine hydroxylase mRNA in neonatal and adult mice*. Cell Mol Neurobiol, 2003. **23**(4-5): p. 507-18.
19. Emborg, M.E., et al., *Age-related declines in nigral neuronal function correlate with motor impairments in rhesus monkeys*. J Comp Neurol, 1998. **401**(2): p. 253-65.
20. McCormack, A.L., et al., *Aging of the nigrostriatal system in the squirrel monkey*. J Comp Neurol, 2004. **471**(4): p. 387-95.
21. Demchyshyn, L.L., et al., *The dopamine D1D receptor. Cloning and characterization of three pharmacologically distinct D1-like receptors from Gallus domesticus*. J Biol Chem, 1995. **270**(8): p. 4005-12.
22. Memo, M., et al., *Pharmacology and biochemistry of dopamine receptors in the central nervous system and peripheral tissue*. J Neural Transm Suppl, 1986. **22**: p. 19-32.

23. Missale, C., et al., *Dopamine receptors: from structure to function*. Physiol Rev, 1998. **78**(1): p. 189-225.
24. Surmeier, D.J., et al., *Modulation of calcium currents by a D1 dopaminergic protein kinase/phosphatase cascade in rat neostriatal neurons*. Neuron, 1995. **14**(2): p. 385-97.
25. Beaulieu, J.M., S. Espinoza, and R.R. Gainetdinov, *Dopamine receptors - IUPHAR Review 13*. Br J Pharmacol, 2015. **172**(1): p. 1-23.
26. Valjent, E., et al., *Haloperidol regulates the state of phosphorylation of ribosomal protein S6 via activation of PKA and phosphorylation of DARPP-32*. Neuropsychopharmacology, 2011. **36**(12): p. 2561-70.
27. Spano, P.F., S. Govoni, and M. Trabucchi, *Studies on the pharmacological properties of dopamine receptors in various areas of the central nervous system*. Adv Biochem Psychopharmacol, 1978. **19**: p. 155-65.
28. Baik, J.H., et al., *Parkinsonian-like locomotor impairment in mice lacking dopamine D2 receptors*. Nature, 1995. **377**(6548): p. 424-8.
29. Toval, A., et al., *Dopaminergic Modulation of Forced Running Performance in Adolescent Rats: Role of Striatal D1 and Extra-striatal D2 Dopamine Receptors*. Mol Neurobiol, 2021.
30. Giros, B., et al., *Hyperlocomotion and indifference to cocaine and amphetamine in mice lacking the dopamine transporter*. Nature, 1996. **379**(6566): p. 606-12.
31. Kristensen, A.S., et al., *SLC6 neurotransmitter transporters: structure, function, and regulation*. Pharmacol Rev, 2011. **63**(3): p. 585-640.
32. Dahlstroem, A. and K. Fuxe, *Evidence for the Existence of Monoamine-Containing Neurons in the Central Nervous System. I. Demonstration of Monoamines in the Cell Bodies of Brain Stem Neurons*. Acta Physiol Scand Suppl, 1964: p. SUPPL 232:1-55.
33. Matsuda, W., et al., *Single nigrostriatal dopaminergic neurons form widely spread and highly dense axonal arborizations in the neostriatum*. J Neurosci, 2009. **29**(2): p. 444-53.
34. Hirsch, E.C., et al., *Neuronal loss in the pedunculopontine tegmental nucleus in Parkinson disease and in progressive supranuclear palsy*. Proc Natl Acad Sci U S A, 1987. **84**(16): p. 5976-80.
35. Pissadaki, E.K. and J.P. Bolam, *The energy cost of action potential propagation in dopamine neurons: clues to susceptibility in Parkinson's disease*. Front Comput Neurosci, 2013. **7**: p. 13.
36. Moss, J. and J.P. Bolam, *A dopaminergic axon lattice in the striatum and its relationship with cortical and thalamic terminals*. J Neurosci, 2008. **28**(44): p. 11221-30.
37. Chaudhuri, K.R. and P. Martinez-Martin, *Quantitation of non-motor symptoms in Parkinson's disease*. Eur J Neurol, 2008. **15 Suppl 2**: p. 2-7.
38. Adalbert, R. and M.P. Coleman, *Review: Axon pathology in age-related neurodegenerative disorders*. Neuropathol Appl Neurobiol, 2013. **39**(2): p. 90-108.
39. Lee, C.S., et al., *In vivo positron emission tomographic evidence for compensatory changes in presynaptic dopaminergic nerve terminals in Parkinson's disease*. Ann Neurol, 2000. **47**(4): p. 493-503.
40. Orimo, S., et al., *Axonal alpha-synuclein aggregates herald centripetal degeneration of cardiac sympathetic nerve in Parkinson's disease*. Brain, 2008. **131**(Pt 3): p. 642-50.
41. Burke, R.E. and K. O'Malley, *Axon degeneration in Parkinson's disease*. Exp Neurol, 2013. **246**: p. 72-83.

42. Bower, J.H., et al., *Influence of strict, intermediate, and broad diagnostic criteria on the age- and sex-specific incidence of Parkinson's disease*. *Mov Disord*, 2000. **15**(5): p. 819-25.
43. Grosch, J., J. Winkler, and Z. Kohl, *Early Degeneration of Both Dopaminergic and Serotonergic Axons - A Common Mechanism in Parkinson's Disease*. *Front Cell Neurosci*, 2016. **10**: p. 293.
44. Cunningham, C., et al., *Central and systemic endotoxin challenges exacerbate the local inflammatory response and increase neuronal death during chronic neurodegeneration*. *J Neurosci*, 2005. **25**(40): p. 9275-84.
45. Ltic, S., et al., *Alpha-synuclein is expressed in different tissues during human fetal development*. *J Mol Neurosci*, 2004. **22**(3): p. 199-204.
46. Fauvet, B., et al., *alpha-Synuclein in central nervous system and from erythrocytes, mammalian cells, and Escherichia coli exists predominantly as disordered monomer*. *J Biol Chem*, 2012. **287**(19): p. 15345-64.
47. Zhang, L., et al., *Semi-quantitative analysis of alpha-synuclein in subcellular pools of rat brain neurons: an immunogold electron microscopic study using a C-terminal specific monoclonal antibody*. *Brain Res*, 2008. **1244**: p. 40-52.
48. Ghosh, D., et al., *alpha-synuclein aggregation and its modulation*. *Int J Biol Macromol*, 2017. **100**: p. 37-54.
49. Abeliovich, A., et al., *Mice lacking alpha-synuclein display functional deficits in the nigrostriatal dopamine system*. *Neuron*, 2000. **25**(1): p. 239-52.
50. Winner, B., et al., *In vivo demonstration that alpha-synuclein oligomers are toxic*. *Proc Natl Acad Sci U S A*, 2011. **108**(10): p. 4194-9.
51. Karpinar, D.P., et al., *Pre-fibrillar alpha-synuclein variants with impaired beta-structure increase neurotoxicity in Parkinson's disease models*. *EMBO J*, 2009. **28**(20): p. 3256-68.
52. Desplats, P., et al., *Inclusion formation and neuronal cell death through neuron-to-neuron transmission of alpha-synuclein*. *Proc Natl Acad Sci U S A*, 2009. **106**(31): p. 13010-5.
53. Volpicelli-Daley, L.A., et al., *Exogenous alpha-synuclein fibrils induce Lewy body pathology leading to synaptic dysfunction and neuron death*. *Neuron*, 2011. **72**(1): p. 57-71.
54. Luk, K.C., et al., *Pathological alpha-synuclein transmission initiates Parkinson-like neurodegeneration in nontransgenic mice*. *Science*, 2012. **338**(6109): p. 949-53.
55. Challis, C., et al., *Gut-seeded alpha-synuclein fibrils promote gut dysfunction and brain pathology specifically in aged mice*. *Nat Neurosci*, 2020. **23**(3): p. 327-336.
56. Kim, S., et al., *Transneuronal Propagation of Pathologic alpha-Synuclein from the Gut to the Brain Models Parkinson's Disease*. *Neuron*, 2019. **103**(4): p. 627-641 e7.
57. Braak, H., et al., *Staging of brain pathology related to sporadic Parkinson's disease*. *Neurobiol Aging*, 2003. **24**(2): p. 197-211.
58. Lionnet, A., et al., *Does Parkinson's disease start in the gut?* *Acta Neuropathol*, 2018. **135**(1): p. 1-12.
59. Klingenhoefer, L. and H. Reichmann, *Pathogenesis of Parkinson disease--the gut-brain axis and environmental factors*. *Nat Rev Neurol*, 2015. **11**(11): p. 625-36.
60. Sampson, T.R., et al., *A gut bacterial amyloid promotes alpha-synuclein aggregation and motor impairment in mice*. *Elife*, 2020. **9**.

61. Singleton, A.B., et al., *alpha-Synuclein locus triplication causes Parkinson's disease*. Science, 2003. **302**(5646): p. 841.
62. Anderson, J.P., et al., *Phosphorylation of Ser-129 is the dominant pathological modification of alpha-synuclein in familial and sporadic Lewy body disease*. J Biol Chem, 2006. **281**(40): p. 29739-52.
63. Giasson, B.I., et al., *Oxidative damage linked to neurodegeneration by selective alpha-synuclein nitration in synucleinopathy lesions*. Science, 2000. **290**(5493): p. 985-9.
64. Pouloupoulos, M., O.A. Levy, and R.N. Alcalay, *The neuropathology of genetic Parkinson's disease*. Mov Disord, 2012. **27**(7): p. 831-42.
65. Chartier, S. and C. Duyckaerts, *Is Lewy pathology in the human nervous system chiefly an indicator of neuronal protection or of toxicity?* Cell Tissue Res, 2018. **373**(1): p. 149-160.
66. Langston, J.W., et al., *Chronic Parkinsonism in humans due to a product of meperidine-analog synthesis*. Science, 1983. **219**(4587): p. 979-80.
67. Javitch, J.A., et al., *Parkinsonism-inducing neurotoxin, N-methyl-4-phenyl-1,2,3,6 - tetrahydropyridine: uptake of the metabolite N-methyl-4-phenylpyridine by dopamine neurons explains selective toxicity*. Proc Natl Acad Sci U S A, 1985. **82**(7): p. 2173-7.
68. Betarbet, R., et al., *Chronic systemic pesticide exposure reproduces features of Parkinson's disease*. Nat Neurosci, 2000. **3**(12): p. 1301-6.
69. Bose, A. and M.F. Beal, *Mitochondrial dysfunction in Parkinson's disease*. J Neurochem, 2016. **139 Suppl 1**: p. 216-231.
70. Liou, H.H., et al., *Environmental risk factors and Parkinson's disease: a case-control study in Taiwan*. Neurology, 1997. **48**(6): p. 1583-8.
71. Lin, M.T. and M.F. Beal, *Mitochondrial dysfunction and oxidative stress in neurodegenerative diseases*. Nature, 2006. **443**(7113): p. 787-95.
72. Matsumine, H., et al., *Localization of a gene for an autosomal recessive form of juvenile Parkinsonism to chromosome 6q25.2-27*. Am J Hum Genet, 1997. **60**(3): p. 588-96.
73. Pickrell, A.M. and R.J. Youle, *The roles of PINK1, parkin, and mitochondrial fidelity in Parkinson's disease*. Neuron, 2015. **85**(2): p. 257-73.
74. Valente, E.M., et al., *Localization of a novel locus for autosomal recessive early-onset parkinsonism, PARK6, on human chromosome 1p35-p36*. Am J Hum Genet, 2001. **68**(4): p. 895-900.
75. Valente, E.M., et al., *PARK6 is a common cause of familial parkinsonism*. Neurol Sci, 2002. **23 Suppl 2**: p. S117-8.
76. Matsuda, N., et al., *PINK1 stabilized by mitochondrial depolarization recruits Parkin to damaged mitochondria and activates latent Parkin for mitophagy*. J Cell Biol, 2010. **189**(2): p. 211-21.
77. Lee, J.Y., et al., *Disease-causing mutations in parkin impair mitochondrial ubiquitination, aggregation, and HDAC6-dependent mitophagy*. J Cell Biol, 2010. **189**(4): p. 671-9.
78. Pickles, S., P. Vigie, and R.J. Youle, *Mitophagy and Quality Control Mechanisms in Mitochondrial Maintenance*. Curr Biol, 2018. **28**(4): p. R170-R185.
79. Clark, I.E., et al., *Drosophila pink1 is required for mitochondrial function and interacts genetically with parkin*. Nature, 2006. **441**(7097): p. 1162-6.

80. Gispert, S., et al., *Parkinson phenotype in aged PINK1-deficient mice is accompanied by progressive mitochondrial dysfunction in absence of neurodegeneration*. PLoS One, 2009. **4**(6): p. e5777.
81. Glasl, L., et al., *Pink1-deficiency in mice impairs gait, olfaction and serotonergic innervation of the olfactory bulb*. Exp Neurol, 2012. **235**(1): p. 214-27.
82. Perez, F.A. and R.D. Palmiter, *Parkin-deficient mice are not a robust model of parkinsonism*. Proc Natl Acad Sci U S A, 2005. **102**(6): p. 2174-9.
83. McWilliams, T.G., et al., *Basal Mitophagy Occurs Independently of PINK1 in Mouse Tissues of High Metabolic Demand*. Cell Metab, 2018. **27**(2): p. 439-449 e5.
84. Matheoud, D., et al., *Parkinson's Disease-Related Proteins PINK1 and Parkin Repress Mitochondrial Antigen Presentation*. Cell, 2016. **166**(2): p. 314-327.
85. Engelhardt, B., P. Vajkoczy, and R.O. Weller, *The movers and shapers in immune privilege of the CNS*. Nat Immunol, 2017. **18**(2): p. 123-131.
86. Ueno, M., et al., *Blood-brain barrier and blood-cerebrospinal fluid barrier in normal and pathological conditions*. Brain Tumor Pathol, 2016. **33**(2): p. 89-96.
87. Aspelund, A., et al., *A dural lymphatic vascular system that drains brain interstitial fluid and macromolecules*. J Exp Med, 2015. **212**(7): p. 991-9.
88. Louveau, A., et al., *Structural and functional features of central nervous system lymphatic vessels*. Nature, 2015. **523**(7560): p. 337-41.
89. Ghersi-Egea, J.F., et al., *Molecular anatomy and functions of the choroidal blood-cerebrospinal fluid barrier in health and disease*. Acta Neuropathol, 2018. **135**(3): p. 337-361.
90. de Graaf, M.T., et al., *Central memory CD4+ T cells dominate the normal cerebrospinal fluid*. Cytometry B Clin Cytom, 2011. **80**(1): p. 43-50.
91. Schlager, C., et al., *Effector T-cell trafficking between the leptomeninges and the cerebrospinal fluid*. Nature, 2016. **530**(7590): p. 349-53.
92. Ho, M.S., *Microglia in Parkinson's Disease*. Adv Exp Med Biol, 2019. **1175**: p. 335-353.
93. Lawson, L.J., et al., *Heterogeneity in the distribution and morphology of microglia in the normal adult mouse brain*. Neuroscience, 1990. **39**(1): p. 151-70.
94. Mogi, M., et al., *Interleukin-1 beta, interleukin-6, epidermal growth factor and transforming growth factor-alpha are elevated in the brain from parkinsonian patients*. Neurosci Lett, 1994. **180**(2): p. 147-50.
95. Blum-Degen, D., et al., *Interleukin-1 beta and interleukin-6 are elevated in the cerebrospinal fluid of Alzheimer's and de novo Parkinson's disease patients*. Neurosci Lett, 1995. **202**(1-2): p. 17-20.
96. Koziorowski, D., et al., *Inflammatory cytokines and NT-proCNP in Parkinson's disease patients*. Cytokine, 2012. **60**(3): p. 762-6.
97. Banks, W.A., et al., *Lipopolysaccharide-induced blood-brain barrier disruption: roles of cyclooxygenase, oxidative stress, neuroinflammation, and elements of the neurovascular unit*. J Neuroinflammation, 2015. **12**: p. 223.
98. Fan, L., et al., *Systemic inflammation induces a profound long term brain cell injury in rats*. Acta Neurobiol Exp (Wars), 2014. **74**(3): p. 298-306.
99. Nadeau, S. and S. Rivest, *Regulation of the gene encoding tumor necrosis factor alpha (TNF-alpha) in the rat brain and pituitary in response in different models of systemic immune challenge*. J Neuropathol Exp Neurol, 1999. **58**(1): p. 61-77.



100. Vallieres, L. and S. Rivest, *Regulation of the genes encoding interleukin-6, its receptor, and gp130 in the rat brain in response to the immune activator lipopolysaccharide and the proinflammatory cytokine interleukin-1beta*. J Neurochem, 1997. **69**(4): p. 1668-83.
101. Grabert, K., et al., *Microglial brain region-dependent diversity and selective regional sensitivities to aging*. Nat Neurosci, 2016. **19**(3): p. 504-16.
102. McGeer, P.L., et al., *Reactive microglia are positive for HLA-DR in the substantia nigra of Parkinson's and Alzheimer's disease brains*. Neurology, 1988. **38**(8): p. 1285-91.
103. Herrera, A.J., et al., *The single intranigral injection of LPS as a new model for studying the selective effects of inflammatory reactions on dopaminergic system*. Neurobiol Dis, 2000. **7**(4): p. 429-47.
104. Castano, A., et al., *Lipopolysaccharide intranigral injection induces inflammatory reaction and damage in nigrostriatal dopaminergic system*. J Neurochem, 1998. **70**(4): p. 1584-92.
105. Kim, C., et al., *Neuron-released oligomeric alpha-synuclein is an endogenous agonist of TLR2 for paracrine activation of microglia*. Nat Commun, 2013. **4**: p. 1562.
106. Daniele, S.G., et al., *Activation of MyD88-dependent TLR1/2 signaling by misfolded alpha-synuclein, a protein linked to neurodegenerative disorders*. Sci Signal, 2015. **8**(376): p. ra45.
107. Hamza, T.H., et al., *Common genetic variation in the HLA region is associated with late-onset sporadic Parkinson's disease*. Nat Genet, 2010. **42**(9): p. 781-5.
108. Brochard, V., et al., *Infiltration of CD4+ lymphocytes into the brain contributes to neurodegeneration in a mouse model of Parkinson disease*. J Clin Invest, 2009. **119**(1): p. 182-92.
109. Magistrelli, L., et al., *Relationship between circulating CD4+ T lymphocytes and cognitive impairment in patients with Parkinson's disease*. Brain Behav Immun, 2020. **89**: p. 668-674.
110. Kustrimovic, N., et al., *Parkinson's disease patients have a complex phenotypic and functional Th1 bias: cross-sectional studies of CD4+ Th1/Th2/T17 and Treg in drug-naive and drug-treated patients*. J Neuroinflammation, 2018. **15**(1): p. 205.
111. Huang, Y., et al., *Treg Cells Attenuate Neuroinflammation and Protect Neurons in a Mouse Model of Parkinson's Disease*. J Neuroimmune Pharmacol, 2020. **15**(2): p. 224-237.
112. Liu, Z., et al., *IL-17A exacerbates neuroinflammation and neurodegeneration by activating microglia in rodent models of Parkinson's disease*. Brain Behav Immun, 2019. **81**: p. 630-645.
113. Sommer, A., et al., *Th17 Lymphocytes Induce Neuronal Cell Death in a Human iPSC-Based Model of Parkinson's Disease*. Cell Stem Cell, 2018. **23**(1): p. 123-131 e6.
114. Sulzer, D., et al., *T cells from patients with Parkinson's disease recognize alpha-synuclein peptides*. Nature, 2017. **546**(7660): p. 656-661.
115. Cebrian, C., et al., *MHC-I expression renders catecholaminergic neurons susceptible to T-cell-mediated degeneration*. Nat Commun, 2014. **5**: p. 3633.
116. Sveinbjornsdottir, S., *The clinical symptoms of Parkinson's disease*. J Neurochem, 2016. **139 Suppl 1**: p. 318-324.
117. Hughes, A.J., et al., *Accuracy of clinical diagnosis of idiopathic Parkinson's disease: a clinico-pathological study of 100 cases*. J Neurol Neurosurg Psychiatry, 1992. **55**(3): p. 181-4.

118. Berardelli, A., et al., *Pathophysiology of bradykinesia in Parkinson's disease*. Brain, 2001. **124**(Pt 11): p. 2131-46.
119. Ross, G.W., et al., *Parkinsonian signs and substantia nigra neuron density in decedents elders without PD*. Ann Neurol, 2004. **56**(4): p. 532-9.
120. de Lau, L.M., et al., *Subjective complaints precede Parkinson disease: the rotterdam study*. Arch Neurol, 2006. **63**(3): p. 362-5.
121. Hughes, A.J., et al., *A clinicopathologic study of 100 cases of Parkinson's disease*. Arch Neurol, 1993. **50**(2): p. 140-8.
122. Shahed, J. and J. Jankovic, *Exploring the relationship between essential tremor and Parkinson's disease*. Parkinsonism Relat Disord, 2007. **13**(2): p. 67-76.
123. Jellinger, K.A., *Post mortem studies in Parkinson's disease--is it possible to detect brain areas for specific symptoms?* J Neural Transm Suppl, 1999. **56**: p. 1-29.
124. Broussolle, E., et al., *Contribution of Jules Froment to the study of parkinsonian rigidity*. Mov Disord, 2007. **22**(7): p. 909-14.
125. Jankovic, J., *Parkinson's disease: clinical features and diagnosis*. J Neurol Neurosurg Psychiatry, 2008. **79**(4): p. 368-76.
126. Williams, D.R., H.C. Watt, and A.J. Lees, *Predictors of falls and fractures in bradykinetic rigid syndromes: a retrospective study*. J Neurol Neurosurg Psychiatry, 2006. **77**(4): p. 468-73.
127. Giladi, N., et al., *Freezing of gait in PD: prospective assessment in the DATATOP cohort*. Neurology, 2001. **56**(12): p. 1712-21.
128. Macht, M., et al., *Predictors of freezing in Parkinson's disease: a survey of 6,620 patients*. Mov Disord, 2007. **22**(7): p. 953-6.
129. Mollenhauer, B., *Prediagnostic presentation of Parkinson's disease in primary care: A case-control study*. Mov Disord, 2015. **30**(6): p. 787.
130. Zesiewicz, T.A., K.L. Sullivan, and R.A. Hauser, *Nonmotor symptoms of Parkinson's disease*. Expert Rev Neurother, 2006. **6**(12): p. 1811-22.
131. Onofrj, M., A. Thomas, and L. Bonanni, *New approaches to understanding hallucinations in Parkinson's disease: phenomenology and possible origins*. Expert Rev Neurother, 2007. **7**(12): p. 1731-50.
132. Chen, H., et al., *Research on the premotor symptoms of Parkinson's disease: clinical and etiological implications*. Environ Health Perspect, 2013. **121**(11-12): p. 1245-52.
133. Broen, M.P., et al., *Prevalence of pain in Parkinson's disease: a systematic review using the modified QUADAS tool*. Mov Disord, 2012. **27**(4): p. 480-4.
134. Doty, R.L., D.A. Deems, and S. Stellar, *Olfactory dysfunction in parkinsonism: a general deficit unrelated to neurologic signs, disease stage, or disease duration*. Neurology, 1988. **38**(8): p. 1237-44.
135. Chen, Z., G. Li, and J. Liu, *Autonomic dysfunction in Parkinson's disease: Implications for pathophysiology, diagnosis, and treatment*. Neurobiol Dis, 2020. **134**: p. 104700.
136. Velseboer, D.C., et al., *Prevalence of orthostatic hypotension in Parkinson's disease: a systematic review and meta-analysis*. Parkinsonism Relat Disord, 2011. **17**(10): p. 724-9.
137. Sung, H.Y., J.W. Park, and J.S. Kim, *The frequency and severity of gastrointestinal symptoms in patients with early Parkinson's disease*. J Mov Disord, 2014. **7**(1): p. 7-12.
138. Langston, J.W. and P.A. Ballard, Jr., *Parkinson's disease in a chemist working with 1-methyl-4-phenyl-1,2,5,6-tetrahydropyridine*. N Engl J Med, 1983. **309**(5): p. 310.

139. Billingsley, K.J., et al., *Genetic risk factors in Parkinson's disease*. Cell Tissue Res, 2018. **373**(1): p. 9-20.
140. Valente, E.M., et al., *PINK1 mutations are associated with sporadic early-onset parkinsonism*. Ann Neurol, 2004. **56**(3): p. 336-41.
141. Klein, C., et al., *Deciphering the role of heterozygous mutations in genes associated with parkinsonism*. Lancet Neurol, 2007. **6**(7): p. 652-62.
142. Mellick, G.D., et al., *Screening PARK genes for mutations in early-onset Parkinson's disease patients from Queensland, Australia*. Parkinsonism Relat Disord, 2009. **15**(2): p. 105-9.
143. Krohn, L., et al., *Comprehensive assessment of PINK1 variants in Parkinson's disease*. Neurobiol Aging, 2020. **91**: p. 168 e1-168 e5.
144. Sim, C.H., et al., *Analysis of the regulatory and catalytic domains of PTEN-induced kinase-1 (PINK1)*. Hum Mutat, 2012. **33**(10): p. 1408-22.
145. Cazeneuve, C., et al., *A new complex homozygous large rearrangement of the PINK1 gene in a Sudanese family with early onset Parkinson's disease*. Neurogenetics, 2009. **10**(3): p. 265-70.
146. Li, Y., et al., *Clinicogenetic study of PINK1 mutations in autosomal recessive early-onset parkinsonism*. Neurology, 2005. **64**(11): p. 1955-7.
147. Camargos, S.T., et al., *Familial Parkinsonism and early onset Parkinson's disease in a Brazilian movement disorders clinic: phenotypic characterization and frequency of SNCA, PRKN, PINK1, and LRRK2 mutations*. Mov Disord, 2009. **24**(5): p. 662-6.
148. Marongiu, R., et al., *Whole gene deletion and splicing mutations expand the PINK1 genotypic spectrum*. Hum Mutat, 2007. **28**(1): p. 98.
149. Kitada, T., et al., *Mutations in the parkin gene cause autosomal recessive juvenile parkinsonism*. Nature, 1998. **392**(6676): p. 605-8.
150. Lucking, C.B., et al., *Association between early-onset Parkinson's disease and mutations in the parkin gene*. N Engl J Med, 2000. **342**(21): p. 1560-7.
151. Hayashi, S., et al., *An autopsy case of autosomal-recessive juvenile parkinsonism with a homozygous exon 4 deletion in the parkin gene*. Mov Disord, 2000. **15**(5): p. 884-8.
152. van de Warrenburg, B.P., et al., *Clinical and pathologic abnormalities in a family with parkinsonism and parkin gene mutations*. Neurology, 2001. **56**(4): p. 555-7.
153. Miyakawa, S., et al., *Lewy body pathology in a patient with a homozygous parkin deletion*. Mov Disord, 2013. **28**(3): p. 388-91.
154. Trempe, J.F., et al., *Structure of parkin reveals mechanisms for ubiquitin ligase activation*. Science, 2013. **340**(6139): p. 1451-5.
155. Wasner, K., A. Grunewald, and C. Klein, *Parkin-linked Parkinson's disease: From clinical insights to pathogenic mechanisms and novel therapeutic approaches*. Neurosci Res, 2020. **159**: p. 34-39.
156. Sironi, F., et al., *Parkin analysis in early onset Parkinson's disease*. Parkinsonism Relat Disord, 2008. **14**(4): p. 326-33.
157. Puschmann, A., *Monogenic Parkinson's disease and parkinsonism: clinical phenotypes and frequencies of known mutations*. Parkinsonism Relat Disord, 2013. **19**(4): p. 407-15.
158. Klein, C. and M.G. Schlossmacher, *The genetics of Parkinson disease: Implications for neurological care*. Nat Clin Pract Neurol, 2006. **2**(3): p. 136-46.

159. Puschmann, A., et al., *A Swedish family with de novo alpha-synuclein A53T mutation: evidence for early cortical dysfunction*. Parkinsonism Relat Disord, 2009. **15**(9): p. 627-32.
160. Giasson, B.I., et al., *A hydrophobic stretch of 12 amino acid residues in the middle of alpha-synuclein is essential for filament assembly*. J Biol Chem, 2001. **276**(4): p. 2380-6.
161. Bertoni, C.W., et al., *Familial mutants of alpha-synuclein with increased neurotoxicity have a destabilized conformation*. J Biol Chem, 2005. **280**(35): p. 30649-52.
162. Nishioka, K., et al., *Clinical heterogeneity of alpha-synuclein gene duplication in Parkinson's disease*. Ann Neurol, 2006. **59**(2): p. 298-309.
163. Ross, O.A., et al., *Genomic investigation of alpha-synuclein multiplication and parkinsonism*. Ann Neurol, 2008. **63**(6): p. 743-50.
164. Bellou, V., et al., *Environmental risk factors and Parkinson's disease: An umbrella review of meta-analyses*. Parkinsonism Relat Disord, 2016. **23**: p. 1-9.
165. Tanner, C.M., et al., *Rotenone, paraquat, and Parkinson's disease*. Environ Health Perspect, 2011. **119**(6): p. 866-72.
166. van der Mark, M., et al., *Is pesticide use related to Parkinson disease? Some clues to heterogeneity in study results*. Environ Health Perspect, 2012. **120**(3): p. 340-7.
167. Pezzoli, G. and E. Cereda, *Exposure to pesticides or solvents and risk of Parkinson disease*. Neurology, 2013. **80**(22): p. 2035-41.
168. Palin, O., et al., *Systematic review and meta-analysis of hydrocarbon exposure and the risk of Parkinson's disease*. Parkinsonism Relat Disord, 2015. **21**(3): p. 243-8.
169. Wang, A., et al., *Macronutrients intake and risk of Parkinson's disease: A meta-analysis*. Geriatr Gerontol Int, 2015. **15**(5): p. 606-16.
170. Jafari, S., et al., *Head injury and risk of Parkinson disease: a systematic review and meta-analysis*. Mov Disord, 2013. **28**(9): p. 1222-9.
171. Stoll, G., S. Jander, and M. Schroeter, *Detrimental and beneficial effects of injury-induced inflammation and cytokine expression in the nervous system*. Adv Exp Med Biol, 2002. **513**: p. 87-113.
172. Adams-Carr, K.L., et al., *Constipation preceding Parkinson's disease: a systematic review and meta-analysis*. J Neurol Neurosurg Psychiatry, 2016. **87**(7): p. 710-6.
173. Noyce, A.J., et al., *Meta-analysis of early nonmotor features and risk factors for Parkinson disease*. Ann Neurol, 2012. **72**(6): p. 893-901.
174. Yang, F., et al., *Physical activity and risk of Parkinson's disease in the Swedish National March Cohort*. Brain, 2015. **138**(Pt 2): p. 269-75.
175. van der Mark, M., et al., *A case-control study of the protective effect of alcohol, coffee, and cigarette consumption on Parkinson disease risk: time-since-cessation modifies the effect of tobacco smoking*. PLoS One, 2014. **9**(4): p. e95297.
176. Poskanzer, D.C. and R.S. Schwab, *Cohort Analysis of Parkinson's Syndrome: Evidence for a Single Etiology Related to Subclinical Infection About 1920*. J Chronic Dis, 1963. **16**: p. 961-73.
177. Ravenholt, R.T. and W.H. Foote, *1918 influenza, encephalitis lethargica, parkinsonism*. Lancet, 1982. **2**(8303): p. 860-4.
178. Jang, H., et al., *Viral parkinsonism*. Biochim Biophys Acta, 2009. **1792**(7): p. 714-21.
179. Martyn, C.N., *Infection in childhood and neurological diseases in adult life*. Br Med Bull, 1997. **53**(1): p. 24-39.

180. Gamboa, E.T., et al., *Influenza virus antigen in postencephalitic parkinsonism brain. Detection by immunofluorescence*. Arch Neurol, 1974. **31**(4): p. 228-32.
181. Kobasa, D., et al., *Aberrant innate immune response in lethal infection of macaques with the 1918 influenza virus*. Nature, 2007. **445**(7125): p. 319-23.
182. Langston, J.W., et al., *Evidence of active nerve cell degeneration in the substantia nigra of humans years after 1-methyl-4-phenyl-1,2,3,6-tetrahydropyridine exposure*. Ann Neurol, 1999. **46**(4): p. 598-605.
183. Wang, H., et al., *Bacterial, viral, and fungal infection-related risk of Parkinson's disease: Meta-analysis of cohort and case-control studies*. Brain Behav, 2020. **10**(3): p. e01549.
184. Huang, H.K., et al., *Helicobacter pylori infection is associated with an increased risk of Parkinson's disease: A population-based retrospective cohort study*. Parkinsonism Relat Disord, 2018. **47**: p. 26-31.
185. Weller, C., et al., *Role of chronic infection and inflammation in the gastrointestinal tract in the etiology and pathogenesis of idiopathic parkinsonism. Part 3: predicted probability and gradients of severity of idiopathic parkinsonism based on H. pylori antibody profile*. Helicobacter, 2005. **10**(4): p. 288-97.
186. Mridula, K.R., et al., *Association of Helicobacter pylori with Parkinson's Disease*. J Clin Neurol, 2017. **13**(2): p. 181-186.
187. Tan, A.H., et al., *Helicobacter pylori Eradication in Parkinson's Disease: A Randomized Placebo-Controlled Trial*. Mov Disord, 2020. **35**(12): p. 2250-2260.
188. Abushouk, A.I., et al., *Evidence for association between hepatitis C virus and Parkinson's disease*. Neurol Sci, 2017. **38**(11): p. 1913-1920.
189. Armstrong, M.J. and M.S. Okun, *Diagnosis and Treatment of Parkinson Disease: A Review*. JAMA, 2020. **323**(6): p. 548-560.
190. Espay, A.J. and A.E. Lang, *Common Myths in the Use of Levodopa in Parkinson Disease: When Clinical Trials Misinform Clinical Practice*. JAMA Neurol, 2017. **74**(6): p. 633-634.
191. Liao, X., et al., *Levodopa/carbidopa/entacapone for the treatment of early Parkinson's disease: a meta-analysis*. Neurol Sci, 2020. **41**(8): p. 2045-2054.
192. Group, P.D.M.C., et al., *Long-term effectiveness of dopamine agonists and monoamine oxidase B inhibitors compared with levodopa as initial treatment for Parkinson's disease (PD MED): a large, open-label, pragmatic randomised trial*. Lancet, 2014. **384**(9949): p. 1196-205.
193. Heumann, R., et al., *Dyskinesia in Parkinson's disease: mechanisms and current non-pharmacological interventions*. J Neurochem, 2014. **130**(4): p. 472-89.
194. Alonso Canovas, A., et al., *Dopaminergic agonists in Parkinson's disease*. Neurologia, 2014. **29**(4): p. 230-41.
195. Garcia-Ruiz, P.J., et al., *Impulse control disorder in patients with Parkinson's disease under dopamine agonist therapy: a multicentre study*. J Neurol Neurosurg Psychiatry, 2014. **85**(8): p. 840-4.
196. Finberg, J.P.M., *Inhibitors of MAO-B and COMT: their effects on brain dopamine levels and uses in Parkinson's disease*. J Neural Transm (Vienna), 2019. **126**(4): p. 433-448.
197. Malek, N., *Deep Brain Stimulation in Parkinson's Disease*. Neurol India, 2019. **67**(4): p. 968-978.

198. Bratsos, S., D. Karponis, and S.N. Saleh, *Efficacy and Safety of Deep Brain Stimulation in the Treatment of Parkinson's Disease: A Systematic Review and Meta-analysis of Randomized Controlled Trials*. Cureus, 2018. **10**(10): p. e3474.
199. Blandini, F. and M.T. Armentero, *Animal models of Parkinson's disease*. FEBS J, 2012. **279**(7): p. 1156-66.
200. Zhang, Q.S., et al., *Reassessment of subacute MPTP-treated mice as animal model of Parkinson's disease*. Acta Pharmacol Sin, 2017. **38**(10): p. 1317-1328.
201. Lai, F., et al., *Intestinal Pathology and Gut Microbiota Alterations in a Methyl-4-phenyl-1,2,3,6-tetrahydropyridine (MPTP) Mouse Model of Parkinson's Disease*. Neurochem Res, 2018. **43**(10): p. 1986-1999.
202. Yang, J., et al., *Nicotine improved the olfactory impairment in MPTP-induced mouse model of Parkinson's disease*. Neurotoxicology, 2019. **73**: p. 175-182.
203. Dutta, D., et al., *RANTES-induced invasion of Th17 cells into substantia nigra potentiates dopaminergic cell loss in MPTP mouse model of Parkinson's disease*. Neurobiol Dis, 2019. **132**: p. 104575.
204. Johnson, M.E. and L. Bobrovskaya, *An update on the rotenone models of Parkinson's disease: their ability to reproduce the features of clinical disease and model gene-environment interactions*. Neurotoxicology, 2015. **46**: p. 101-16.
205. Inden, M., et al., *Neurodegeneration of mouse nigrostriatal dopaminergic system induced by repeated oral administration of rotenone is prevented by 4-phenylbutyrate, a chemical chaperone*. J Neurochem, 2007. **101**(6): p. 1491-1504.
206. Dodiya, H.B., et al., *Chronic stress-induced gut dysfunction exacerbates Parkinson's disease phenotype and pathology in a rotenone-induced mouse model of Parkinson's disease*. Neurobiol Dis, 2020. **135**: p. 104352.
207. Ungerstedt, U., T. Ljungberg, and G. Steg, *Behavioral, physiological, and neurochemical changes after 6-hydroxydopamine-induced degeneration of the nigro-striatal dopamine neurons*. Adv Neurol, 1974. **5**: p. 421-6.
208. Tronci, E. and V. Francardo, *Animal models of L-DOPA-induced dyskinesia: the 6-OHDA-lesioned rat and mouse*. J Neural Transm (Vienna), 2018. **125**(8): p. 1137-1144.
209. Qin, L., et al., *Systemic LPS causes chronic neuroinflammation and progressive neurodegeneration*. Glia, 2007. **55**(5): p. 453-62.
210. La Vitola, P., et al., *Peripheral inflammation exacerbates alpha-synuclein toxicity and neuropathology in Parkinson's models*. Neuropathol Appl Neurobiol, 2020.
211. Chesselet, M.F., et al., *A progressive mouse model of Parkinson's disease: the Thyl-aSyn ("Line 61") mice*. Neurotherapeutics, 2012. **9**(2): p. 297-314.
212. Fleming, S.M., et al., *Olfactory deficits in mice overexpressing human wildtype alpha-synuclein*. Eur J Neurosci, 2008. **28**(2): p. 247-56.
213. Lam, H.A., et al., *Elevated tonic extracellular dopamine concentration and altered dopamine modulation of synaptic activity precede dopamine loss in the striatum of mice overexpressing human alpha-synuclein*. J Neurosci Res, 2011. **89**(7): p. 1091-102.
214. Watson, M.B., et al., *Regionally-specific microglial activation in young mice overexpressing human wildtype alpha-synuclein*. Exp Neurol, 2012. **237**(2): p. 318-34.
215. Goldberg, M.S., et al., *Parkin-deficient mice exhibit nigrostriatal deficits but not loss of dopaminergic neurons*. J Biol Chem, 2003. **278**(44): p. 43628-35.
216. Dawson, T.M., H.S. Ko, and V.L. Dawson, *Genetic animal models of Parkinson's disease*. Neuron, 2010. **66**(5): p. 646-61.

217. Bian, M., et al., *Overexpression of parkin ameliorates dopaminergic neurodegeneration induced by 1-methyl-4-phenyl-1,2,3,6-tetrahydropyridine in mice*. PLoS One, 2012. **7**(6): p. e39953.
218. Greenwood-Van Meerveld, B., A.C. Johnson, and D. Grundy, *Gastrointestinal Physiology and Function*. Handb Exp Pharmacol, 2017. **239**: p. 1-16.
219. McCormick, B.J.J. and D.R. Lang, *Diarrheal disease and enteric infections in LMIC communities: how big is the problem?* Trop Dis Travel Med Vaccines, 2016. **2**: p. 11.
220. Fischer Walker, C.L., et al., *Diarrhea incidence in low- and middle-income countries in 1990 and 2010: a systematic review*. BMC Public Health, 2012. **12**: p. 220.
221. Reed, K.K. and R. Wickham, *Review of the gastrointestinal tract: from macro to micro*. Semin Oncol Nurs, 2009. **25**(1): p. 3-14.
222. Clevers, H., *The intestinal crypt, a prototype stem cell compartment*. Cell, 2013. **154**(2): p. 274-84.
223. Furness, J.B., *The enteric nervous system and neurogastroenterology*. Nat Rev Gastroenterol Hepatol, 2012. **9**(5): p. 286-94.
224. Sender, R., S. Fuchs, and R. Milo, *Revised Estimates for the Number of Human and Bacteria Cells in the Body*. PLoS Biol, 2016. **14**(8): p. e1002533.
225. Rowland, I., et al., *Gut microbiota functions: metabolism of nutrients and other food components*. Eur J Nutr, 2018. **57**(1): p. 1-24.
226. Takiishi, T., C.I.M. Fenero, and N.O.S. Camara, *Intestinal barrier and gut microbiota: Shaping our immune responses throughout life*. Tissue Barriers, 2017. **5**(4): p. e1373208.
227. Gensollen, T., et al., *How colonization by microbiota in early life shapes the immune system*. Science, 2016. **352**(6285): p. 539-44.
228. Baumler, A.J. and V. Sperandio, *Interactions between the microbiota and pathogenic bacteria in the gut*. Nature, 2016. **535**(7610): p. 85-93.
229. Peterson, L.W. and D. Artis, *Intestinal epithelial cells: regulators of barrier function and immune homeostasis*. Nat Rev Immunol, 2014. **14**(3): p. 141-53.
230. Abreu, M.T., *Toll-like receptor signalling in the intestinal epithelium: how bacterial recognition shapes intestinal function*. Nat Rev Immunol, 2010. **10**(2): p. 131-44.
231. Vaishnava, S., et al., *The antibacterial lectin RegIIIgamma promotes the spatial segregation of microbiota and host in the intestine*. Science, 2011. **334**(6053): p. 255-8.
232. Ngo, V.L., et al., *A cytokine network involving IL-36gamma, IL-23, and IL-22 promotes antimicrobial defense and recovery from intestinal barrier damage*. Proc Natl Acad Sci U S A, 2018. **115**(22): p. E5076-E5085.
233. Mukherjee, S., et al., *Antibacterial membrane attack by a pore-forming intestinal C-type lectin*. Nature, 2014. **505**(7481): p. 103-7.
234. Mabbott, N.A., et al., *Microfold (M) cells: important immunosurveillance posts in the intestinal epithelium*. Mucosal Immunol, 2013. **6**(4): p. 666-77.
235. Hase, K., et al., *Uptake through glycoprotein 2 of FimH(+) bacteria by M cells initiates mucosal immune response*. Nature, 2009. **462**(7270): p. 226-30.
236. Bevins, C.L. and N.H. Salzman, *Paneth cells, antimicrobial peptides and maintenance of intestinal homeostasis*. Nat Rev Microbiol, 2011. **9**(5): p. 356-68.
237. Salzman, N.H., et al., *Protection against enteric salmonellosis in transgenic mice expressing a human intestinal defensin*. Nature, 2003. **422**(6931): p. 522-6.

238. Vaishnava, S., et al., *Paneth cells directly sense gut commensals and maintain homeostasis at the intestinal host-microbial interface*. Proc Natl Acad Sci U S A, 2008. **105**(52): p. 20858-63.
239. Johansson, M.E., et al., *The inner of the two Muc2 mucin-dependent mucus layers in colon is devoid of bacteria*. Proc Natl Acad Sci U S A, 2008. **105**(39): p. 15064-9.
240. Van der Sluis, M., et al., *Muc2-deficient mice spontaneously develop colitis, indicating that MUC2 is critical for colonic protection*. Gastroenterology, 2006. **131**(1): p. 117-29.
241. Velcich, A., et al., *Colorectal cancer in mice genetically deficient in the mucin Muc2*. Science, 2002. **295**(5560): p. 1726-9.
242. Gribble, F.M. and F. Reimann, *Enteroendocrine Cells: Chemosensors in the Intestinal Epithelium*. Annu Rev Physiol, 2016. **78**: p. 277-99.
243. Wichmann, A., et al., *Microbial modulation of energy availability in the colon regulates intestinal transit*. Cell Host Microbe, 2013. **14**(5): p. 582-90.
244. Li, H.J., et al., *Distinct cellular origins for serotonin-expressing and enterochromaffin-like cells in the gastric corpus*. Gastroenterology, 2014. **146**(3): p. 754-764 e3.
245. Reimann, F., et al., *Glucose sensing in L cells: a primary cell study*. Cell Metab, 2008. **8**(6): p. 532-9.
246. Suzuki, T., *Regulation of intestinal epithelial permeability by tight junctions*. Cell Mol Life Sci, 2013. **70**(4): p. 631-59.
247. Van Itallie, C.M. and J.M. Anderson, *Claudins and epithelial paracellular transport*. Annu Rev Physiol, 2006. **68**: p. 403-29.
248. Baum, B. and M. Georgiou, *Dynamics of adherens junctions in epithelial establishment, maintenance, and remodeling*. J Cell Biol, 2011. **192**(6): p. 907-17.
249. Madara, J.L., R. Moore, and S. Carlson, *Alteration of intestinal tight junction structure and permeability by cytoskeletal contraction*. Am J Physiol, 1987. **253**(6 Pt 1): p. C854-61.
250. Bruewer, M., et al., *Proinflammatory cytokines disrupt epithelial barrier function by apoptosis-independent mechanisms*. J Immunol, 2003. **171**(11): p. 6164-72.
251. Burgueno, J.F. and M.T. Abreu, *Epithelial Toll-like receptors and their role in gut homeostasis and disease*. Nat Rev Gastroenterol Hepatol, 2020. **17**(5): p. 263-278.
252. Mowat, A.M. and W.W. Agace, *Regional specialization within the intestinal immune system*. Nat Rev Immunol, 2014. **14**(10): p. 667-85.
253. Cornes, J.S., *Number, size, and distribution of Peyer's patches in the human small intestine: Part I The development of Peyer's patches*. Gut, 1965. **6**(3): p. 225-9.
254. Masahata, K., et al., *Generation of colonic IgA-secreting cells in the caecal patch*. Nat Commun, 2014. **5**: p. 3704.
255. Farache, J., et al., *Luminal bacteria recruit CD103+ dendritic cells into the intestinal epithelium to sample bacterial antigens for presentation*. Immunity, 2013. **38**(3): p. 581-95.
256. Habtezion, A., et al., *Leukocyte Trafficking to the Small Intestine and Colon*. Gastroenterology, 2016. **150**(2): p. 340-54.
257. Toivonen, R., et al., *Activation of Plasmacytoid Dendritic Cells in Colon-Draining Lymph Nodes during Citrobacter rodentium Infection Involves Pathogen-Sensing and Inflammatory Pathways Distinct from Conventional Dendritic Cells*. J Immunol, 2016. **196**(11): p. 4750-9.



258. Stagg, A.J., M.A. Kamm, and S.C. Knight, *Intestinal dendritic cells increase T cell expression of alpha4beta7 integrin*. Eur J Immunol, 2002. **32**(5): p. 1445-54.
259. Coombes, J.L., et al., *A functionally specialized population of mucosal CD103+ DCs induces Foxp3+ regulatory T cells via a TGF-beta and retinoic acid-dependent mechanism*. J Exp Med, 2007. **204**(8): p. 1757-64.
260. Liu, Z.M., et al., *The role of all-trans retinoic acid in the biology of Foxp3+ regulatory T cells*. Cell Mol Immunol, 2015. **12**(5): p. 553-7.
261. Ueno, A., et al., *Th17 plasticity and its relevance to inflammatory bowel disease*. J Autoimmun, 2018. **87**: p. 38-49.
262. Lee, S.H., P.M. Starkey, and S. Gordon, *Quantitative analysis of total macrophage content in adult mouse tissues. Immunochemical studies with monoclonal antibody F4/80*. J Exp Med, 1985. **161**(3): p. 475-89.
263. Smythies, L.E., et al., *Human intestinal macrophages display profound inflammatory anergy despite avid phagocytic and bacteriocidal activity*. J Clin Invest, 2005. **115**(1): p. 66-75.
264. Bain, C.C., et al., *Resident and pro-inflammatory macrophages in the colon represent alternative context-dependent fates of the same Ly6Chi monocyte precursors*. Mucosal Immunol, 2013. **6**(3): p. 498-510.
265. Niess, J.H., et al., *CX3CR1-mediated dendritic cell access to the intestinal lumen and bacterial clearance*. Science, 2005. **307**(5707): p. 254-8.
266. Kuhn, R., et al., *Interleukin-10-deficient mice develop chronic enterocolitis*. Cell, 1993. **75**(2): p. 263-74.
267. Bain, C.C. and A.M. Mowat, *Macrophages in intestinal homeostasis and inflammation*. Immunol Rev, 2014. **260**(1): p. 102-17.
268. Serbina, N.V. and E.G. Pamer, *Monocyte emigration from bone marrow during bacterial infection requires signals mediated by chemokine receptor CCR2*. Nat Immunol, 2006. **7**(3): p. 311-7.
269. Sadik, C.D., N.D. Kim, and A.D. Luster, *Neutrophils cascading their way to inflammation*. Trends Immunol, 2011. **32**(10): p. 452-60.
270. Zhou, G.X. and Z.J. Liu, *Potential roles of neutrophils in regulating intestinal mucosal inflammation of inflammatory bowel disease*. J Dig Dis, 2017. **18**(9): p. 495-503.
271. Kucharzik, T., et al., *Acute induction of human IL-8 production by intestinal epithelium triggers neutrophil infiltration without mucosal injury*. Gut, 2005. **54**(11): p. 1565-72.
272. Gaffen, S.L., et al., *The IL-23-IL-17 immune axis: from mechanisms to therapeutic testing*. Nat Rev Immunol, 2014. **14**(9): p. 585-600.
273. Pelletier, M., et al., *Evidence for a cross-talk between human neutrophils and Th17 cells*. Blood, 2010. **115**(2): p. 335-43.
274. Maynard, C.L. and C.T. Weaver, *Intestinal effector T cells in health and disease*. Immunity, 2009. **31**(3): p. 389-400.
275. Ueno, A., et al., *Increased prevalence of circulating novel IL-17 secreting Foxp3 expressing CD4+ T cells and defective suppressive function of circulating Foxp3+ regulatory cells support plasticity between Th17 and regulatory T cells in inflammatory bowel disease patients*. Inflamm Bowel Dis, 2013. **19**(12): p. 2522-34.
276. Cerutti, A., *The regulation of IgA class switching*. Nat Rev Immunol, 2008. **8**(6): p. 421-34.

277. Mann, E.R. and X. Li, *Intestinal antigen-presenting cells in mucosal immune homeostasis: crosstalk between dendritic cells, macrophages and B-cells*. World J Gastroenterol, 2014. **20**(29): p. 9653-64.
278. Carter, N.A., et al., *Mice lacking endogenous IL-10-producing regulatory B cells develop exacerbated disease and present with an increased frequency of Th1/Th17 but a decrease in regulatory T cells*. J Immunol, 2011. **186**(10): p. 5569-79.
279. Pabst, O. and E. Slack, *IgA and the intestinal microbiota: the importance of being specific*. Mucosal Immunol, 2020. **13**(1): p. 12-21.
280. Geremia, A. and C.V. Arancibia-Carcamo, *Innate Lymphoid Cells in Intestinal Inflammation*. Front Immunol, 2017. **8**: p. 1296.
281. Kramer, B., et al., *Compartment-specific distribution of human intestinal innate lymphoid cells is altered in HIV patients under effective therapy*. PLoS Pathog, 2017. **13**(5): p. e1006373.
282. Sonnenberg, G.F., et al., *CD4(+) lymphoid tissue-inducer cells promote innate immunity in the gut*. Immunity, 2011. **34**(1): p. 122-34.
283. Backhed, F., et al., *Host-bacterial mutualism in the human intestine*. Science, 2005. **307**(5717): p. 1915-20.
284. Donaldson, G.P., S.M. Lee, and S.K. Mazmanian, *Gut biogeography of the bacterial microbiota*. Nat Rev Microbiol, 2016. **14**(1): p. 20-32.
285. Geva-Zatorsky, N., et al., *In vivo imaging and tracking of host-microbiota interactions via metabolic labeling of gut anaerobic bacteria*. Nat Med, 2015. **21**(9): p. 1091-100.
286. Rooks, M.G. and W.S. Garrett, *Gut microbiota, metabolites and host immunity*. Nat Rev Immunol, 2016. **16**(6): p. 341-52.
287. Heiss, C.N. and L.E. Olofsson, *Gut Microbiota-Dependent Modulation of Energy Metabolism*. J Innate Immun, 2018. **10**(3): p. 163-171.
288. Turnbaugh, P.J., et al., *An obesity-associated gut microbiome with increased capacity for energy harvest*. Nature, 2006. **444**(7122): p. 1027-31.
289. McNeil, N.I., *The contribution of the large intestine to energy supplies in man*. Am J Clin Nutr, 1984. **39**(2): p. 338-42.
290. Kelly, C.J., et al., *Crosstalk between Microbiota-Derived Short-Chain Fatty Acids and Intestinal Epithelial HIF Augments Tissue Barrier Function*. Cell Host Microbe, 2015. **17**(5): p. 662-71.
291. Brown, A.J., et al., *The Orphan G protein-coupled receptors GPR41 and GPR43 are activated by propionate and other short chain carboxylic acids*. J Biol Chem, 2003. **278**(13): p. 11312-9.
292. Schele, E., et al., *The gut microbiota reduces leptin sensitivity and the expression of the obesity-suppressing neuropeptides proglucagon (Gcg) and brain-derived neurotrophic factor (Bdnf) in the central nervous system*. Endocrinology, 2013. **154**(10): p. 3643-51.
293. Samuel, B.S., et al., *Effects of the gut microbiota on host adiposity are modulated by the short-chain fatty-acid binding G protein-coupled receptor, Gpr41*. Proc Natl Acad Sci U S A, 2008. **105**(43): p. 16767-72.
294. Psichas, A., et al., *The short chain fatty acid propionate stimulates GLP-1 and PYY secretion via free fatty acid receptor 2 in rodents*. Int J Obes (Lond), 2015. **39**(3): p. 424-9.

295. Morland, B. and T. Midtvedt, *Phagocytosis, peritoneal influx, and enzyme activities in peritoneal macrophages from germfree, conventional, and ex-germfree mice*. Infect Immun, 1984. **44**(3): p. 750-2.
296. Ohkubo, T., et al., *Impaired superoxide production in peripheral blood neutrophils of germ-free rats*. Scand J Immunol, 1990. **32**(6): p. 727-9.
297. Clarke, T.B., et al., *Recognition of peptidoglycan from the microbiota by Nod1 enhances systemic innate immunity*. Nat Med, 2010. **16**(2): p. 228-31.
298. Cario, E., G. Gerken, and D.K. Podolsky, *Toll-like receptor 2 controls mucosal inflammation by regulating epithelial barrier function*. Gastroenterology, 2007. **132**(4): p. 1359-74.
299. Bhattarai, Y. and P.C. Kashyap, *Germ-Free Mice Model for Studying Host-Microbial Interactions*. Methods Mol Biol, 2016. **1438**: p. 123-35.
300. Tao, R., et al., *Deacetylase inhibition promotes the generation and function of regulatory T cells*. Nat Med, 2007. **13**(11): p. 1299-307.
301. Mazmanian, S.K., J.L. Round, and D.L. Kasper, *A microbial symbiosis factor prevents intestinal inflammatory disease*. Nature, 2008. **453**(7195): p. 620-5.
302. Ivanov, II, et al., *Induction of intestinal Th17 cells by segmented filamentous bacteria*. Cell, 2009. **139**(3): p. 485-98.
303. Allam-Ndoul, B., S. Castonguay-Paradis, and A. Veilleux, *Gut Microbiota and Intestinal Trans-Epithelial Permeability*. Int J Mol Sci, 2020. **21**(17).
304. Zackular, J.P., et al., *Dietary zinc alters the microbiota and decreases resistance to Clostridium difficile infection*. Nat Med, 2016. **22**(11): p. 1330-1334.
305. Miao, W., et al., *Sodium Butyrate Promotes Reassembly of Tight Junctions in Caco-2 Monolayers Involving Inhibition of MLCK/MLC2 Pathway and Phosphorylation of PKCbeta2*. Int J Mol Sci, 2016. **17**(10).
306. Braniste, V., et al., *The gut microbiota influences blood-brain barrier permeability in mice*. Sci Transl Med, 2014. **6**(263): p. 263ra158.
307. Li, H., et al., *Sodium butyrate exerts neuroprotective effects by restoring the blood-brain barrier in traumatic brain injury mice*. Brain Res, 2016. **1642**: p. 70-78.
308. Mark, K.S. and D.W. Miller, *Increased permeability of primary cultured brain microvessel endothelial cell monolayers following TNF-alpha exposure*. Life Sci, 1999. **64**(21): p. 1941-53.
309. Adak, A. and M.R. Khan, *An insight into gut microbiota and its functionalities*. Cell Mol Life Sci, 2019. **76**(3): p. 473-493.
310. Sarkar, A., et al., *Psychobiotics and the Manipulation of Bacteria-Gut-Brain Signals*. Trends Neurosci, 2016. **39**(11): p. 763-781.
311. Vuong, H.E., et al., *The Microbiome and Host Behavior*. Annu Rev Neurosci, 2017. **40**: p. 21-49.
312. Bayliss, W.M. and E.H. Starling, *The movements and innervation of the small intestine*. J Physiol, 1899. **24**(2): p. 99-143.
313. Furness, J.B., et al., *Intrinsic primary afferent neurons and nerve circuits within the intestine*. Prog Neurobiol, 2004. **72**(2): p. 143-64.
314. Bertrand, P.P., et al., *Analysis of the responses of myenteric neurons in the small intestine to chemical stimulation of the mucosa*. Am J Physiol, 1997. **273**(2 Pt 1): p. G422-35.

315. Reigstad, C.S., et al., *Gut microbes promote colonic serotonin production through an effect of short-chain fatty acids on enterochromaffin cells*. FASEB J, 2015. **29**(4): p. 1395-403.
316. Obata, Y. and V. Pachnis, *The Effect of Microbiota and the Immune System on the Development and Organization of the Enteric Nervous System*. Gastroenterology, 2016. **151**(5): p. 836-844.
317. Brun, P., et al., *Toll-like receptor 2 regulates intestinal inflammation by controlling integrity of the enteric nervous system*. Gastroenterology, 2013. **145**(6): p. 1323-33.
318. Anitha, M., et al., *Gut microbial products regulate murine gastrointestinal motility via Toll-like receptor 4 signaling*. Gastroenterology, 2012. **143**(4): p. 1006-16 e4.
319. Yang, Y.X., X. Chen, and H.T. Gan, *Toll-like receptor 2 regulates intestinal inflammation by controlling integrity of the enteric nervous system: why were TLR3's roles not tested?* Gastroenterology, 2014. **146**(5): p. 1428.
320. Muller, P.A., et al., *Crosstalk between muscularis macrophages and enteric neurons regulates gastrointestinal motility*. Cell, 2014. **158**(2): p. 300-313.
321. Bonaz, B., V. Sinniger, and S. Pellissier, *Vagus Nerve Stimulation at the Interface of Brain-Gut Interactions*. Cold Spring Harb Perspect Med, 2019. **9**(8).
322. Berthoud, H.R., *Vagal and hormonal gut-brain communication: from satiation to satisfaction*. Neurogastroenterol Motil, 2008. **20 Suppl 1**: p. 64-72.
323. Cailotto, C., et al., *Neuro-anatomical evidence indicating indirect modulation of macrophages by vagal efferents in the intestine but not in the spleen*. PLoS One, 2014. **9**(1): p. e87785.
324. Harris, G.W., *The hypothalamus and endocrine glands*. Br Med Bull, 1950. **6**(4): p. 345-50.
325. Bercik, P., et al., *Chronic gastrointestinal inflammation induces anxiety-like behavior and alters central nervous system biochemistry in mice*. Gastroenterology, 2010. **139**(6): p. 2102-2112 e1.
326. De Palma, G., S.M. Collins, and P. Bercik, *The microbiota-gut-brain axis in functional gastrointestinal disorders*. Gut Microbes, 2014. **5**(3): p. 419-29.
327. Catanzaro, R., et al., *Irritable bowel syndrome: new findings in pathophysiological and therapeutic field*. Minerva Gastroenterol Dietol, 2014. **60**(2): p. 151-63.
328. Viswanathan, V.K., K. Hodges, and G. Hecht, *Enteric infection meets intestinal function: how bacterial pathogens cause diarrhoea*. Nat Rev Microbiol, 2009. **7**(2): p. 110-9.
329. Petri, W.A., Jr., et al., *Enteric infections, diarrhea, and their impact on function and development*. J Clin Invest, 2008. **118**(4): p. 1277-90.
330. Gill, R.K., et al., *Mechanism underlying inhibition of intestinal apical Cl/OH exchange following infection with enteropathogenic E. coli*. J Clin Invest, 2007. **117**(2): p. 428-37.
331. Guttman, J.A., et al., *Aquaporins contribute to diarrhoea caused by attaching and effacing bacterial pathogens*. Cell Microbiol, 2007. **9**(1): p. 131-41.
332. Simonovic, I., et al., *Enteropathogenic Escherichia coli dephosphorylates and dissociates occludin from intestinal epithelial tight junctions*. Cell Microbiol, 2000. **2**(4): p. 305-15.
333. Borenshtein, D., et al., *Development of fatal colitis in FVB mice infected with Citrobacter rodentium*. Infect Immun, 2007. **75**(7): p. 3271-81.
334. Giron, J.A., A.S. Ho, and G.K. Schoolnik, *An inducible bundle-forming pilus of enteropathogenic Escherichia coli*. Science, 1991. **254**(5032): p. 710-3.

335. McDaniel, T.K., et al., *A genetic locus of enterocyte effacement conserved among diverse enterobacterial pathogens*. Proc Natl Acad Sci U S A, 1995. **92**(5): p. 1664-8.
336. Kenny, B., et al., *Enteropathogenic E. coli (EPEC) transfers its receptor for intimate adherence into mammalian cells*. Cell, 1997. **91**(4): p. 511-20.
337. Kalman, D., et al., *Enteropathogenic E. coli acts through WASP and Arp2/3 complex to form actin pedestals*. Nat Cell Biol, 1999. **1**(6): p. 389-91.
338. Deng, W., et al., *Citrobacter rodentium translocated intimin receptor (Tir) is an essential virulence factor needed for actin condensation, intestinal colonization and colonic hyperplasia in mice*. Mol Microbiol, 2003. **48**(1): p. 95-115.
339. Petty, N.K., et al., *The Citrobacter rodentium genome sequence reveals convergent evolution with human pathogenic Escherichia coli*. J Bacteriol, 2010. **192**(2): p. 525-38.
340. Gomes, T.A., et al., *Diarrheagenic Escherichia coli*. Braz J Microbiol, 2016. **47 Suppl 1**: p. 3-30.
341. Tacket, C.O., et al., *Role of EspB in experimental human enteropathogenic Escherichia coli infection*. Infect Immun, 2000. **68**(6): p. 3689-95.
342. Levine, M.M. and R. Edelman, *Enteropathogenic Escherichia coli of classic serotypes associated with infant diarrhea: epidemiology and pathogenesis*. Epidemiol Rev, 1984. **6**: p. 31-51.
343. Lindberg, A.A., et al., *Identification of the carbohydrate receptor for Shiga toxin produced by Shigella dysenteriae type 1*. J Biol Chem, 1987. **262**(4): p. 1779-85.
344. Endo, Y., et al., *Site of action of a Vero toxin (VT2) from Escherichia coli O157:H7 and of Shiga toxin on eukaryotic ribosomes. RNA N-glycosidase activity of the toxins*. Eur J Biochem, 1988. **171**(1-2): p. 45-50.
345. Karmali, M.A., et al., *The association between idiopathic hemolytic uremic syndrome and infection by verotoxin-producing Escherichia coli*. J Infect Dis, 1985. **151**(5): p. 775-82.
346. Schuller, S., *Shiga toxin interaction with human intestinal epithelium*. Toxins (Basel), 2011. **3**(6): p. 626-39.
347. Yang, B., et al., *Enterohemorrhagic Escherichia coli senses low biotin status in the large intestine for colonization and infection*. Nat Commun, 2015. **6**: p. 6592.
348. Schmidt, M.A., *LEEways: tales of EPEC, ATEC and EHEC*. Cell Microbiol, 2010. **12**(11): p. 1544-52.
349. Allen-Vercoe, E., et al., *Amino acid residues within enterohemorrhagic Escherichia coli O157:H7 Tir involved in phosphorylation, alpha-actinin recruitment, and Nck-independent pedestal formation*. Infect Immun, 2006. **74**(11): p. 6196-205.
350. Ugalde-Silva, P., O. Gonzalez-Lugo, and F. Navarro-Garcia, *Tight Junction Disruption Induced by Type 3 Secretion System Effectors Injected by Enteropathogenic and Enterohemorrhagic Escherichia coli*. Front Cell Infect Microbiol, 2016. **6**: p. 87.
351. McNamara, B.P., et al., *Translocated EspF protein from enteropathogenic Escherichia coli disrupts host intestinal barrier function*. J Clin Invest, 2001. **107**(5): p. 621-9.
352. Peralta-Ramirez, J., et al., *EspF Interacts with nucleation-promoting factors to recruit junctional proteins into pedestals for pedestal maturation and disruption of paracellular permeability*. Infect Immun, 2008. **76**(9): p. 3854-68.
353. Thanabalasuriar, A., et al., *The bacterial virulence factor NleA is required for the disruption of intestinal tight junctions by enteropathogenic Escherichia coli*. Cell Microbiol, 2010. **12**(1): p. 31-41.

354. Kim, J., et al., *The bacterial virulence factor NleA inhibits cellular protein secretion by disrupting mammalian COPII function*. Cell Host Microbe, 2007. **2**(3): p. 160-71.
355. Selyunin, A.S., et al., *Selective protection of an ARF1-GTP signaling axis by a bacterial scaffold induces bidirectional trafficking arrest*. Cell Rep, 2014. **6**(5): p. 878-91.
356. Glotfelty, L.G., et al., *Enteropathogenic E. coli effectors EspG1/G2 disrupt microtubules, contribute to tight junction perturbation and inhibit restoration*. Cell Microbiol, 2014. **16**(12): p. 1767-83.
357. Singh, A.P. and S. Aijaz, *Enteropathogenic E. coli: breaking the intestinal tight junction barrier*. F1000Res, 2015. **4**: p. 231.
358. Nougayrede, J.P. and M.S. Donnenberg, *Enteropathogenic Escherichia coli EspF is targeted to mitochondria and is required to initiate the mitochondrial death pathway*. Cell Microbiol, 2004. **6**(11): p. 1097-111.
359. Nougayrede, J.P., G.H. Foster, and M.S. Donnenberg, *Enteropathogenic Escherichia coli effector EspF interacts with host protein Abcf2*. Cell Microbiol, 2007. **9**(3): p. 680-93.
360. Papatheodorou, P., et al., *The enteropathogenic Escherichia coli (EPEC) Map effector is imported into the mitochondrial matrix by the TOM/Hsp70 system and alters organelle morphology*. Cell Microbiol, 2006. **8**(4): p. 677-89.
361. Marches, O., et al., *EspF of enteropathogenic Escherichia coli binds sorting nexin 9*. J Bacteriol, 2006. **188**(8): p. 3110-5.
362. Barthold, S.W., et al., *The etiology of transmissible murine colonic hyperplasia*. Lab Anim Sci, 1976. **26**(6 Pt 1): p. 889-94.
363. Schauer, D.B. and S. Falkow, *The eae gene of Citrobacter freundii biotype 4280 is necessary for colonization in transmissible murine colonic hyperplasia*. Infect Immun, 1993. **61**(11): p. 4654-61.
364. Mullineaux-Sanders, C., et al., *Citrobacter rodentium-host-microbiota interactions: immunity, bioenergetics and metabolism*. Nat Rev Microbiol, 2019. **17**(11): p. 701-715.
365. Deng, W., et al., *Locus of enterocyte effacement from Citrobacter rodentium: sequence analysis and evidence for horizontal transfer among attaching and effacing pathogens*. Infect Immun, 2001. **69**(10): p. 6323-35.
366. Mundy, R., et al., *Citrobacter rodentium of mice and man*. Cell Microbiol, 2005. **7**(12): p. 1697-706.
367. Wiles, S., et al., *Organ specificity, colonization and clearance dynamics in vivo following oral challenges with the murine pathogen Citrobacter rodentium*. Cell Microbiol, 2004. **6**(10): p. 963-72.
368. Mallick, E.M., et al., *A novel murine infection model for Shiga toxin-producing Escherichia coli*. J Clin Invest, 2012. **122**(11): p. 4012-24.
369. Papapietro, O., et al., *R-spondin 2 signalling mediates susceptibility to fatal infectious diarrhoea*. Nat Commun, 2013. **4**: p. 1898.
370. Koroleva, E.P., et al., *Citrobacter rodentium-induced colitis: A robust model to study mucosal immune responses in the gut*. J Immunol Methods, 2015. **421**: p. 61-72.
371. Kang, E., M. Yousefi, and S. Gruenheid, *R-Spondins Are Expressed by the Intestinal Stroma and are Differentially Regulated during Citrobacter rodentium- and DSS-Induced Colitis in Mice*. PLoS One, 2016. **11**(4): p. e0152859.
372. Kang, E., et al., *Loss of disease tolerance during Citrobacter rodentium infection is associated with impaired epithelial differentiation and hyperactivation of T cell responses*. Sci Rep, 2018. **8**(1): p. 847.

373. Kamada, N., et al., *Regulated virulence controls the ability of a pathogen to compete with the gut microbiota*. Science, 2012. **336**(6086): p. 1325-9.
374. Berger, C.N., et al., *Citrobacter rodentium Subverts ATP Flux and Cholesterol Homeostasis in Intestinal Epithelial Cells In Vivo*. Cell Metab, 2017. **26**(5): p. 738-752 e6.
375. Hopkins, E.G.D., et al., *Intestinal Epithelial Cells and the Microbiome Undergo Swift Reprogramming at the Inception of Colonic Citrobacter rodentium Infection*. mBio, 2019. **10**(2).
376. Fabich, A.J., et al., *Comparison of carbon nutrition for pathogenic and commensal Escherichia coli strains in the mouse intestine*. Infect Immun, 2008. **76**(3): p. 1143-52.
377. Burger-van Paassen, N., et al., *The regulation of intestinal mucin MUC2 expression by short-chain fatty acids: implications for epithelial protection*. Biochem J, 2009. **420**(2): p. 211-9.
378. Desai, M.S., et al., *A Dietary Fiber-Deprived Gut Microbiota Degrades the Colonic Mucus Barrier and Enhances Pathogen Susceptibility*. Cell, 2016. **167**(5): p. 1339-1353 e21.
379. Buschor, S., et al., *Innate immunity restricts Citrobacter rodentium A/E pathogenesis initiation to an early window of opportunity*. PLoS Pathog, 2017. **13**(6): p. e1006476.
380. Gibson, D.L., et al., *Toll-like receptor 2 plays a critical role in maintaining mucosal integrity during Citrobacter rodentium-induced colitis*. Cell Microbiol, 2008. **10**(2): p. 388-403.
381. Khan, M.A., et al., *Toll-like receptor 4 contributes to colitis development but not to host defense during Citrobacter rodentium infection in mice*. Infect Immun, 2006. **74**(5): p. 2522-36.
382. Gibson, D.L., et al., *MyD88 signalling plays a critical role in host defence by controlling pathogen burden and promoting epithelial cell homeostasis during Citrobacter rodentium-induced colitis*. Cell Microbiol, 2008. **10**(3): p. 618-31.
383. Wang, Y., et al., *Lymphotoxin beta receptor signaling in intestinal epithelial cells orchestrates innate immune responses against mucosal bacterial infection*. Immunity, 2010. **32**(3): p. 403-13.
384. Guo, X., et al., *Induction of innate lymphoid cell-derived interleukin-22 by the transcription factor STAT3 mediates protection against intestinal infection*. Immunity, 2014. **40**(1): p. 25-39.
385. Spehlmann, M.E., et al., *CXCR2-dependent mucosal neutrophil influx protects against colitis-associated diarrhea caused by an attaching/effacing lesion-forming bacterial pathogen*. J Immunol, 2009. **183**(5): p. 3332-43.
386. Longman, R.S., et al., *CX(3)CR1(+) mononuclear phagocytes support colitis-associated innate lymphoid cell production of IL-22*. J Exp Med, 2014. **211**(8): p. 1571-83.
387. Schreiber, H.A., et al., *Intestinal monocytes and macrophages are required for T cell polarization in response to Citrobacter rodentium*. J Exp Med, 2013. **210**(10): p. 2025-39.
388. Bry, L. and M.B. Brenner, *Critical role of T cell-dependent serum antibody, but not the gut-associated lymphoid tissue, for surviving acute mucosal infection with Citrobacter rodentium, an attaching and effacing pathogen*. J Immunol, 2004. **172**(1): p. 433-41.

389. Simmons, C.P., et al., *Central role for B lymphocytes and CD4+ T cells in immunity to infection by the attaching and effacing pathogen Citrobacter rodentium*. Infect Immun, 2003. **71**(9): p. 5077-86.
390. Ishigame, H., et al., *Differential roles of interleukin-17A and -17F in host defense against mucoepithelial bacterial infection and allergic responses*. Immunity, 2009. **30**(1): p. 108-19.
391. Basu, R., et al., *Th22 cells are an important source of IL-22 for host protection against enteropathogenic bacteria*. Immunity, 2012. **37**(6): p. 1061-75.
392. Kamada, N., et al., *Humoral Immunity in the Gut Selectively Targets Phenotypically Virulent Attaching-and-Effacing Bacteria for Intraluminal Elimination*. Cell Host Microbe, 2015. **17**(5): p. 617-27.
393. Cryan, J.F., et al., *The Microbiota-Gut-Brain Axis*. Physiol Rev, 2019. **99**(4): p. 1877-2013.
394. Brudek, T., *Inflammatory Bowel Diseases and Parkinson's Disease*. J Parkinsons Dis, 2019. **9**(s2): p. S331-S344.
395. Sun, M.F. and Y.Q. Shen, *Dysbiosis of gut microbiota and microbial metabolites in Parkinson's Disease*. Ageing Res Rev, 2018. **45**: p. 53-61.
396. Nerius, M., G. Doblhammer, and G. Tamguney, *GI infections are associated with an increased risk of Parkinson's disease*. Gut, 2020. **69**(6): p. 1154-1156.
397. Perez-Pardo, P., et al., *Role of TLR4 in the gut-brain axis in Parkinson's disease: a translational study from men to mice*. Gut, 2019. **68**(5): p. 829-843.
398. Hasegawa, S., et al., *Intestinal Dysbiosis and Lowered Serum Lipopolysaccharide-Binding Protein in Parkinson's Disease*. PLoS One, 2015. **10**(11): p. e0142164.
399. Forsyth, C.B., et al., *Increased intestinal permeability correlates with sigmoid mucosa alpha-synuclein staining and endotoxin exposure markers in early Parkinson's disease*. PLoS One, 2011. **6**(12): p. e28032.
400. Campos-Acuna, J., D. Elgueta, and R. Pacheco, *T-Cell-Driven Inflammation as a Mediator of the Gut-Brain Axis Involved in Parkinson's Disease*. Front Immunol, 2019. **10**: p. 239.
401. Devos, D., et al., *Colonic inflammation in Parkinson's disease*. Neurobiol Dis, 2013. **50**: p. 42-8.
402. Chen, Y., et al., *Clinical characteristics and peripheral T cell subsets in Parkinson's disease patients with constipation*. Int J Clin Exp Pathol, 2015. **8**(3): p. 2495-504.
403. Hui, K.Y., et al., *Functional variants in the LRRK2 gene confer shared effects on risk for Crohn's disease and Parkinson's disease*. Sci Transl Med, 2018. **10**(423).
404. Park, S., et al., *Patients with Inflammatory Bowel Disease Are at an Increased Risk of Parkinson's Disease: A South Korean Nationwide Population-Based Study*. J Clin Med, 2019. **8**(8).
405. Villumsen, M., et al., *Inflammatory bowel disease increases the risk of Parkinson's disease: a Danish nationwide cohort study 1977-2014*. Gut, 2019. **68**(1): p. 18-24.
406. Weimers, P., et al., *Inflammatory Bowel Disease and Parkinson's Disease: A Nationwide Swedish Cohort Study*. Inflamm Bowel Dis, 2019. **25**(1): p. 111-123.
407. Peter, I., et al., *Anti-Tumor Necrosis Factor Therapy and Incidence of Parkinson Disease Among Patients With Inflammatory Bowel Disease*. JAMA Neurol, 2018. **75**(8): p. 939-946.



408. Lin, J.C., et al., *Association Between Parkinson's Disease and Inflammatory Bowel Disease: a Nationwide Taiwanese Retrospective Cohort Study*. *Inflamm Bowel Dis*, 2016. **22**(5): p. 1049-55.
409. Magro, F., et al., *Impaired synthesis or cellular storage of norepinephrine, dopamine, and 5-hydroxytryptamine in human inflammatory bowel disease*. *Dig Dis Sci*, 2002. **47**(1): p. 216-24.
410. Pacheco, R., *Targeting dopamine receptor D3 signalling in inflammation*. *Oncotarget*, 2017. **8**(5): p. 7224-7225.
411. Contreras, F., et al., *Dopamine Receptor D3 Signaling on CD4+ T Cells Favors Th1- and Th17-Mediated Immunity*. *J Immunol*, 2016. **196**(10): p. 4143-9.
412. Villaran, R.F., et al., *Ulcerative colitis exacerbates lipopolysaccharide-induced damage to the nigral dopaminergic system: potential risk factor in Parkinson's disease*. *J Neurochem*, 2010. **114**(6): p. 1687-700.
413. Kishimoto, Y., et al., *Chronic Mild Gut Inflammation Accelerates Brain Neuropathology and Motor Dysfunction in alpha-Synuclein Mutant Mice*. *Neuromolecular Med*, 2019. **21**(3): p. 239-249.
414. Braak, H., et al., *Gastric alpha-synuclein immunoreactive inclusions in Meissner's and Auerbach's plexuses in cases staged for Parkinson's disease-related brain pathology*. *Neurosci Lett*, 2006. **396**(1): p. 67-72.
415. Svensson, E., et al., *Vagotomy and subsequent risk of Parkinson's disease*. *Ann Neurol*, 2015. **78**(4): p. 522-9.
416. Uemura, N., et al., *Inoculation of alpha-synuclein preformed fibrils into the mouse gastrointestinal tract induces Lewy body-like aggregates in the brainstem via the vagus nerve*. *Mol Neurodegener*, 2018. **13**(1): p. 21.
417. Killinger, B.A., et al., *The vermiform appendix impacts the risk of developing Parkinson's disease*. *Sci Transl Med*, 2018. **10**(465).
418. Lu, H.T., et al., *Lack of association between appendectomy and Parkinson's disease: a systematic review and meta-analysis*. *Aging Clin Exp Res*, 2020. **32**(11): p. 2201-2209.
419. Scheperjans, F., et al., *Gut microbiota are related to Parkinson's disease and clinical phenotype*. *Mov Disord*, 2015. **30**(3): p. 350-8.
420. Unger, M.M., et al., *Short chain fatty acids and gut microbiota differ between patients with Parkinson's disease and age-matched controls*. *Parkinsonism Relat Disord*, 2016. **32**: p. 66-72.
421. Bedarf, J.R., et al., *Functional implications of microbial and viral gut metagenome changes in early stage L-DOPA-naïve Parkinson's disease patients*. *Genome Med*, 2017. **9**(1): p. 39.
422. Petrov, V.A., et al., *Analysis of Gut Microbiota in Patients with Parkinson's Disease*. *Bull Exp Biol Med*, 2017. **162**(6): p. 734-737.
423. Tetz, G., et al., *Parkinson's disease and bacteriophages as its overlooked contributors*. *Sci Rep*, 2018. **8**(1): p. 10812.
424. Shen, L., *Gut, oral and nasal microbiota and Parkinson's disease*. *Microb Cell Fact*, 2020. **19**(1): p. 50.
425. Lin, C.H., et al., *Altered gut microbiota and inflammatory cytokine responses in patients with Parkinson's disease*. *J Neuroinflammation*, 2019. **16**(1): p. 129.
426. Arumugam, M., et al., *Enterotypes of the human gut microbiome*. *Nature*, 2011. **473**(7346): p. 174-80.

427. Mulak, A. and B. Bonaz, *Brain-gut-microbiota axis in Parkinson's disease*. World J Gastroenterol, 2015. **21**(37): p. 10609-20.
428. Furusawa, Y., et al., *Commensal microbe-derived butyrate induces the differentiation of colonic regulatory T cells*. Nature, 2013. **504**(7480): p. 446-50.
429. Lopez, C.A., et al., *Virulence factors enhance Citrobacter rodentium expansion through aerobic respiration*. Science, 2016. **353**(6305): p. 1249-53.
430. Fasano, A., et al., *The role of small intestinal bacterial overgrowth in Parkinson's disease*. Mov Disord, 2013. **28**(9): p. 1241-9.
431. Vizcarra, J.A., et al., *Small intestinal bacterial overgrowth in Parkinson's disease: Tribulations of a trial*. Parkinsonism Relat Disord, 2018. **54**: p. 110-112.
432. Li, W., et al., *Structural changes of gut microbiota in Parkinson's disease and its correlation with clinical features*. Sci China Life Sci, 2017. **60**(11): p. 1223-1233.
433. Hill-Burns, E.M., et al., *Parkinson's disease and Parkinson's disease medications have distinct signatures of the gut microbiome*. Mov Disord, 2017. **32**(5): p. 739-749.
434. Ottman, N., et al., *Action and function of Akkermansia muciniphila in microbiome ecology, health and disease*. Best Pract Res Clin Gastroenterol, 2017. **31**(6): p. 637-642.
435. Sampson, T.R., et al., *Gut Microbiota Regulate Motor Deficits and Neuroinflammation in a Model of Parkinson's Disease*. Cell, 2016. **167**(6): p. 1469-1480 e12.
436. Sun, M.F., et al., *Neuroprotective effects of fecal microbiota transplantation on MPTP-induced Parkinson's disease mice: Gut microbiota, glial reaction and TLR4/TNF-alpha signaling pathway*. Brain Behav Immun, 2018. **70**: p. 48-60.
437. Seregin, S.S., et al., *NLRP6 Protects Il10(-/-) Mice from Colitis by Limiting Colonization of Akkermansia muciniphila*. Cell Rep, 2017. **19**(4): p. 733-745.
438. Everard, A., et al., *Cross-talk between Akkermansia muciniphila and intestinal epithelium controls diet-induced obesity*. Proc Natl Acad Sci U S A, 2013. **110**(22): p. 9066-71.
439. Xing, J., et al., *Comparative genomic and functional analysis of Akkermansia muciniphila and closely related species*. Genes Genomics, 2019. **41**(11): p. 1253-1264.
440. Johnson, M.E., et al., *Triggers, Facilitators, and Aggravators: Redefining Parkinson's Disease Pathogenesis*. Trends Neurosci, 2019. **42**(1): p. 4-13.
441. Kannarkat, G.T., J.M. Boss, and M.G. Tansey, *The role of innate and adaptive immunity in Parkinson's disease*. J Parkinsons Dis, 2013. **3**(4): p. 493-514.
442. Farrer, M.J., *Genetics of Parkinson disease: paradigm shifts and future prospects*. Nat Rev Genet, 2006. **7**(4): p. 306-18.
443. Narendra, D., et al., *Parkin is recruited selectively to impaired mitochondria and promotes their autophagy*. J Cell Biol, 2008. **183**(5): p. 795-803.
444. Allen, G.F., et al., *Loss of iron triggers PINK1/Parkin-independent mitophagy*. EMBO Rep, 2013. **14**(12): p. 1127-35.
445. Kageyama, Y., et al., *Parkin-independent mitophagy requires Drp1 and maintains the integrity of mammalian heart and brain*. EMBO J, 2014. **33**(23): p. 2798-813.
446. McWilliams, T.G., et al., *Phosphorylation of Parkin at serine 65 is essential for its activation in vivo*. Open Biol, 2018. **8**(11).
447. Oliveras-Salva, M., et al., *Loss-of-function rodent models for parkin and PINK1*. J Parkinsons Dis, 2011. **1**(3): p. 229-51.
448. Mueller, S.N., et al., *Rapid cytotoxic T lymphocyte activation occurs in the draining lymph nodes after cutaneous herpes simplex virus infection as a result of early antigen presentation and not the presence of virus*. J Exp Med, 2002. **195**(5): p. 651-6.

449. Tanaka, A., P.S. Leung, and M.E. Gershwin, *Environmental basis of primary biliary cholangitis*. Exp Biol Med (Maywood), 2018. **243**(2): p. 184-189.
450. Sliter, D.A., et al., *Parkin and PINK1 mitigate STING-induced inflammation*. Nature, 2018. **561**(7722): p. 258-262.
451. Ghaem-Maghami, M., et al., *Intimin-specific immune responses prevent bacterial colonization by the attaching-effacing pathogen Citrobacter rodentium*. Infect Immun, 2001. **69**(9): p. 5597-605.
452. Nishimura, M., et al., *Dual functions of fractalkine/CX3C ligand 1 in trafficking of perforin+/granzyme B+ cytotoxic effector lymphocytes that are defined by CX3CR1 expression*. J Immunol, 2002. **168**(12): p. 6173-80.
453. Nishiyori, A., et al., *Localization of fractalkine and CX3CR1 mRNAs in rat brain: does fractalkine play a role in signaling from neuron to microglia?* FEBS Lett, 1998. **429**(2): p. 167-72.
454. Kageyama, S., et al., *Potent cytolytic response by a CD8+ CTL clone to multiple peptides from the same protein in association with an allogeneic class I MHC molecule*. J Immunol, 2001. **166**(5): p. 3028-34.
455. Dave, K.D., et al., *Phenotypic characterization of recessive gene knockout rat models of Parkinson's disease*. Neurobiol Dis, 2014. **70**: p. 190-203.
456. Matsuura, K., et al., *Pole test is a useful method for evaluating the mouse movement disorder caused by striatal dopamine depletion*. J Neurosci Methods, 1997. **73**(1): p. 45-8.
457. Kelm-Nelson, C.A., et al., *Characterization of early-onset motor deficits in the Pink1-/- mouse model of Parkinson disease*. Brain Res, 2018. **1680**: p. 1-12.
458. Kitada, T., et al., *Impaired dopamine release and synaptic plasticity in the striatum of PINK1-deficient mice*. Proc Natl Acad Sci U S A, 2007. **104**(27): p. 11441-6.
459. Holmqvist, S., et al., *Direct evidence of Parkinson pathology spread from the gastrointestinal tract to the brain in rats*. Acta Neuropathol, 2014. **128**(6): p. 805-20.
460. Houser, M.C. and M.G. Tansey, *The gut-brain axis: is intestinal inflammation a silent driver of Parkinson's disease pathogenesis?* NPJ Parkinsons Dis, 2017. **3**: p. 3.
461. Fasano, C., D. Thibault, and L.E. Trudeau, *Culture of postnatal mesencephalic dopamine neurons on an astrocyte monolayer*. Curr Protoc Neurosci, 2008. **Chapter 3**: p. Unit 3 21.
462. Gundersen, H.J., et al., *The new stereological tools: disector, fractionator, nucleator and point sampled intercepts and their use in pathological research and diagnosis*. APMIS, 1988. **96**(10): p. 857-81.
463. Dutz, J.P., et al., *A cytotoxic T lymphocyte clone can recognize the same naturally occurring self peptide in association with a self and nonself class I MHC protein*. Mol Immunol, 1994. **31**(13): p. 967-75.
464. Tysnes, O.B. and A. Storstein, *Epidemiology of Parkinson's disease*. J Neural Transm (Vienna), 2017. **124**(8): p. 901-905.
465. Pringsheim, T., et al., *The prevalence of Parkinson's disease: a systematic review and meta-analysis*. Mov Disord, 2014. **29**(13): p. 1583-90.
466. Gelb, D.J., E. Oliver, and S. Gilman, *Diagnostic criteria for Parkinson disease*. Arch Neurol, 1999. **56**(1): p. 33-9.
467. Dauer, W. and S. Przedborski, *Parkinson's disease: mechanisms and models*. Neuron, 2003. **39**(6): p. 889-909.


468. Wong, Y.C., et al., *Neuronal vulnerability in Parkinson disease: Should the focus be on axons and synaptic terminals?* *Mov Disord*, 2019. **34**(10): p. 1406-1422.
469. Brooks, J., et al., *Parkin and PINK1 mutations in early-onset Parkinson's disease: comprehensive screening in publicly available cases and control.* *J Med Genet*, 2009. **46**(6): p. 375-81.
470. Jin, S.M., et al., *Mitochondrial membrane potential regulates PINK1 import and proteolytic destabilization by PARL.* *J Cell Biol*, 2010. **191**(5): p. 933-42.
471. Wright Willis, A., et al., *Geographic and ethnic variation in Parkinson disease: a population-based study of US Medicare beneficiaries.* *Neuroepidemiology*, 2010. **34**(3): p. 143-51.
472. Ben-Joseph, A., et al., *Ethnic Variation in the Manifestation of Parkinson's Disease: A Narrative Review.* *J Parkinsons Dis*, 2020. **10**(1): p. 31-45.
473. Tremlett, H., et al., *The gut microbiome in human neurological disease: A review.* *Ann Neurol*, 2017. **81**(3): p. 369-382.
474. Shao, Q.H., et al., *TLR4 deficiency has a protective effect in the MPTP/probenecid mouse model of Parkinson's disease.* *Acta Pharmacol Sin*, 2019. **40**(12): p. 1503-1512.
475. Matheoud, D., et al., *Intestinal infection triggers Parkinson's disease-like symptoms in Pink1(-/-) mice.* *Nature*, 2019. **571**(7766): p. 565-569.
476. Lupp, C., et al., *Host-mediated inflammation disrupts the intestinal microbiota and promotes the overgrowth of Enterobacteriaceae.* *Cell Host Microbe*, 2007. **2**(2): p. 119-29.
477. Vallance, B.A., et al., *Host susceptibility to the attaching and effacing bacterial pathogen Citrobacter rodentium.* *Infect Immun*, 2003. **71**(6): p. 3443-53.
478. Bolyen, E., et al., *Reproducible, interactive, scalable and extensible microbiome data science using QIIME 2.* *Nat Biotechnol*, 2019. **37**(8): p. 852-857.
479. Ghosh, S., et al., *Colonic microbiota alters host susceptibility to infectious colitis by modulating inflammation, redox status, and ion transporter gene expression.* *Am J Physiol Gastrointest Liver Physiol*, 2011. **301**(1): p. G39-49.
480. Willing, B.P., et al., *Altering host resistance to infections through microbial transplantation.* *PLoS One*, 2011. **6**(10): p. e26988.
481. Osbelt, L., et al., *Variations in microbiota composition of laboratory mice influence Citrobacter rodentium infection via variable short-chain fatty acid production.* *PLoS Pathog*, 2020. **16**(3): p. e1008448.
482. Schneeberger, M., et al., *Akkermansia muciniphila inversely correlates with the onset of inflammation, altered adipose tissue metabolism and metabolic disorders during obesity in mice.* *Sci Rep*, 2015. **5**: p. 16643.
483. Keshavarzian, A., et al., *Colonic bacterial composition in Parkinson's disease.* *Mov Disord*, 2015. **30**(10): p. 1351-60.
484. Zhou, Z.L., et al., *Neuroprotection of Fasting Mimicking Diet on MPTP-Induced Parkinson's Disease Mice via Gut Microbiota and Metabolites.* *Neurotherapeutics*, 2019. **16**(3): p. 741-760.
485. Liu, H., et al., *Butyrate: A Double-Edged Sword for Health?* *Adv Nutr*, 2018. **9**(1): p. 21-29.
486. Mariadason, J.M., D.H. Barkla, and P.R. Gibson, *Effect of short-chain fatty acids on paracellular permeability in Caco-2 intestinal epithelium model.* *Am J Physiol*, 1997. **272**(4 Pt 1): p. G705-12.

487. Takaishi, H., et al., *Imbalance in intestinal microflora constitution could be involved in the pathogenesis of inflammatory bowel disease*. Int J Med Microbiol, 2008. **298**(5-6): p. 463-72.
488. Silva, J.P.B., et al., *Protective Mechanisms of Butyrate on Inflammatory Bowel Disease*. Curr Pharm Des, 2018. **24**(35): p. 4154-4166.
489. Arpaia, N., et al., *Metabolites produced by commensal bacteria promote peripheral regulatory T-cell generation*. Nature, 2013. **504**(7480): p. 451-5.
490. Jiminez, J.A., et al., *Butyrate Supplementation at High Concentrations Alters Enteric Bacterial Communities and Reduces Intestinal Inflammation in Mice Infected with Citrobacter rodentium*. mSphere, 2017. **2**(4).
491. Choi, J.G., et al., *Oral administration of Proteus mirabilis damages dopaminergic neurons and motor functions in mice*. Sci Rep, 2018. **8**(1): p. 1275.
492. Takeda, K. and S. Akira, *TLR signaling pathways*. Semin Immunol, 2004. **16**(1): p. 3-9.
493. Tanaka, Y. and Z.J. Chen, *STING specifies IRF3 phosphorylation by TBK1 in the cytosolic DNA signaling pathway*. Sci Signal, 2012. **5**(214): p. ra20.
494. Hopfner, K.P. and V. Hornung, *Molecular mechanisms and cellular functions of cGAS-STING signalling*. Nat Rev Mol Cell Biol, 2020. **21**(9): p. 501-521.
495. Smith, J.A., *Regulation of Cytokine Production by the Unfolded Protein Response; Implications for Infection and Autoimmunity*. Front Immunol, 2018. **9**: p. 422.
496. Wang, Y., et al., *Lipopolysaccharide Activates the Unfolded Protein Response in Human Periodontal Ligament Fibroblasts*. J Periodontol, 2016. **87**(5): p. e75-81.
497. Bellucci, A., et al., *Induction of the unfolded protein response by alpha-synuclein in experimental models of Parkinson's disease*. J Neurochem, 2011. **116**(4): p. 588-605.
498. Hoozemans, J.J., et al., *Activation of the unfolded protein response in Parkinson's disease*. Biochem Biophys Res Commun, 2007. **354**(3): p. 707-11.
499. Heo, J.M., et al., *The PINK1-PARKIN Mitochondrial Ubiquitylation Pathway Drives a Program of OPTN/NDP52 Recruitment and TBK1 Activation to Promote Mitophagy*. Mol Cell, 2015. **60**(1): p. 7-20.
500. MacVicar, T.D., et al., *Targeted siRNA Screens Identify ER-to-Mitochondrial Calcium Exchange in Autophagy and Mitophagy Responses in RPE1 Cells*. Int J Mol Sci, 2015. **16**(6): p. 13356-80.
501. Youle, R.J. and D.P. Narendra, *Mechanisms of mitophagy*. Nat Rev Mol Cell Biol, 2011. **12**(1): p. 9-14.
502. Klein, L., E.A. Robey, and C.S. Hsieh, *Central CD4(+) T cell tolerance: deletion versus regulatory T cell differentiation*. Nat Rev Immunol, 2019. **19**(1): p. 7-18.
503. Stegall, M.D., et al., *The 2C T-cell transgenic mouse: an in vivo model of allospecific cytotoxic T-cell activation and homing*. Transplant Proc, 1999. **31**(1-2): p. 779.
504. Bogdanos, D.P. and D. Vergani, *Bacteria and primary biliary cirrhosis*. Clin Rev Allergy Immunol, 2009. **36**(1): p. 30-9.
505. Borsche, M., et al., *Mitochondrial damage-associated inflammation highlights biomarkers in PRKN/PINK1 parkinsonism*. Brain, 2020. **143**(10): p. 3041-3051.
506. Gubser, P.M., et al., *Rapid effector function of memory CD8+ T cells requires an immediate-early glycolytic switch*. Nat Immunol, 2013. **14**(10): p. 1064-72.
507. Yanamandra, K., et al., *alpha-synuclein reactive antibodies as diagnostic biomarkers in blood sera of Parkinson's disease patients*. PLoS One, 2011. **6**(4): p. e18513.

- 508. Pigeyre, M., et al., *Recent progress in genetics, epigenetics and metagenomics unveils the pathophysiology of human obesity*. Clin Sci (Lond), 2016. **130**(12): p. 943-86.
- 509. Karlsson, F.H., et al., *Symptomatic atherosclerosis is associated with an altered gut metagenome*. Nat Commun, 2012. **3**: p. 1245.
- 510. Ducarmon, Q.R., et al., *Gut Microbiota and Colonization Resistance against Bacterial Enteric Infection*. Microbiol Mol Biol Rev, 2019. **83**(3).

## APPENDIX

### Written agreement for a co-first authored article (Chapter 2) to be published in this thesis:

**From:** Matheoud Diana [diana.matheoud@umontreal.ca](mailto:diana.matheoud@umontreal.ca)   
**Subject:** RE: Sharing Information for "Intestinal infection triggers Parkinson's disease-like symptoms in Pink1(-/-) mice": Manuscript  
Permission for PhD Thesis  
**Date:** February 22, 2021 at 3:49 PM  
**To:** Tyler Cannon [tyler.cannon2@mail.mcgill.ca](mailto:tyler.cannon2@mail.mcgill.ca)

---

Dear Tyler,

Yes, I grant you the permission to use this manuscript for your thesis.

Best,

Diana Matheoud, PhD  
Département de Neurosciences, Université de Montréal  
CRCHUM, Tour Viger R09.418  
[900 St-Denis, Montréal, Qc, Canada, H2X 0A9](#)  
Téléphone [514-890-8000](tel:514-890-8000) X: 14090  
[diana.matheoud@umontreal.ca](mailto:diana.matheoud@umontreal.ca)

---

**De :** Tyler Cannon <[tyler.cannon2@mail.mcgill.ca](mailto:tyler.cannon2@mail.mcgill.ca)>

**Envoyé :** lundi 22 février 2021 15:47

**À :** Matheoud Diana <[diana.matheoud@umontreal.ca](mailto:diana.matheoud@umontreal.ca)>

**Objet :** Sharing Information for "Intestinal infection triggers Parkinson's disease-like symptoms in Pink1(-/-) mice": Manuscript Permission for PhD Thesis

Hello Dr. Matheoud,

I am in the process of submitting my Ph.D. thesis and was hoping that you would grant me permission to use the following manuscript in my thesis:

Matheoud, D., Cannon, T., et al. (2019). "Intestinal infection triggers Parkinson's disease-like symptoms in Pink1(-/-) mice." Nature **571**(7766): 565-569.

Thank you,  
Tyler Cannon